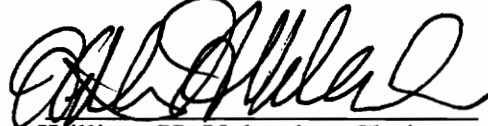# DESIGN OF ANION EXCHANGE CELLULOSE HYDROGEL FOR LARGE PROTEINS

by

Guneet Kumar

Dissertation submitted to the Faculty of the
Virginia Polytechnic Institute and State University
in partial fulfillment of the requirements for the degree of

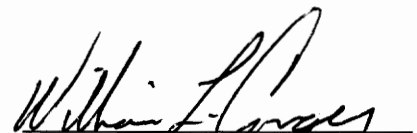Doctor of Philosophy

in

Chemical Engineering
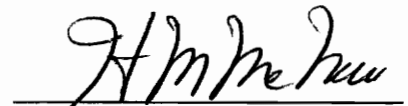
APPROVED:

William H. Velander, Chairman

Richey M. Davis

William L. Conger

Wolfgang G. Glasser

Harold M. McNair

March 1994
Blacksburg, Virginia

Design of Anion Exchange DEAE Cellulose

Hydrogel for Large Proteins

by

Guneet Kumar

William H. Velander, Chairman

Chemical Engineering

(ABSTRACT)

In our previous studies, uncross-linked large diameter cellulose beads were optimized for solids content, bead size, pressure-flow limits, molecular accessibility and performance as an immunosorbent. Here, anion exchange (DEAE) cellulose beads were derivatized by two different procedures (defined as A and B) and the changes in bead morphology were correlated with transport and sorption kinetics. The kinetic characteristics clearly defined a minimum of two different types of protein binding site architecture. DEAE cellulose beads exhibited molecular exclusion of BSA near the edge of the bead in contrast to greater permeability seen in underivatized beads. Thus, accessible BSA binding sites are present only on the surface of the derivatized beads. DEAE cellulose beads derivatized by procedure B gave higher density of DEAE ligand as compared to beads derivatized by procedure A, as well as higher static and dynamic capacity for BSA. Even though DEAE cellulose beads (DP 2070, 450 μm diameter,

derivatized by procedure B) have lower small ion capacity than DEAE cross-linked agarose beads, as well as ¼ the surface area, they exhibit equivalent binding capacity for BSA per volume of support. Thus, DEAE cellulose beads possess more sites per surface area as well as have lower ligand density per BSA site. Furthermore, BSA adsorption sites on DEAE cellulose beads derivatized by procedure B exhibit slow binding kinetics as compared to those derivatized by procedure A and also compared to DEAE cross-linked agarose beads. Thus, the rate limiting step for the adsorption of BSA on DEAE cellulose beads was not diffusion as suggested by the large diameter of the bead. Feasibility studies were performed for process scale applications to fixed and expanded bed anion exchange purification. The large diameter DEAE cellulose beads of this study maybe useful for process scale anion exchange as evident from purification of immunoglobulins from hybridoma cell culture in fixed bed. The balance of large diameter and density of these DEAE cellulose beads enable stable expanded bed purification of proteins such as recombinant human protein C from transgenic porcine whey.

Dedication

This work is dedicated with love and affection, to the memory of my father, who has always been my inspiration.

Acknowledgements

I would like to thank my committee members, Professors Velander, Davis, McNair, Glasser, and Conger for their help and guidance. I would like to extend an additional thanks to Dr. Velander for his support and encouragement that made this work possible. Thanks also go to Willer de Oliveira for the many batches of cellulose beads provided in a timely fashion. I would like to especially thank Tom. E. Glass, and Dan Hahn, for giving me their valuable time to teach me NMR and FTIR instrument techniques.

I would like to take this opportunity to thank my colleagues, Jeffrey Kaster, Anuradha Subramanian, Arthur Degner, and Kevin Van Cott for their support and friendliness which helped make my stay both fruitful and enjoyable.

I would like to extend a special thanks to my mother, without whose help I could not have written my dissertation in time. Thanks to my son, Abhik, for his smiles and

Table of Contents

LIST OF ILLUSTRATIONS

List of Tables

Preface

In previous studies, large cellulose beads have been studied for use as hydrogel supports for protein affinity column chromatography. Affinity chromatography is an expensive purification process, which is used as a high resolution step in the downstream processing of proteins. High resolution processing is usually preceded by low resolution and volume reduction steps. Ion exchange chromatography is an important low cost technique used to achieve volume reduction and low resolution protein purification.

Here we extend the application of large cellulose beads to anion exchange protein purification. In order for it to be effective in low resolution and volume reduction processing, it must have inexpensive and chemically robust ligands such that it can withstand harsh loading and sanitization conditions. Thus packed bed processing of crude starting materials having dilute target solutes are used as one of the first steps in the sequence of various purification procedures.

In Chapter 1 we review the literature and discuss the various theoretical models which address transport and adsorption kinetics. These models are useful for understanding the behavior of anion exchange cellulose beads (presented later in Chapter 4). We summarize models which help to explain both simple and complex adsorption

1

kinetics and the nature of molecule transport in derivatized cellulose beads.

Chapter 2 introduces the requirements of an ideal support for protein purification and also discusses the different commercially available supports. The techniques and example proteins used to study the anion exchange cellulose beads have been detailed in Chapter 3. Novel applications of solid state NMR and FTIR spectra have been used to study the degree of substitution and spatial distribution of the ligand on the bead respectively.

In previous studies, no apparent physical changes in bead morphology were observed when antibody ligands were attached to CNBr derivatized cellulose beads. The cost of the affinity column prevented permeation studies. Hence, it was necessary to assume that the behavior of affinity columns would be similar to that of underivatized beads. However, for anion exchange beads a decrease in bead diameter and increase in solids content was observed upon derivatization. In comparison to affinity beads, the inexpensive nature of anion exchange cellulose beads enabled molecular permeation studies to be carried out. Our studies on the effect of derivatization are presented in Chapter 4.

In Chapters 5 and 6 we report some important applications of the large anion exchange cellulose beads. The performance of anion exchange cellulose beads in

expanded bed configuration has been studied in Chapter 5. Because of the large diameter and associated low pressure drops in columns we have applied DEAE cellulose to the preparative scale purification of monoclonal antibodies and discussed this application in Chapter 6.

Conclusions of the research and recommendations for future follow-up work based on the studies accomplished herein are presented in Chapters 7 and 8.

Chapter 1:

Theoretical Models of Ion Exchange Chromatography of Proteins

Introduction

Ion exchange chromatography has been an important tool for chemical separation since the turn of the century, and it is particularly useful for protein separation. Like many other chromatographies used for protein purification, ion exchange is usually performed with aqueous flow through a fixed particulate bed. Separation is achieved due to the constitutive differences in charge which appear on the surface of the proteins.

Proteins constitute a major fraction of the mass of all organisms and are macromolecules consisting of different amino acids joined by peptide bonds. These biomolecules have a distinct three-dimensional structure with a specific distribution of polar and ionic amino acids on the surface. This three-dimensional structure imparts the biochemical function of proteins. For example, an enzyme maintains a specific spatial configuration of very reactive amino acids resulting in catalytic activity. Hence, the maintenance of the constitutive distribution of exposed surface and internal charge is not only a basis for purification but is important to obtain biological active product upon purification.

A protein's ion exchange properties can be easily changed by pH and salt concentration. Since temperature changes the activity of acids, bases and other salts, temperature can affect the ion exchange properties of proteins. The isoelectric point (pI)

of most proteins range between 4.5 to 6.0 and thus are negatively charged at pH 7 or above. Most proteins tend to adsorb to surfaces which have positively charged residues at pH 7 or above. The tertiary amine of the anion exchange group diethylaminoethane has a pK_a of 9.5 and thus loses its capacity for adsorption of proteins at pH 10.5.

The design of particulate chromatographic supports for proteins has evolved over the past thirty-eight years with gains in the understanding of intraparticle transport phenomena and surface kinetics. Three rate limiting steps have been identified as film transport, intraparticle transport and sorption kinetics. It is noted that both convection and diffusion can contribute to each of the individual transport steps. In most cases intraparticle convection is ignored and transport inside the support is assumed to occur solely by diffusion [1]. The slow nature of diffusion of proteins in aqueous solutions has been a major consideration in the design of protein purification supports so far. For example, Bovine Serum Albumin (BSA) has a relative molecular weight of 66,000 Daltons and has a diffusion coefficient of 6×10^{-7} cm^2 sec^{-1} [2] in water. But the diffusivity and the diffusion coefficient of BSA inside the aqueous intraparticle voids can be much lower in the presence of hydrated support material [3]. Thus, most efforts in support design have strived to minimize the length a protein molecule has to diffuse through to reach the majority of available adsorption sites within the support. In the case of hydrogels, small diameter spheres have frequently been used. In summary, to minimize the diffusion length many theoretical models have emphasized transport as the

rate limiting step.

The use of simple equilibrium expressions between point charges on protein and surfaces have also been used as a guiding rationale for designing ion exchange supports for protein purification. This can be described by a simple equilibrium expression:

$$X^+P^- + Y^-R^+\text{-support} \leftrightarrows P^-R^+\text{-support} + X^+Y^-$$

where: P = Protein

                                         R^+ = Ion exchange ligand

                                         X^+ & Y^- = counter ions

The above equilibrium expression describes gross Le Chatelier responses to the adsorption/desorption of proteins in the presence of low/high salts. However, complex adsorption and elution behavior due to three-dimensional structure of proteins, the presence of different surface charges, and dynamic interaction of multiple charges on the protein with multiple charges on the surface are not well described by simple adsorption isotherms. Very little theoretical knowledge for the dynamic interaction of complex protein structure and support charge architecture has been reported. The adsorption step has been frequently modeled using very simple Langmuir kinetics which are correlated by measurements of adsorption isotherm. Simple Langmuir kinetics are limited in their ability to describe surface site architecture and how it impacts the multipoint adsorption

7

of large macromolecules like proteins. In limited models, as suggested by Velayudhan and Horvath [4], proteins have multivalent attachment between several groups on the surface of the protein and the adsorbent. Brooks and Cramer [5], have included a specifying parameter for multipoint attachment of proteins and steric hindrance of ion exchange sites as part of their Steric Mass Action isotherm model for ion exchangers.

In the next section, we present the salient features of the above models for transport and adsorption phenomena. These models provide some theoretical guiding principles of the material manipulation introduced by our work with the design of protein chromatography using cellulose adsorbents.

Theoretical Models

Models useful for the analysis of anion exchange chromatography are presented in this section while comparison with experimental results are discussed in Chapter 4. The major theories used to describe these models can be divided into two categories: the "plate theory" and the "rate theory" [6]. The former approach seeks to first ignore transport effects and then correlate the difference found from equilibrium sorption predictions with transport effects. The latter introduces directly the sequential transport processes of film and intraparticle diffusion, and subsequent surface sorption kinetics.

"Plate Theory" was first introduced by Martin and Synge [7] as the *equilibrium-stage model*. This model depicts the column as a succession of well mixed equilibrium stages. The adsorbent (stationary phase) is contained within each stage and the carrier liquid (mobile phase) passes continuously through stages in series carrying adsorbate from stage to stage. By assuming that equilibrium is always attained between the two phases in each stage, the process can be treated as a series of ideal mixed-flow "contactors". Assuming a linear equilibrium isotherm and small sample size, the material balance equations obtained can be solved analytically, to yield a chromatogram represented by a Poisson distribution function. The number of equilibrium stages of the column can be determined experimentally from the elution profile resulting from a pulse response. The plate theory analysis is dependent on the characteristic dimensions of the

9

system, the physico-chemical properties of adsorbate and the operating variables governing fluid flow.

The "plate theory" has limited utility in the analysis of zonal solute migration, spreading and resolution between solute zones. Plate theory is less useful in the prediction of eluate patterns resulting from columnwise saturation loading with solute (called "frontal elution"). The shortcomings of the original plate theory were the inability to predict the number of plates, the effective plate height, and the failure to provide information as to how a change in operating conditions could affect the column performance. Much of this limitation is inherently due to the exclusion of transport phenomena. Another limitation of the plate theory is that it is only applicable to linear isotherms, because the plate height is a function of the fixed linear equilibrium constant or partition ratio [8].

"Rate Theory" or the mass balance model is a more rigorous model than the plate theory. In rate theory, no assumptions regarding local equilibrium in the individual "stages" or statistical distribution among phases are made. This model mechanistically separates out the transport of target molecules to the adsorption site from the adsorption step. The transport to the sorption site consists of bulk fluid flow in the column, diffusion through a laminar flow film near the surface of the bead, diffusion into the solid support and then, diffusion through the pore wall surface. The intraparticle diffusion is

treated as slow diffusion within a homogenous liquid phase. Once the protein to be adsorbed is transported to the adsorption site, the adsorption step is treated as a reaction between the ion-exchange ligand and the target protein with the release of the counter ions. The elution of the protein from the column is assumed to follow the reverse sequence. A schematic representation of this model is given in Figure 1.

Based upon these assumptions, the rate theory model can be described with the equations governing conservation of mass (species continuity equation), and the constitutive equations describing Fickian diffusion and adsorption. Due to the complexities of fluid flow in a packed bed, the fluid mechanics in the void volume are constrained by a dispersion coefficient rather than exact determination of the velocity profile by the equation of motion which govern conservation of momentum. The species mass balance over the column gives a form of the continuity equation for the packed bed:

$$D_z \frac{\delta^2 C}{\delta z^2} - v \frac{\delta C}{\delta z} - R = \frac{\delta C}{\delta t} \tag{1}$$

where: D_z = axial dispersion coefficient

C = concentration of solute in the bulk fluid

v = superficial liquid velocity

R = rate of interface mass transfer

The diversity of the existing rate theory models in the literature is attributed to the formulation of the R term in Eq. (1). The rate determining step may be attributed to one or a combination of the following resistances: film diffusion resistance, pore diffusion or particle diffusion resistance, and surface reaction or adsorption resistance.

Film Diffusion Rate Controlling: The film diffusion step can become rate controlling in cases where the particle size is small or the intraparticle effective diffusivity is large. Under film diffusion control, the concentration inside the particle is constant and the mass transfer rate is modelled as follows:

$$R = K_f a \ (C - C_i) \tag{2}$$

where: K_f = laminar film mass transfer coefficient

a = interface area per unit interstitial void volume

C_i = concentration inside the particle

Eqs. (1) and (2), with the assumptions of plug flow and linear isotherm, have been solved by Anzelius [9], Schumann [10], and Furnas [11] and used for analysis of solute frontal elution patterns.

Particle Diffusion Resistance Rate Controlling: Much of the literature in the area of fixed-bed adsorption belongs to this category. The adsorbent particle is considered to be porous by nature and the rate equation is constructed for pore diffusion resistance. Conservation of species mass states that the overall rate of change of the solute concentration in the support material is equal to the flux of solute from the bulk fluid into the support material. The intraparticle material balance is as follows:

$$\frac{\delta C_i}{\delta t} + \frac{\rho_P}{\epsilon_i} \frac{\delta q}{\delta t} = D_P \nabla^2 C_i \tag{3}$$

where: D_P = effective intraparticle diffusivity

ρ_P = density of packing material

ϵ_i = intraparticle void fraction

q = concentration of sorbate on the stationary phase

The rate equation can be expressed by the Fickian constitutive equation and is as follows:

$$R = -a\ \epsilon_i\ D_P\ \frac{\delta C_i}{\delta r}\bigg|_{r=r_o} \tag{4}$$

where: r_s = particle radius

Analytical solution of porous particle models have mostly been obtained for linear isotherm cases. Film and pore resistance was accounted for by Kasten *et al* [12], as well as plug flow assumption was made. Kubin [13] and Kucera [14] used the moment theory for the analysis of solute elution profiles of anion exchange chromatography.

The Surface Adsorption Rate Controlling: In this case, the surface reaction rate is slow compared to the mass transfer rate so that the concentration is uniform throughout the aqueous void of particles and the rate function assumes the form of a kinetic rate equation as follows:

$$R = k_a C_i (Q_{max} - q) - k_d q \tag{5}$$

where: Q_{max} = maximum sorbate concentration

k_a = rate of adsorption

k_d = rate of desorption

Considering proper initial boundary conditions and assuming no dispersion effects, Eqs. (1) and (5) have been solved by Thomas [15] and is called the Thomas' solution.

The approximate solutions for frontal and elution profiles mentioned above can be used to identify limitations caused by either film diffusion, intraparticle diffusion or

14

surface adsorption being the rate determining step. These approximate solutions have been refined over time, as advances in numerical analysis have permitted. For example, Lee *et al* [16] have simulated the effluent histories of multicomponent ion exchange systems using a rate equation model which accounts for axial dispersion, film mass transfer, intraparticle diffusion, size exclusion and nonlinear isotherms.

We now introduce the concepts of equilibrium adsorption and the respective isotherm behavior as a function of increasing concentration of protein solution. Several forms of constitutive isotherms will be discussed.

Expressions which describe Isothermal Adsorption

The complexity of experiments describing surface adsorption for ion exchange chromatography has increased, from simple adsorption equilibrium isotherms to detailed kinetic models which incorporate information about the tertiary conformation of the protein structure and how it interacts with the surface. This schematic is shown in Figure 2. While Langmuir adsorption isotherm is very often used due to its simplicity, the more advanced concept of multipoint attachment has been put forth by Velayudhun and Horvath [4] for its use to describe the equilibrium between protein and ion exchangers. Further advancement of this approach of multivalent attachment of proteins to the ion exchanger, has been made by defining a steric factor for proteins by Brooks and Cramer

[5]. This model has been termed as Steric Mass Action Isotherm.

The equilibrium relationship between the concentration of the biomolecules between the mobile phase and the stationary phase can be represented by an adsorption isotherm which has a general form:

$$q_i = f (c_1, c_2, \ldots\ldots\ldots, c_n) \qquad i = 1, 2, \ldots\ldots, n. \qquad (6)$$

where: q_i = concentration of sorbate in the stationary phase

c_i = concentration of the sorbate in the mobile phase

Langmuir Adsorption Isotherm: Many isotherms have been described in the literature [17], but the simplest functional form for single and multicomponent adsorption in a wide concentration range is the Langmuir adsorption isotherm and has been used in the models described by Helfferich [18,19]. At equilibrium the isotherm is described as follows:

$$q_i = \frac{a_i \, c_i}{1 + \sum_{j=1}^{n} b_j c_j} \qquad\qquad i = 1,2,......n. \qquad\qquad (7)$$

where the parameters a_i and b_i are derived from the respective single component isotherms. For single component adsorption isotherm the following equation is usually used:

$$q = \frac{Q_{max} \, K_L \, c}{1 + K_L \, c} \qquad\qquad (8)$$

where: K_L =   adsorption equilibrium constant

The adsorption equilibrium constant is defined as follows:

$$K_L = \frac{k_a}{k_d} \qquad\qquad (9)$$

17

Velayudhan and Horvath [4] have recently pointed out that the adsorption of the three dimensional nature of the protein to ion exchangers indicates that multivalent attachment occurs between several functional groups on the protein surface with the adsorbent. The drawbacks of Langmuir isotherm are: the assumption that adsorption of the protein takes place at individual and independent sites, and its inability to account for the change in protein retention with change in salt concentration. Multivalent adsorption has been demonstrated by several authors in different systems including Whitley *et al* [20] and Regnier *et al* [21].

Steric Mass-Action Isotherm: The steric mass-action (SMA) isotherm assumes not only multipoint nature of protein binding, but also the steric hindrance of salt counter-ions caused by the binding of these large macromolecules. These salt counter-ions are subsequently unavailable for exchange with other protein molecules in the mobile phase. The advantage of the SMA isotherm is that, once the proteins equilibrium parameters are determined the SMA isotherm at any mobile phase salt concentration can be constructed, whereas equilibrium parameters at each mobile phase salt concentration need to be measured for Langmuir isotherm.

Kinetic Model

For chromatographic processes it is usually assumed that the rate of adsorption

18

and desorption are fast enough that equilibrium is achieved between the solute in the mobile and stationary phase. The rate of adsorption of proteins to ion exchangers being a rate limiting step has been recently acknowledged by various authors, including Whitley *et al* [22] who have used the VErsatile Reaction SEparation in Liquid Chromatography (VERSE-LC) to verify their model with experimental data of a Lysozyme breakthrough curve on S-Sepharose FF. The VERSE model accounts for convection, axial dispersion, film diffusion, intraparticle diffusion and nonequilibrium adsorption/desorption kinetics. They have also perturbed the rate of adsorption/desorption and studied the effects on the breakthrough curves and elution profiles as the kinetics decreased.

The Thomas solution, has been extended for proteins by Chase [23] to predict the change in breakthrough curves by changing operational parameters, one at a time and keeping all others constant. They also see the breakthrough curve sharpening as the rate of adsorption is increased. This is achieved easily in a chromatographic system by increasing the temperature, as temperature has a minimal effect on film and intraparticle diffusion.

Summary

From a theoretical perspective, the design of an ion exchanger for preparative chromatography for protein separation requires knowledge of equilibrium ("static") and

dynamic capacity of adsorption of proteins by the hydrogels. We focus upon material manipulation which yield changes in both the static and dynamic adsorption behavior of proteins on DEAE cellulose. Thus, our determinations of "equilibrium behavior" uses experimental time frames which exceed by an order of magnitude asymptotic approach to steady state predicted by the characteristic times for unsteady diffusional transport [24]. The batch adsorption of proteins at long times are compared with those obtained from dynamic loadings of protein solutes (at breakthrough of inlet solute concentration at column exit) at fluid velocities which result in short particle contacting times.

References

1. Afeyan N.B., Fulton S.P., Gordon N.F., Mazaroff I., Varady L., and Regnier F.E., *Bio/technology*, (1990) **8**: 203-206.

2. *Mass Transfer Operations*, 3rd ed., Treybal R.E., McGraw-Hill, NY, (1980) pp.

3. Skidmore G.L., Horstmann B.J., and Chase H.A., *J. Chromatogr.*, (1990) **498**: 113-128.

4. Velayudhan A., and Horvath Cs., *J. Chromatogr.*, (1988) **443**: 13-29.

5. Brooks C.A., and Cramer S.M., *AICHE*, (1992) **38 (12)**: 1969-1978.

6. Yang C.-M., and Tsao G.T., *Adv. Biochem. Eng.*, (1982) **25**: 1-18.

7. Martin A.J.P., and Synge R.L.M., *Biochem. J.*, (1941) **35**: 1358.

8. van Deemter J.J., Zuiderweg F.J., and Klinkenberg A., *Chem. Eng. Sci.*, (1956) **5**: 271.

9. Anzelius A.Z., *Angew. Math. und Mech.*, (1926) **6**: 291.

10. Schumann T.E.W., *J. Franklin Inst.*, (1929) **208**: 405.

11. Furnas C.C., *Trans. Am. Inst. Chem. Engr.*, (1930) **24**: 142.

12. Kasten P.R., Lapidus L., and Amundson N.R., *J. Phys. Chem.*, (1952) **56**: 683.

13. Kubin M., *Collect. Czech. Chem. Commun.*, (1965) **30**: 1104.

14. Kucera E., *J. Chromatogr.*, (1965) **19**: 237.

15. Thomas H.C., *J. Am. Chem. Soc.*, (1944) **66**: 1664.

16. Lee C.K., Yu Q., Kim S.U., and Wang N.-H.L., *J. Chromatogr.*, (1989) **484**: 29-59.

17. Ruthven D.M., *Principles of Adsorption and Adsorption Processes,* John Wiley, New York, (1984).

18. Helfferich F.G., *Ion Exchange,* Mcgraw Hill, New York, (1962).

19. Helfferich F.G., and Klein G., *Multicomponent Chromatography Theory of Interference*, Marcel Dekker, NY, (1970).

20. Whitley R.D., Wachter R., Liu F., and Wang N.-H.L., *J. Chromatogr.*, (1989) **465**: 137-156.

21. Regnier F.E., and Marzaroff I., *Biotechnol. Progress*, (1987) **3**: 22.

22. Whitley R.D., Van Cott K.E., and Wang N.-H.L., *Ind. Eng. Chem. Res.*, (1993) **32**: 149-159.

23. Chase H.A., *J. Chromatogr.*, (1984) **297**: 179.

24. Kaster J.A., Ph.D dissertation.
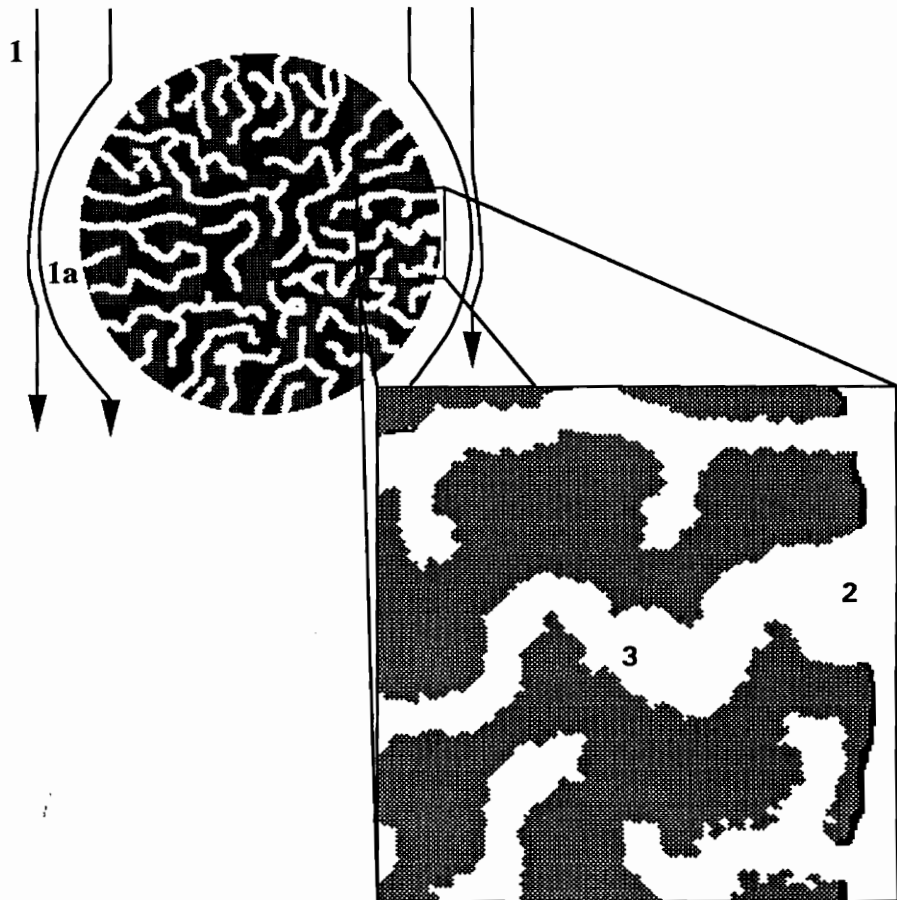
Step 1. Convection past the particle
Step 1a. Diffusion through laminar film
Step 2. Diffusion into the particle
Step 3. Adsorption (simple sorption, ion exchange
                    sorption, etc.)

Figure 1: Classical model for adsorption chromatography

a.
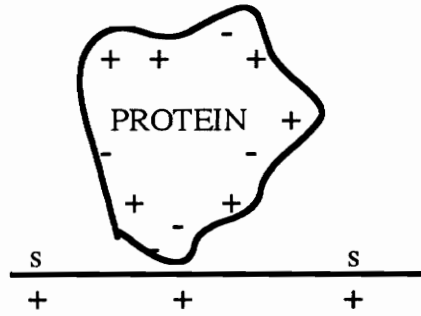
b.
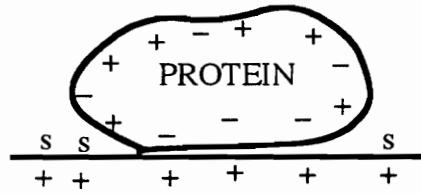
c.
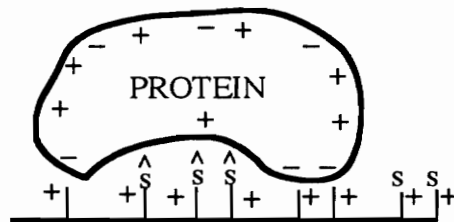
$\hat{s}$: Salt counter-ion not available for ion exchange

s : Salt counter-ion available for ion exchange

Figure 2: Protein adsorption on the surface of a hydrogel
a. Adsorption as described by Langmuir isotherm
b. Multipoint adsorption
c. Adsorption as described by SMA isotherm

Chapter 2:

Material Aspects of Anion Exchange Hydrogels

Introduction

Previous studies showed that cellulose based immunoaffinity sorbent could be optimized by "material design approach". The "material design approach" emphasizes molecular accessibility and fluid flow conditions. It scales the particle size optimization using the theoretical characteristic time of intraparticle diffusion [1] with the pressure drop predicted by the particle size [2]. We here extend those previous studies of cellulose beads for affinity chromatography to anion exchange chromatography. While our studies emphasize on anion exchange of proteins, the applicability of our design can be extended to cation exchange. Several practical design questions sought in our studies are:

1. Does a cellulose hydrogel at low solids contents really have a well defined porous structure or in what way does it approach an aqueous continuum ?

2. To what extent does hydrogel accessiblity change in the presence of convection?

3. Does intraparticle convection play a role in intraparticle transport ?

4. Does hydrodynamic strength of a hydrogel change after derivatization ?

5. Does the interior aqueous structure of the cellulose change after derivatization ?

6. Can transport or adsorption kinetics be identified as the rate limiting step in a column mode operation for a given protein ?

7. What is the stoichiometric ratio of the DEAE ligand to BSA for cellulose beads

versus other adsorbents ?

8.   How does anion ion exchange ligand density affect site architecture on cellulose hydrogels for a given protein like BSA ?

9.   Does degree of polymerization impact on anion exchange capacity for proteins ?

10.   Under what conditions does simple adsorption describe the adsorption of a particular protein and the hydrogel in column mode operation ?

11.   Can a anion exchange cellulose hydrogel be designed to manipulate steric hindrance and adsorption kinetics ?

We have discussed important theoretical views of anion exchange chromatography of proteins in Chapter 1 and will here discuss material aspects. These material aspects include ion exchange moieties, chemistry of derivatization and hydrogel supports.

Ion Exchange Moieties

On the material level, the presence of a charged group on a gel imparts the property of an ion exchanger [3]. There are different moieties which can be attached on the gel as shown in Table 1. This gives a variety of ion exchangers: strong, intermediate, and weak. The strength of the ion exchanger is measured as the extent of the variation of ionization with pH. For weak ion exchangers like diethylaminoethyl and

carboxymethyl, the degree of dissociation is sensitive to change in pH. Strong ion exchangers like sulfonic and quaternary amino groups are completely ionized over a wide range of pH.

TABLE 1: Functional Groups for Ion Exchangers

ANION EXCHANGERS	FUNCTIONAL GROUP
Aminoethyl (AE-)	$-OCH_2CH_2NH_3^+$
Diethylaminoethyl (DEAE-)	$-OCH_2CH_2N^+H\ (CH_2CH_3)_2$
Quaternary aminoethyl (QAE-)	$-OCH_2CH_2N^+(C_2H_5)_2CH_2CH(OH)CH_3$
CATION EXCHANGERS	
Carboxymethyl (CM-)	$-OCH_2COO^-$
Phospho	$-PO_4H_2^-$
Sulphopropyl (SP-)	$-CH_2CH_2CH_2SO_3^-$

Chemistry of Derivatization

Any physical form of cellulose can be easily derivatized to produce an ion exchange matrix, as it possesses primary hydroxyl groups. Attachment of the Diethylaminoethyl (DEAE-) or the Carboxymethyl (CM-) groups is carried out by the classical Williamson ether synthesis. The preparation of diethylaminoethyl cellulose was first reported by Hartmann who used cotton as the source of cellulose [4]. Its extensive use as an ion exchange matrix for biological molecules is largely due to the work of Sober, *et al*, who used purified wood pulp as their starting material [5].

For most purposes only a small proportion of the hydroxyl groups need to be converted; in fact, overderivatization of cellulose with diethylaminoethyl groups makes the ion exchanger soluble in water [6]. The optimum conditions as determined by Kalman *et al* were used to modify large cellulose beads [7]. Another procedure of derivatization i.e. keeping the reagent concentration constant but changing the temperature and length of reaction time, was used to improve the degree of substitution on the beads.

Type of Supports

As ion exchange chromatography of proteins has matured, the need for better chromatographic supports has become apparent. The first experiments were performed in the early fifties with resin ion exchangers such as Amberlite IRC-50 for the fractionation of low molecular weight proteins such as ribonuclease [8]. The main drawbacks of resins as matrices for protein chromatography were recognized as hydrophobicity and low accessibility to the support interior. To overcome this problem cellulose ion exchangers were introduced by Peterson and Sober [9]. In these early studies, cellulose was used in a fibrous form which gave rise to poor flow characteristics and high pressure drop across the column [10].

Thus the properties required by an ion exchange matrix can be summed up as follows:

- Hydrophilicity
- Macroporosity and Permeability
- Rigidity and Physical shape
- Inertness (minimal non-specific adsorption)
- Insolubility and Chemical stability
- Ease of Derivatization
- Cost and Reusability

Traditionally the most important matrix for ion exchange chromatography is cellulose substituted with either diethylaminoethyl (DEAE-) or carboxymethyl (CM-) groups. Other matrices which are also popular and commercially available are: cross-linked dextran, cross-linked agarose and semisynthetic acrylic copolymers. Novel matrices can also be found in the literature, for example, kieselguhr-agarose composite [11], hollow fibres [12], etcetera. Kieselguhr-agarose composite is made of porous kieselguhr beads which have been partially filled with derivatized cross-linked agarose.

Beaded Cellulose Supports

The physical form of the cellulose ion exchanger is important, especially in large scale operations. In addition to the fibrous form of cellulose ion exchangers, microgranular and beaded form of cellulose ion exchangers are also available commercially. The advantage of beaded cellulose is that it has an acceptable geometric shape in that spheres pack well in a column and can have more desirable flow properties than amorphous materials. It also has superior behavior in the regeneration step, whereas the microgranular cellulose has a tendency to generate substantial amount of fines which have to be removed by repeated decantation. The beaded form of cellulose ion exchanger is commercially available under the name of DEAE Sephacel sold by Pharmacia Fine Chemicals. These beads have a diameter of 40-160 μm, 6-7% solids content and are cross-linked to give mechanical strength. Anion exchange cellulose in the microgranular form is sold by Whatman Biochemicals Ltd. under the name of DE52.

Cellulose is a natural occuring polymer of β-1,4 linked glucose units. Cellulose is structurally strong and does not tend to crush unlike agaroses and dextrans. Several methods of producing cellulose beads have been developed since the first successful beading procedure was discovered by O'Neill and Reichardts [13]. Cellulose ion exchangers were prepared in the optimal bead form by Determen *et al* in 1969 [14]. The commercially available beaded cellulose supports crush at lower superficial velocities as compared to fast flow cross-linked agarose matrices, and also tend to have a molecular sieving effect on large proteins. Large cellulose beads have been optimized by Kaster *et al* [15], such that the matrix has low pressure drop through the column, good mechanical or hydrodynamic strength, as well as permeability for affinity chromatography of large protein molecules. For these cellulose beads, the cellulose has been dissolved in DMAC/LiCl and regenerated into beads by atomization [16]. Affinity columns made from CNBr activated cellulose beads, were assumed to have the same properties as underivatized beads, as the high cost of antibodies prevented any solids content, pressure drop and permeation studies. The window describing the limitations for the solids content of the cellulose bead having these properties is shown in Figure 1. This material window defined the salient principles of the "material design approach". This window appears as a shaded section of the plot bounded by molecular accessibity and the flow rate at which bed crushing occurs in a 15 cm bed. These beads have been derivatized and characterized as described in Chapter 3 for purposes of using them as anion exchangers for large proteins. Our work focusses on a more detailed study of

changes in cellulose beads upon derivatization.

Cross-linked Agarose

Agarose is a polymer of d-galactose and 3,6-anhydro-l-galactose that is produced by sea weed. Agarose is mechanically weak because adjacent polymer chains interact weakly due to steric hinderance and reduced hydrogen bonding. Agarose can be cross-linked with epichlorohydrin, bisepoxide, or divinyl sulphone to produce mechanically stronger cross-linked agarose beads [17,18].

Cross-linked agarose beads are currently the standard chromatography support for laboratory and industrial scale separations. The beads have an open structure, thus having molecular exclusion limits greater than one million daltons. This allows the interior and exterior of the bead to be used for separations of large biomolecules. Cross-linked agarose matrices are derivatized with charged groups like Diethylaminoethyl (DEAE-) and carboxymethyl (CM-) to give ion exchangers, commercially known as DEAE-Sepharose CL-6B and CM-Sepharose CL-6B. These beads are marketed by Pharmacia Fine Chemicals. Among the commercially available ion exchange matrices, cross-linked agarose beads are considered highly rigid, with excellent bed packing qualities like high flow rates and volume stability during changes in ionic strength and pH of different buffers.

Cross-linked Dextran

Dextrans are branched chain polymers of glucose that are normally cross-linked with 1-chloro-2,3-epoxypropane to enhance mechanical strength. Dextran are mechanically less sturdy than agaroses especially in their highly porous forms [19]. Ion exchangers are produced easily because of the many available hydroxyl groups on the polymer. The ion exchange matrices are known commercially as Sephadex. Pharmacia Fine Chemicals has two products, namely the Sephadex G-50 and Sephadex G-25. Sephadex G-50 is normally preferred for protein chromatography, because of their higher porosity and capacity, but have low rigidity and a tendency to swell and shrink when exposed to varying ionic strength of buffers.

Semisynthetic Copolymers

A new kind of matrix available in the market is the Trisacryl M, which has been derivatized to give ion exchange matrices, namely the DEAE Trisacryl M and the CM Trisacryl M. This matrix has an open structure and has been shown to have very similar properties to cross-linked agarose but is based on acrylic copolymers. We do not use this material as reference material but instead compare cross-linked agarose to cellulose beads.

References

1.   Kaster J. A., Oliviera W.de., Glasser W.G., and Velander W.H., *J. Chromatogr.*, (1993) **648**: 79-90.

2.   *Mass Transfer Operations*, 3rd. Ed., Treybal R.E., Mcgraw-Hill, NY, (1980) pp. 200.

3.   *Ion exchange Chromatography, Principles and Methods,* Pharmacia Fine Chemicals.

4.   Hartmann M., *U.S. Patent No.* 1,777,970 (1930).

5.   Sober H.A., Gutter F.J., Wyckoff M.M., and Peterson E.A., *J. Am. Chem. Soc.*, (1956) **78**: 756.

6.   Glasser W.G., intercommunication.

7.   Kalman F., Borsa J., Kemeny S., and Rusznak I., *Colloid and Polymer Science,* (1988) **266**: 716-720.

8.   Hirs C.W.H., Stein W.S., and Moore S., *J. Am. Chem. Soc.*, (1951) **73**: 1893.

9.   Peterson E.A., and Sober H.A., *J. Am. Chem. Soc.*, (1956) **78**: 751.

10. James K., and Stanworth D. R., *J. Chromatogr.* (1964) **15**:324-335.

11. Goward C.R., Stevens G.B., Collins I.J., Wilkinson I.R., and Scawen M.D., *Enzyme Microb. Technol.*, (1989) **11**: 810-814.

12. Tsuei A.C.R., and Yang V.C., *Polymer Preprints, Division of Polymer Chemistry, American Chemical Society*, (1990) **30(1)**: 238-239.

13. O'Neill J.J.Jr., Reichardt R., and Reichardt E.P., *U.S. Patent No.* 2,543,928 (1951).

14. Determan H., Meyer N., and Wieland T., *Nature*, (1969), **223**: 499-500.

15. Velander W.H., Kaster J.A., and Glasser W.G., *U.S. Pat. Appl.,* 07/496314.

16. Kaster J. A., Oliviera W.de., Glasser W.G., and Velander W.H., *J. Chromatogr.,* (1993) **648**: 79-90.

17. Porath J., Janson J.-C., and Laas T., *Journal of Chromatography,* (1971) **60**: 167-177.

18. Porath J., Laas T., and Janson J.-C., *Journal of Chromatography,* (1975) **103**: 49-62.

19. *Affinity Chromatography: A Practical Approach,* Dean P.D.G., Johnson W.S., and Middle F.A., (Eds.), IRL Press, Washington D.C. (1985).
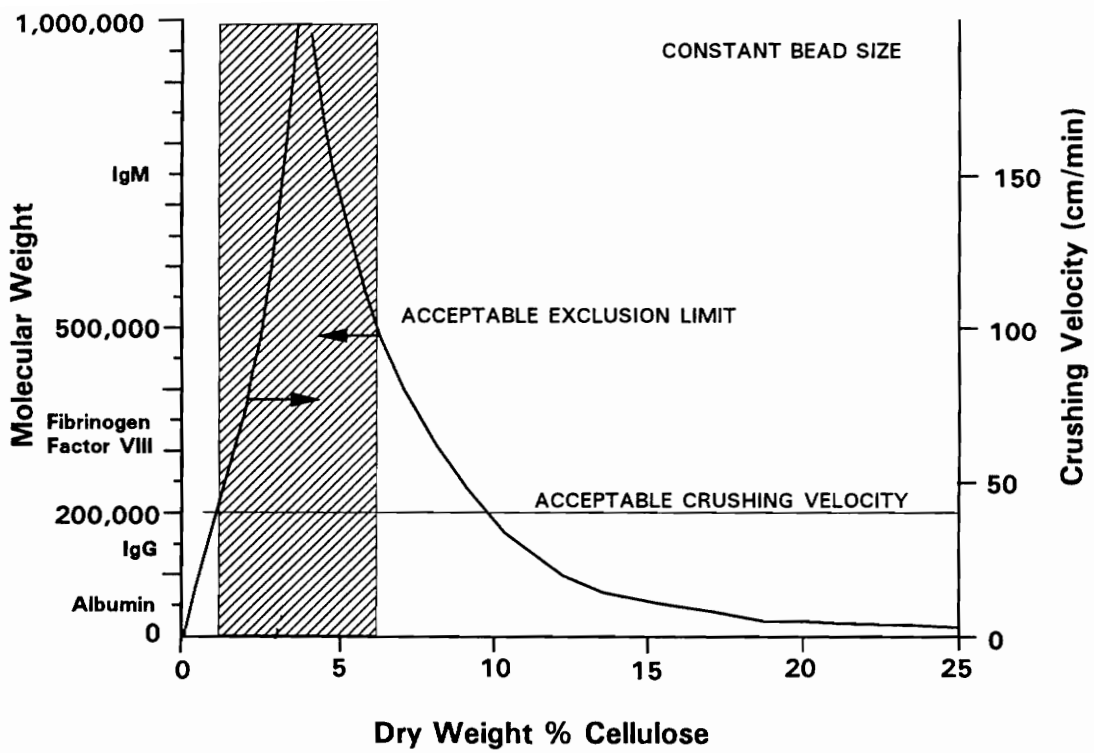
Figure 1: Design characteristics for cellulose supports

Chapter 3:

Techniques for Characterizing Derivatized Hydrogels

Introduction

We now introduce several techniques for studying changes in material upon derivatization. Molecular accessibility has been studied using gel permeation chromatography at nonbinding conditions. Degree of substitution of anion exchange ligand is determined by solid state Nuclear Magnetic Resonance (NMR) spectroscopy. Spatial distribution of anion exchange ligand is determined by Fourier Transform Infra Red spectroscopy (FTIR).

Gel Permeation Chromatography

As discussed before chromatography performance is affected by transport phenomena and the kinetics of surface adsorption. The technique of gel permeation chromatography can be used to obtain information on the nature of transport phenomena which occurs in the hydrogel [1]. The most important feature is the applicability to matrices in the wet state, to which conventional porosimetry cannot be applied.

Gel permeation chromatography is a technique which predominantly separates biomolecules based on their molecular weight, although nonspecific adsorption phenomena can always play a role. The separation mechanism is governed in general, by the relation between the molecular size of solute and the pore size distribution of

39

packed gel. For long column residence times Casassa [2,3] and Giddings *et al* [4] have shown that equilibrium partitioning of solute between the inside and outside of gel phase is a dominant mechanism for gel permeation chromatography.

A theoretical or equivalent pore size is often assumed to exist in hydrogels. Determination of the effective pore size distribution in the hydrogel, is done by studying the resultant elution pattern of probe solutes introduced to a column. Once the void volume (column volume not occupied by the hydrogel), elution volume (volume of solute leaving the column), and the volume of the bed are determined, the fraction of the volume of the gel that is accessible for a particular solute can then be deduced [5] and hence the characteristics of the transport phenomena.

However, for the present research, studies were performed to determine the structural change of the gel after derivatization, as well as the change of penetration depth of the protein in the gel at different superficial velocities. Bovine Serum Albumin (BSA) was chosen as the probe solute.

Evaluation of Derivatization by NMR

Until a few years ago, solid-state nuclear magnetic resonance (NMR) yielded spectra containing broad lines only. Since the introduction of CP/MAS (cross

polarization, magic angle spin) NMR spectroscopy has provided a method which gives narrow nuclear resonance lines from a solid-state specimen as well. This yields a ^{13}C-NMR spectra, the signals of which can be correlated with a chemical structure. Not only can the chemical structure be determined by this approach but quantitation, and comparison of quantitation of different samples with the same structure can be done with a high degree of accuracy [6]. Here we have used solid state NMR spectroscopy to quantitate the degree of substitution on DEAE cellulose beads.

In the solid state, the orientation dependence of the chemical shift (chemical shift anisotropy, CSA) is generally not averaged to δ_{iso} because large-amplitude, rapid motion is absent. The geometric relationship in which the orientation dependence of the chemical shift tensor is embodied contains the factor $(1-3 \cos^2 \theta)$, where θ represents the angle between the magnetic field direction and an axis of the atom-based principal axis system of the chemical shift tensor. The geometric factor offers an alternative averaging scheme to the random Brownian motion of solutions. If the sample is rotated rapidly about an axis inclined at an angle β to the magnetic field direction, the CSA will be scaled by the factor $(1-3 \cos^2 \beta)$. At $\beta = 54.7^0$, this factor becomes zero and the broadening effect of the CSA vanishes, hence the term "magic angle spin" [7].

In most solid samples, a given nucleus will experience dipolar interactions with several neighboring nuclei, resulting in line broadening by several tens of kHz. MAS

at routine speeds is usually ineffective at removing the ^{13}C-^{1}H dipolar couplings, as the MAS rate would have to be much faster than the ^{1}H-^{1}H dipolar coupling frequency. However, the protons can be decoupled from each other and from the carbons with a strong radio frequency field. The strong ^{13}C-^{1}H dipolar coupling is turned to advantage in the cross polarization technique, where a transfer of magnetization from ^{1}H to ^{13}C takes place. To achieve the transfer of magnetization, a "Hartmann-Hahn contact" is made i.e. the simultaneous application of two radio-frequency fields in resonance with ^{13}C and ^{1}H with the same frequency as the nuclei in the rotating coordinate system. The reason for using cross polarization for enhancing the ^{13}C signal resides in the ratio of the gyromagnetic ratios $\gamma_H / \gamma_C \approx 4$. Moreover it allows signal averaging to be carried out with repetition rates governed by the much faster ^{1}H relaxation times (T_{1H}) rather than by the ^{13}C relaxation times (T_{1C}). In favorable circumstances it is possible to achieve an enhancement factor of 20 in the signal to noise ratio.

In the CP (cross polarization) experiment, the spin locked ^{1}H magnetization decays toward zero during the CP or "contact" time (τ) with a time constant of $T_{1\rho H}$. The ^{13}C CP intensity grows during the CP period with an exponential time constant, T_{CH}, and, at sufficiently long contact time, decays with a time constant of $T_{1\rho H}$. A sample often contains carbons with various strengths of ^{13}C-^{1}H dipolar coupling and T_{CH} is dependent on the ^{13}C-^{1}H dipolar coupling.

In single phase systems with adequate dipole-dipole interaction between the protons, the signal intensity, $I(\tau)$, passes through a maximum and then falls off exponentially with increasing contact time. For quantitative assays based on ^{13}C CP/ MAS, T_{CH} and $T_{1\rho H}$ need to be determined for each peak of interest. This is achieved by plotting the ^{13}C intensity (I) of the peak versus contact time (τ), and curve fitting the data iteratively as shown in Figure 1 by using the following equation:

$$I(\tau) = I_0 \left[\frac{T_{1\rho H}}{T_{1\rho H} - T_{CH}}\right] \times \left[\exp(\frac{-\tau}{T_{1\rho H}}) - \exp(\frac{-\tau}{T_{CH}})\right] \tag{1}$$

I_0 is the "corrected" ^{13}C intensity, the signal intensity which would be obtained if CP was infinitely rapid and $T_{1\rho H}$ decay was infinitely slow. Once the I_0 of each peak of interest has been determined, the ratio of the abundance of the carbon atoms can be found as it is directly proportional to the ratios of the signal intensity.

Spatial Evaluation of Derivatization by FTIR

The reflection infrared technique was used to determine the $N-C$ stretching on the cross-section of a DEAE cellulose bead using a FTIR spectrometer, which gives information of spatial derivatization on the bead. Spectra between 990-1220 cm^{-1} wavenumber were scanned as a weak N-C stretching adsorption band in this region

usually shows the presence of a tertiary amine.

Infrared spectroscopy (IR) has been widely used to identify molecular structures present at the surface of catalysts and other surfaces. In most instances, dispersive spectrometers, utilizing either a prism or a grating as the dispersing element have proven to be satisfactory for such studies. Limitations of such instruments have been encountered, especially for samples exhibiting weak adsorption bands. The introduction of commercial Fourier Transform (FT) spectrometers in the early 1960's has made it possible, in part, to overcome the limitations associated with dispersive instruments and has helped to broaden the scope of problems amenable to investigation by infrared spectroscopy. FT spectrometers can offer significantly superior performance over grating spectrometers. The optical advantage of an FT spectrometer is the higher signal to noise ratio for an equivalent data acquisition time [8].

Transmission infrared spectroscopy is one of the simplest and widely used methods to use experimentally but is not sufficiently sensitive for detecting flat thin films on a smooth surface. The reflection infrared techniques on the other hand are sufficiently sensitive for flat monolayers [9]. Some examples of thin and thick films can be found in the literature [10,11].

Proteins useful for Probing Anion Exchange Properties of DEAE Cellulose

Bovine Serum Albumin

Bovine serum albumin (BSA) was chosen as a reference protein for the study of capacity of DEAE cellulose beads. It is a cheap, commercially available protein and the data obtained can be easily compared with data found in the literature, as BSA has been used by many other researchers [12,13]. The molecular weight is 66,000 daltons, which size range is typically found for many therapeutic proteins. The isoelectric point of BSA is 4.9. Thus at pH 7.0 the molecule is strongly anionic and binds easily to DEAE matrices.

The three dimensional structure of serum albumin has not yet been determined, but possesses at least two folded domains, and has a high α helix content. The molecule consists of two globular parts which are firmly associated at neutral pH but can rotate more or less independently at acidic conditions [14,15]. It has a total of 32 glutamic and aspartic amino acid which give the negative charge to the molecule at a pH higher than its isoelectric point.

Albumin is a cross-linked transporter containing 21 intrachain bridges. It is known for its ability to bind diversified substances such as fatty acids, bilirubin,

tryptophan, various metal ions, some hormones and numerous drugs. As a therapeutic, albumin is primarily used as an electrolyte replacer to maintain proper osmolarity [16,17]. Because albumin is a key binding protein it can be expected to generally exert specific interactions with charged molecules.

Protein C

We present here a discussion of the structure and properties of Protein C which has uses as a therapeutic protein. Protein C is a vitamin K dependent coagulation regulating protein. It is a serine protease anticoagulant in the clotting cascade. In the human body it works to stop the conversion of prothrombin to thrombin by inactivating Factors Va and VIIIa. The molecular weight of the protein is 62,000 and it consists of two chains. The heavy chain has a molecular weight of 42,000, and the light chain has a molecular weight of 20,000. The two chains are joined by a single disulfide bond. Protein C is approximately 23% carbohydrates by weight [18,19]. The isoelectric point of Protein C ranges from 4.4-4.8. Thus at pH 7.0 the protein is strongly anionic and can adsorb to DEAE matrices. The "gla" region of the molecule which have negatively charged residues is not available in the presence of Ca^{2+}, Mg^{2+}, and Zn^{2+} ions. Thus Protein C can be eluted at mild conditions in the presence of 25 mM Ca^{2+} ions.

Protein C is present in human plasma at a concentration of 4 μg/ml [20]. Protein C has been produced in the milk of transgenic swine at greater than 100 μg/ml

[21]. The abundance of the recombinant human protein C has facilitated its use as a feedstock for examining the performance of ion exchange cellulose beads in an expanded bed presented herein.

Monoclonal Antibodies

We here present some discussion on the structure and manufacturing process of monoclonal antibodies, which have uses in purification and disease therapy. They are routinely isolated from myelomian cell culture and ascites fluid by a sequence of precipitation and ion exchange chromatography.

Antibodies belong to a group of proteins called "Immunoglobulins". They are all made up of a common structural unit comprising two heavy and two light chains. The heavy chain constant region determines the class and subclass of the immunoglobulin, whilst the light chains (either kappa or lambda) are common to all classes. The variable regions of both heavy and light chains determine the antigen binding specificity [22].

Immunoglobulins are made *in vivo* as a response to the presence of a foreign substance and specifically by disease fighting cells called lymphocytes. Certain chemical moieties of the foreign substance are recognized by the immune system; a given cell line of lymphocytes is programmed by the immune system to recognize a given chemical moiety. Thus, the immune system strives to produce as many lymphocyte cell lines (a

47

single or monoclonal lymphocyte subtype) as there are recognizable chemical moieties contained within the foreign substance. Together these differently programmed lymphocytes produce a (polyclonal) mixture of immunoglobulin which all recognize some part of the foreign substance.

For example, when a foreign substance, such as a protein, is introduced into the body of a mammal such as a mouse, a variety of differently programmed lymphocytes are produced each making an antibody which will recognize a specific chemical moiety within the target protein. These lymphocytes can be harvested from the mouse, but not stably grown in culture. To introduce culturing stability, the unregulated growth of a cancer cell is introduced by random fusion of the harvested lymphocytes with myeloma cells or neoplastic (cancerous) B lymphocyte cells [23]. The resultant fusion cells are called hybridomas. From the population of fusion cells, clonal lines having culturing stability are selected using a sequence of repetitive serial dilutions and subsequent culturing of the original mixture of hybridomas. Individual or monoclonal lines (each having arisen from a single lymphocyte and each producing a monoclonal antibody) are then screened for the production of an antibody *in vitro* with desirable interactions with the target protein.

The usefulness of monoclonal antibodies has spawned a hybridoma industry for therapeutics, diagnostics and protein purification. 7D7B10 is an anti Human Protein C

murine monoclonal antibody, which belongs to the immunoglobulin G class. It was produced *in vitro* using the hybridoma technology and the cell culture supernatant originally generated for purification of hPC was supplied to our laboratory by the American Red Cross. This supernatant was used to examine the performance of DEAE cellulose beads at the preparative scale and the results presented herein.

References

1. Kuga S., *Aqueous Size-Exclusion Chromatography, J. of Chromatography Library*, (1988) **40**: 157.

2. Casassa E.F., *J. Polym. Sci., Part B,* (1967) **5**: 773-778.

3. Casassa E.F., *J. Phys. Chem.,* (1971) **75**: 3929-3939.

4. Giddings J.C., Kucera E., Russel C.P., and Myers M.N., *J. Phys. Chem.,* (1968) **72**: 4397-4408.

5. Laurent T.C., and Killander J., *Jornal of Chromatography,* (1964) **14**: 317-330.

6. Voelkel R., *Angew. Chem. Int. Ed. Engl.,* (1988) **27**: 1468-1483.

7. Frye J.S., and Maciel G.E., Solid State NMR approaches for resolving components of Plant Materials, Chapter 14, 389-402.

8. Bell A.T., *Vibrational spectroscopies for Adsorbed Species, American Chemical Society,* (1980) **137**: 13.

9. Allara D.L., *Vibrational spectroscopies for Adsorbed Species, American Chemical Society,* (1980) **137**: 37.

10. Ito M., and Suetaka W., *J. Phys. Chem.,* (1975) **79**: 1190.

11. Boerio F.J., and Chen S.L., *Applied Spectroscopy,* (1979) **33**: 121.

12. Tsai A.M., Englert D., and Graham E.E., *J. Chromatogr.,* (1990) **504(1)**: 89-95.

13. Draeger N.M., and Chase H.A., I.Chem.E. Symposium Series No. 118, () 161-172.

14. Harrington W.F., Johnson P., and Ottewill R.H., *Biochem. J.*, (1956) **62**: 569-582.

15. Brown J.R., *Federation Proc.*, (1975) **34**: 591.

16. Peters T. Jr., and Reed R.G., *Federation of EuropeanBiochemical Societies, Proceedings of the 11th Meeting Copenhagen,* (1977) **50**: 11-20.

17. Foster J.F., *Albumin Structure, Function and Uses*, Pergamon Press Inc., (1977), 53-84.

18. Esmon C.T., Stenflo J., Suttie J.W., and Jackson C.M., *Journal of Biological Chemistry,* (1976) **251**: 3052-3056.

19. Kisiel w., "Human Plasma Protein C. Isolation Characterization, and Mechanism of Activation by α-Thrombin", *Journal of Clinical Investigation*, (1979) **64**: 761-769.

20. Yamaji T., *Advances in Applied Biotechnology*, (1990) **11**: 125-138.

21. Velander W,H., Johnson J.L., Page R.L., Russell C.G., Subramanian A., Morcol T., Gwasdaukas F.C., Pittius C., and Drohan W.N., *The Proceedings of the National Academy of Sciences*, (1992) **89**: 12003-12007.

22. Johnstone A., and Thorpe R., *Immunochemistry in Practise, 2nd Edition,* Blackwell Scientific, Boston, (1987) pp 30-49.

23. Kohler G., and Milstein C., Continuous cultures of fused cells secreting antibody of predefined specificity. *Nature* (1975) **256**: 495.
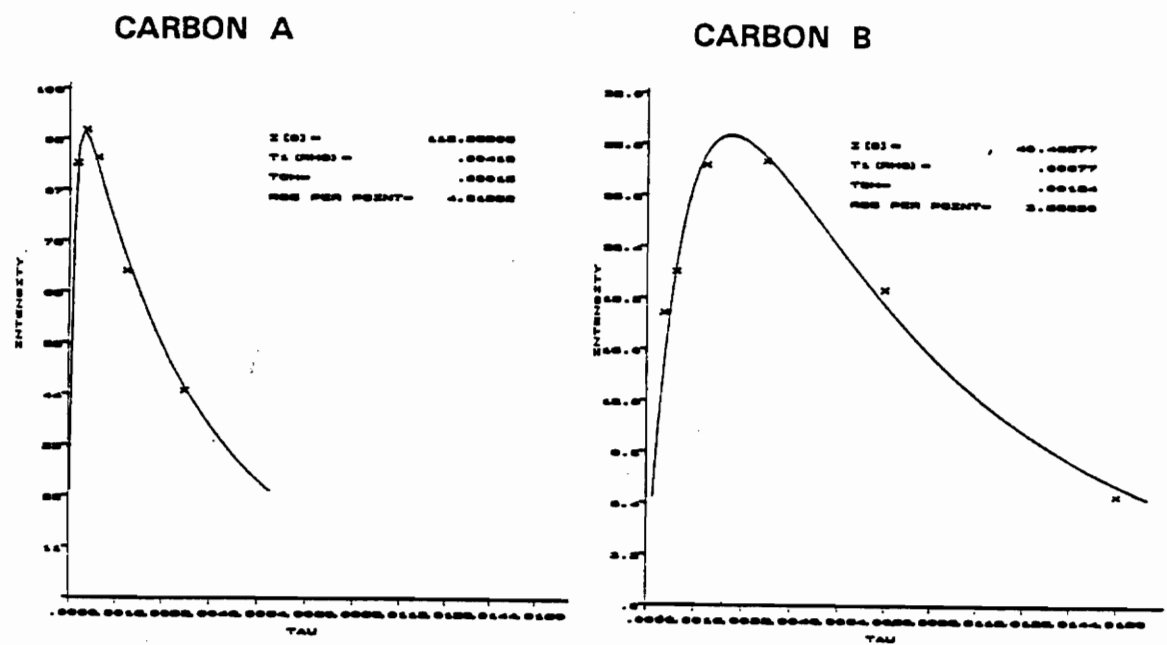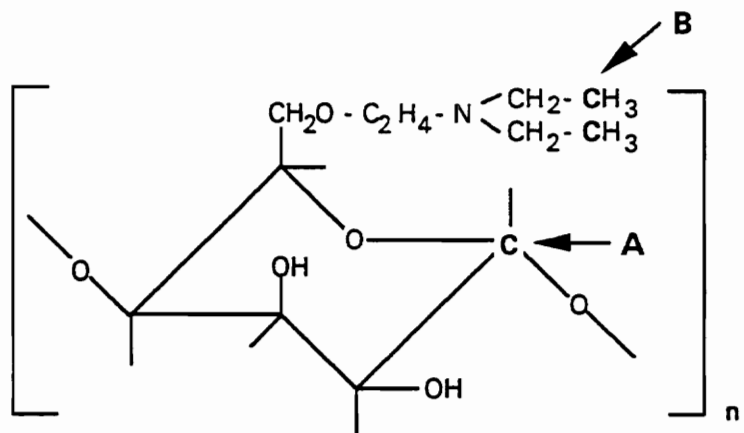
Figure 1: Partial molecular structure of DEAE cellulose and intensity as a function of contact time for carbon atoms A and B of DEAE cellulose

Chapter 4:

Engineering Protein Binding Site Architecture of Uncross-Linked DEAE Cellulose Beads

Abstract

In our previous studies, uncross-linked large diameter cellulose beads were optimized for solids content, bead size, pressure-flow limits, molecular accessibility and performance as an immunosorbent. Here, anion exchange (DEAE) cellulose beads were derivatized by two different procedures (defined as A and B) and the changes in bead morphology were correlated with transport and sorption kinetics. The kinetic characteristics clearly defined a minimum of two different types of protein binding site architecture. DEAE cellulose beads exhibited molecular exclusion of BSA near the edge of the bead in contrast to greater permeability seen in underivatized beads. Thus, accessible BSA binding sites are present only on the surface of the derivatized beads. DEAE cellulose beads derivatized by procedure B gave higher density of DEAE ligand as compared to beads derivatized by procedure A, as well as higher static and dynamic capacity for BSA. Even though DEAE cellulose beads (DP 2070, 450 μm diameter, derivatized by procedure B) have lower small ion capacity than DEAE cross-linked agarose beads, as well as ¼ the surface area, they exhibit equivalent binding capacity for BSA per volume of support. Thus, DEAE cellulose beads possess more sites per surface area as well as have lower ligand density per BSA site. Furthermore, BSA adsorption sites on DEAE cellulose beads derivatized by procedure B exhibit slow binding kinetics as compared to those derivatized by procedure A and also compared to DEAE cross-linked agarose beads.

54

Introduction

The design optimal for hydrogels use in ion exchange chromatography strives to minimize the rate limiting phenomena (transport phenomena and/or adsorption-desorption kinetics) for protein adsorption. The physical properties of the adsorbent i.e. particle diameter, and hydrogel mesh or mesh distribution can be perturbed by solids content to change the transport phenomena. The protein binding site architecture of the ion exchange adsorbent i.e. nature of ligand, total number of ligands, ligand density per accessible site and structure of the binding site can effect the kinetics of adsorption-desorption as well as total protein capacity.

The adsorbents used for column mode operation are usually small beaded hydrogels. In the absence of intraparticle convection, the transport of a protein in and out of the bead is rate limited by diffusion [1,2], which is inversely proportional to the square of the bead diameter. The diffusion rates of most proteins are on the order of 10^{-7} cm^2 sec^{-1} or slower [3]. Thus, to maintain high efficiency the length over which diffusion occurs is usually kept small. As a result, most beaded hydrogel supports are less than 200 μm in diameter.

In contrast to diffusional transport, the pressure drop due to fluid drag in a packed bed increases linearly as bead area to volume ratio increases. Thus, the pressure drop

increases linearly as bead diameter decreases. However, the use of large beaded hydrogels can lessen pressure drop by lowering the surface area per volume exposed to flow. The strength or resistance to crushing at a given pressure drop is a function of hydrogel solids content. Solids content, bead size, pressure-flow limits, and molecular accessibility of cellulose beads have been optimized by Kaster *et al* [4].

While adsorption chromatography of protein is frequently limited by diffusional mass transfer it can also be limited by sorption kinetics. In addition, studies by Arnold and Blanch [5] have shown that binding rate constant for Bovine Serum Albumin (BSA) interacting with immobilized blue dye is three orders of magnitude smaller than rate constants of diffusion-controlled biological binding reactions in solution. For example, studies by Wu and Walters [6] have shown that the Z number or the number of binding sites on a protein surface interacting with the hydrogel is directly proportional to the ligand density for an ion exchange support giving rise to slow desorption of proteins at high ligand density. Thus nonequilibrium adsorption-desorption of proteins on chromatographic hydrogel can be attributed to protein binding site architecture as well as operating conditions (i.e. low concentration of protein feed).

In our previous studies we have defined a "window of acceptable support characteristics" for protein affinity chromatography based upon prederivatized bead properties, as there was no change in bead morphology upon CNBr derivatization. Here,

we have produced large uncross-linked anion exchange (DEAE) cellulose beads for protein chromatography. The present studies report the impact of two different reaction conditions used to derivatize cellulose beads with DEAE ligand. We characterize the BSA binding site architecture which governs the intraparticle transport and sorption kinetics of protein on DEAE cellulose beads.

Methods and Materials

Cellulose beads were produced from pure alpha cellulose by the methods reported by Kaster *et al.* [4]. Cellulose beads having degree of polymerization of ~200, 1200 ± 200 μm diameter and 3.2 ± 0.2 % solids content, degree of polymerization of ~870, 1200 ± 150 μm diameter and 2.1 ± 0.2 % solids content, degree of polymerization of ~2070, 1250 ± 200 μm diameter and 2.3 ± 0.1 % solids content, and degree of polymerization of ~2070, 600 ± 100 μm diameter and 4.2 ± 0.1 solids content were beaded.

The solids content of the beads was determined before and after derivatization, by weight loss after freeze drying of the beads. Similarly, the diameter of the beads was determined before and after derivatization by photomicroscopy of random samples of 15 to 20 beads using a Nikkon microscope.

Bovine Serum Albumin (BSA), colorimetric Albumin reagent and Tryptophan were purchased from Sigma Chemical Company. Polystyrene latex microspheres used to determine bed void volume were obtained from Duke Scientific. JB-4 embedding resin for bead cross-sectioning was purchased from Polysciences. All other reagents used were of the highest grade available.

Modification of Cellulose Beads

Modification of the beads was performed using two different reaction times and temperature, while keeping the reagent-to-bead ratio constant. The first procedure described here is a modification of the method as optimized by Kalman *et al* [7] and has been used in our previous studies [8].

Procedure A: About 50 ml of cellulose beads were thoroughly washed in 0.1 M NaCl. A slurry of the beads with 75 ml 0.1 M NaCl solution was stirred gently with a magnetic stirring bar in a three-necked round bottomed flask. 6 M NaOH solution was slowly added to a pH of 12.5, and then heated and thermostated at 70°C using a Thermowatch L6 1000 SS. About 100 ml of 1.5 M aqueous solution of 2-diethylaminoethyl hydrochloride was slowly added while maintaining the reaction mixture at pH 12.5 by slow addition of 6 M NaOH solution. A total of 75 ml of the NaOH solution was added. The reaction mixture was allowed to stir for one hour. The beads were then filtered on a glass sintered funnel and washed with 250 ml of 0.1 M NaCl solution. The beads were stored in 0.1 M NaCl solution at 4°C.

Procedure B: About 100 ml of 1.5 M aqueous 2-Diethylaminoethyl hydrochloride was added to a slurry of cellulose beads in 0.1 M NaCl and allowed to stir for 30 minutes. A pH of 12.5 was never exceeded during the slow addition of 150 ml of 3 M NaOH solution. The reaction was allowed to run at room temperature for 24 hours. The beads

were then filtered on a glass sintered funnel and washed with 250 ml of 0.1 M NaCl solution. The beads were stored in 0.1 M NaCl solution at 4˚C.

Pressure Drop Studies

The pressure drop across a column of DEAE cellulose beads was measured at various flow rates of 13, 25, 38, 51, 64, 76, and 89 cm/min. Beads were packed as an aqueous slurry into a 1.0 x 15 cm column (C10/20, Pharmacia). Degassed deionized water was pumped through the column using a Rainin HPX HPLC pump with a 2070 kPa in line valve before the column to maintain backpressure on the pump. A KM 5007 I.S. digital pressure gauge (Kane-May, Ltd.) was attached by a three-way valve above the column. The column bed was first consolidated for a minimum of 30 minutes at a flow rate that gave a pressure drop of at least 3.4 kPa across the column. The flow rate was then increased incrementally with a minimum of 5 minutes allowed for the pressure drop across the column to come to equilibrium.

Gel Permeation Studies

Solute permeation in underivatized and DEAE cellulose beads was studied by elution behavior of pulses of single component solutions of BSA and tryptophan relative to that obtained for 0.269 μm latex beads. The elution profiles as detected at O.D. 280 nm were studied at different superficial velocities. The column bed was allowed to consolidate at each superficial velocity for 30 minutes before a sample was introduced.

The chromatographies were run using degassed Tris buffered saline solution (pH 7.0) for underivatized beads and Tris buffered with 0.5 M salt solution (pH 7.0), i.e. non-binding conditions, for derivatized beads. The void volume of the column was determined using an aqueous pulse of polystyrene latex microspheres having a diameter of 0.269 ± 0.007 μm.

Titration of DEAE ligand

Titration of DEAE ligand on cellulose beads (DP 200) derivatized by procedures A and B was performed to determine small ion capacity of the hydrogel as well as to detect any difference due to DEAE derivatization procedure. About 12 ml of cellulose beads were thoroughly washed in 1M NaCl (pH 12). Successive changes of beads slurried with 5 ml 10 mM hydrochloric acid were made. Each slurry was stirred for 15 minutes on a rotator mixer. The pH of the bead slurries were measured using a Fischer Scientific Accumet 25 digital pHmeter.

Solid State NMR studies

Solid state NMR was used to determine the degree of substitution on the derivatized beads. DE52 (Whatman), a amorphous cellulose support derivatized with DEAE was used as the reference material. All samples were freeze dried. To obtain CP/MAS ^{13}C-NMR spectra of the samples, MSL Bruker 300 MHz instrument with a 7 mm diameter probe was used. The operating frequency of 300.13 MHz was used for the

proton channel and 75.47 MHz for the carbon channel. For the reference material, a CP/MAS ^{13}C-NMR spectrum with a contact time of 2 milliseconds was determined and the two carbon peaks were identified, which when integrated gave a quantitative measure of the degree of substitution. A CP/MAS ^{13}C-NMR spectra with varying contact time from 0.5 to 20 milliseconds was obtained on all the samples, and values of I_0, T_{CH}, and $T_{1\rho H}$ were determined for both the peaks. The I_0 value of the sample was compared to the I_0 value of the reference material and hence the degree of substitution was determined [9,10].

Fourier Transform Infra Red Spectroscopy

FTIR spectroscopy was used to study the spatial distribution of DEAE on the cellulose bead. The beads were embedded in a resin and cross-sections of the bead were analyzed by reflectance FTIR technique. The beads were prepared for embedding by dewatering with successive 20 minute incubation in ethanol solutions of 30, 50, 70, 80, and 95%. Dewatered beads were infiltrated and embedded in JB-4 embedding resin, as per the manufacturers' instructions. Blocks of embedded beads were allowed to cure overnight before sectioning. Cross-sections, 8 μm thick, were cut with a glass knife using a Reichert-Jung Ultracut E Ultramicrotome. Bead slices were placed on a gold plated mirror and viewed under a IR Plane Microscope and irradiated with an infra red (IR) beam from a Nicolet 800 IR Spectroscope. The spectrum was determined in reflectance mode, and was averaged over 128 scans. All cellulose bead spectrums were

normalized to the gold mirror and JB-4 polymer background spectrum. The IR beam diameter was 250 μm, so a 1000 μm bead could be divided into four equal sections, and IR spectrum of each section was determined. An underivatized cellulose bead was chosen as the reference material. The IR spectra of the underivatized bead was compared with that of the derivatized bead, between the wavenumbers 990-1220 cm^{-1}, where N-C stretching band is usually present.

Adsorption Isotherms

Adsorption isotherms of underivatized and DEAE cellulose beads were compared with that of DEAE Fast Flow Sepharose (Pharmacia). BSA stock solutions ranging from 0.5 to 30 mg/ml in Tris saline buffer, pH 8.5, were made. Triplicate samples of cellulose or agarose adsorbents, were suspended in a buffer slurry (1 ml in each test tube), and placed in a 50 ml tube. The adsorbent was allowed to settle and the excess buffer was removed with a Pasteur pipette. Then 20 ml of BSA solution was added to each tube containing adsorbent. The tubes were then sealed by plastic cap and agitated at room temperature. After a 24 hour incubation, a 1.5 ml sample was removed from each tube in an Eppendorf centrifuge tube and centrifuged at 1000 x g for five minutes to pellet the adsorbent. The concentration of BSA in the supernatant was measured using both dye binding assay and optical density measurement at 280 nm at the Beer's law extinction coefficient of BSA $\epsilon = 6$ g cm^{-2}.

Column Configuration

DEAE cellulose beads or DEAE fast flow sepharose beads were packed into a C10/20 jacketed column (Pharmacia) for the study of dynamic binding capacity (DBC) of the beads. Experiments were performed at room temperature and 37°C. For gel permeation studies the beads were loaded into a 1.6 x 100 cm column (C16/100, Pharmacia) and a bed height of 90 cm was used. Two Rainin HPX pump modules with 5 ml/min and 100 ml/min pump heads were used for buffer delivery. A Masterflex peristaltic pump (Cole-Parmer) with a 7013 head and latex rubber tubing of 0.8 mm i.d. was used for buffer delivery as well as for feeding the BSA solution for DBC studies.

Protein content of the column effluent was continuously measured by absorbance at 280 nm with a Knauer Variable Wavelength Monitor UV detector with 1.0 mm variable path length flow cell (Sonntek). Eluate fractions were measured with a Spectronic 1201 Milton Roy UV Spectroscope and random samples were verified by dye binding assay. Buffer delivery for the HPLC pumps and data collection was controlled using a Rainin Dynamax system.

Dynamic Binding Capacity

Dynamic Binding Capacity (DBC) is here defined as the milligrams of protein bound per ml of gel, when the sample concentration of the effluent is 70-80% of the initial concentration. The DBC of adsorbents was evaluated using BSA. BSA, dissolved

in 50 mM Tris-Base, 0.1 M NaCl, pH 8.5 at 1 mg/ml was loaded on the column at superficial velocities of 1, 5 and 10 cm/min. During each run, the columns were washed with loading buffer and the bound protein was eluted with 1 M NaCl solution. All data for DBC was collected in triplicate.

Dye Binding Assay for BSA

BSA was determined spectrophotometrically with a specific reaction of BSA with calorimetric Albumin reagent. Briefly, 3 μl of BSA standard or unknown were added to microtiter plate wells containing 300 μl of Albumin reagent. Microtiter plate was then gently agitated for 10 minutes and absorbance was measured at 595 nm using a EL308 microplate reader (Bio-Tek).

Results

The effect of derivatization using procedure A and B, on the solids content, diameter, and varying the degree of polymerization of cellulose, on the beads is presented in Table 1. Cellulose beads, DP 200, derivatized by procedure A shrank by 50% of their volume from a diameter of 1200 ± 200 μm to 900 ± 100 μm and had an increase in solids content from 3.2 ± 0.2 % to 7.1 ± 0.2 %. Cellulose beads, DP 200, derivatized by procedure B shrank by 5% of their volume from a diameter of 1200 ± 200 μm to 1100 ± 150 μm and had an increase in solids content from 3.2 ± 0.2 % to 6.2 ± 0.3 %. Cellulose beads, DP 870, derivatized by procedure B shrank by 25% of their volume from a diameter of 1200 ± 150 μm to 1000 ± 100 μm and had an increase in solids content from 2.1 ± 0.2 % to 3.5 ± 0.2 %. Cellulose beads, DP 2070, derivatized by procedure B shrank by 40% of their volume from a diameter of 1250 ± 50 μm to 1000 ± 50 μm and had an increase in solids content from 2.3 ± 0.1 % to 5.3 ± 0.1 %.

The pressure drop versus linear velocities through a 15 cm column of underivatized and derivatized beads and comparison with theoretical curves is presented in Figure 1. Underivatized beads (DP 200, diameter 1200 ± 200 μm, solids content 3.2%) did not exhibit a pressure exponentiation at flow rates upto 100 cm/min and had a pressure drop of 6 kPa/cm bed height. DEAE beads (DP 200, diameter 900 ± 100

μm, solids content 7.1%) derivatized by procedure A, did not exhibit a pressure exponentiation at flow rates upto 90 cm/min and had a pressure drop of 13 kPa/cm bed height. DEAE beads (DP 200, diameter 1100 $\pm$ 150 μm, solids content 6.2%) derivatized by procedure B had the same pressure flow behavior as underivatized beads (data not shown). The pressure drop predicted from semi-empirical Ergun correlation for 1.2 mm diameter beads exhibited a slope of 400 (line 1). The prediction curve for 0.9 mm diameter beads exhibited a slope of 200 (line 2). The underivatized cellulose beads (DP 200, diameter 1200 $\pm$ 200 μm, solids content 3.2%) exhibited a slope of 13 (line 3). DEAE cellulose beads (DP 200, diameter 900 $\pm$ 100 μm, solids content 7.1%) derivatized by procedure A, exhibited a slope of 6 (line 4).

Solute permeation studies were conducted on cellulose beads with varying degree of polymerization as well as of the effect of varying the procedure of derivatization. Since neither of the above variables gave a significant change in data, the following beads were chosen as an example to show the effect of derivatization on cellulose beads. Figure 2a presents permeation chromatography of underivatized cellulose beads (DP 2070, 650 μm diameter, 3.5% solids content) at 2 cm/min of polystyrene latex microspheres, tryptophan and BSA. Figure 2b presents permeation chromatography of DEAE cellulose beads (DP 2070, 500 μm diameter, 6.8% solids content, derivatized by procedure B) at 2 cm/min of polystyrene latex microspheres, tryptophan and BSA. Figure 2c presents permeation chromatography of underivatized cellulose beads (DP

2070, 650 μm diameter, 3.5% solids content) at superficial velocities of 1, 2, and 5 cm/min of BSA. Figure 2d presents permeation chromatography on DEAE cellulose beads (DP 2070, 500 μm diameter, 6.8% solids content) at superficial velocities of 1, 2, and 5 cm/min of BSA. The void volume ranged from 0.45-0.50 column volumes (CV) for underivatized as well as derivatized beads, as indicated by a sharp elution peak of 0.269 μm diameter latex polymer spheres (see panel a of Figures 2a and 2b). The void volumes did not vary with linear velocity. For any of the biochemical species evaluated in these permeation experiments; after about 1.5 column volumes, no absorbance was detected in the subsequent 10 column volumes. Tryptophan gave an elution peak centered about 1.0 CV for underivatized and derivatized beads (see panel b of Figure 2a and 2b) at all linear velocities studied, although at higher linear velocities peak broadening did occur.

Permeation experiments using BSA (M_r 66,000 Da) on underivatized cellulose beads produced an elution profile with a maxima centering at 1.0, 0.85, and 0.7, column volumes for superficial velocities 1, 2 and 5 cm/min respectively (see panel a, b, and c of Figure 2c respectively). Similarly permeation studies were done on derivatized beads. The maxima of the elution profile centered at 0.60, 0.55, and 0.45 column volumes for superficial velocity 1, 2, and 5 cm/min respectively (see panel a, b, and c of Figure 2d respectively).

The pH of DEAE cellulose beads derivatized by procedure A and B versus microequivalent hydrochloric acid added to titrate the DEAE ligand is presented in Figure 3. DEAE cellulose beads (DP 200, 900 μm diameter, 7.1% solids content) derivatized by procedure A exhibit a single pK_a of 10 and a small ion capacity of 0.03 meq/ml gel. DEAE cellulose beads (DP 200, 1100 μm diameter, 6.2% solids content) derivatized by procedure B exhibit two pK_a's, a pK_{a1} of 10, pK_{a2} of 5 and a small ion capacity of 0.05 meq/ml gel.

Figure 4 presents the CP/MAS ^{13}C-NMR spectra of DE52, and partial molecular structure of DEAE cellulose. The peak labeled as A is the signal generated by carbon atom at position 5 of the pyranose ring. The position 5 carbon has two adjacent oxygen atoms and has a signature shift of ~ 105 ppm. Peak B is characteristic of methyl carbons of the DEAE ligand, which have a shift of ~ 10 ppm. The degree of substitution (DS) calculated from relative peak area of carbon A : carbon B was 0.20. The DS of various samples was also calculated from the ratio of I_0 values of the two carbon atoms, and is presented in Table 2. The DS of various samples of DEAE cellulose beads was calculated by normalizing I_0 value of carbon A of sample with respect to I_0 value of carbon A of DE52, and then calculating the relative intensity of carbon B with respect to carbon A. The DS of DE52 by I_0 calculation was 0.17. The DS of cellulose beads (DP 200) derivatized by procedure A was 0.04. The DS of beads derivatized by procedure B was similar for DP 200, 870 and 2070 beads with a value of about 0.11-

0.12.

Figure 5 presents the FTIR spectra across a DEAE cellulose bead as compared to an underivatized cellulose bead. The FTIR spectra of DP 200, diameter 1100 ± 150 μm, solids content 6.2%, and derivatized by procedure B was chosen as an example from the different samples of DEAE cellulose beads, as no variation in the FTIR spectra was noticed among different samples. FTIR spectra a, b, c, and d, are the spectra across the DEAE cellulose bead which was divided into four equal sections, and spectra e is an example of a FTIR spectra of an underivatized bead. The FTIR spectra of the derivatized bead show a N-H stretching band at 1000 cm^{-1} at all positions across the bead. No N-H stretching band was observed in the FTIR spectra of underivatized cellulose beads.

Adsorption isotherms of DEAE cellulose beads derivatized by Procedure A and Procedure B are presented in Figure 6a. Adsorption isotherms of DEAE cellulose beads with varying DP are presented in Figure 6b. The comparison of adsorption isotherm of one example of DEAE cellulose beads derivatized by procedure B with respect to DEAE fast flow sepharose is presented in Figure 6c. The maximum adsorption capacity of DEAE cellulose beads, DP 200 derivatized by procedure A had a value between 18-20 mg BSA/ml of gel. The maximum adsorption capacity of DEAE cellulose beads, DP 200 derivatized by procedure B had a value between 60-65 mg BSA/ml of gel. The

maximum adsorption capacity of DEAE cellulose beads, DP 2070 (diameter 1000 ± 50 μm) derivatized by procedure B also had a value between 60-65 mg BSA/ml of gel. The maximum adsorption capacity of DEAE cellulose beads, DP 870 derivatized by procedure B had a value of 30 mg BSA/ml of gel. The maximum adsorption capacity of DEAE cellulose beads, DP 2070 (diameter 450 ± 100 μm) derivatized by procedure B had a value of 100 mg BSA/ml of gel. DEAE fast flow sepharose had a maximum adsorption capacity of 40 mg BSA/ml of gel at the same conditions.

Table 3 presents the dynamic binding capacity of various DEAE cellulose beads and DEAE fast flow sepharose at superficial velocities 1, 5, and 10 cm/min. DEAE cellulose beads, DP 200 and 900 ± 100 μm diameter, derivatized by procedure A had a capacity of 1.8 mg BSA/ml of gel at a linear velocity of 5cm/min. All the following beads were derivatized by procedure B. DEAE cellulose beads, DP 2070 and 450 ± 100 μm diameter had a capacity of 11.7 mg BSA/ml of gel at a superficial velocity of 5 cm/min. DEAE cellulose beads, DP 2070 and 1000 ± 50 μm diameter had a capacity of 6.4 mg BSA/ml of gel at a superficial velocity of 5 cm/min. DEAE cellulose beads, DP 870 and 1000 ± 100 μm diameter had a capacity of 3.0 mg BSA/ml of gel at a superficial velocity of 5 cm/min. DEAE cellulose beads, DP 200 and 1100 ± 150 μm diameter had a capacity of 5.5 mg BSA/ml of gel at a superficial velocity of 5 cm/min. DEAE fast flow sepharose had a capacity of 8.3 mg BSA/ml of gel at a superficial velocity of 5 cm/min.

A typical chromatogram for BSA adsorption/elution onto DEAE cellulose beads (DP 200, 900 μm diameter) derivatized by procedure A at a superficial velocity of 5 cm/min is presented in Figure 7a. The breakthrough occurs at 0.6 column volumes, and required 9 column volumes to reach 75% of the inlet concentration. The column was washed for 2 column volumes and the peak eluted in 2 column volumes. A typical chromatogram for BSA adsorption/elution onto DEAE cellulose beads (DP 2070, 450 μm diameter) derivatized by procedure B at a superficial velocity of 5 cm/min is presented in Figure 7b. The breakthrough occurs at 0.6 column volumes, and required 30 column volumes to reach 75% of the inlet concentration. The column was washed for 5 column volumes and the peak eluted in 6 column volumes. A typical chromatogram for BSA adsorption/elution onto DEAE fast flow sepharose is presented in Figure 7c. The breakthrough occurs at 8 column volumes, and required 25 column volumes to reach 80% of the inlet concentration. The column was washed for 16 column volumes and the peak eluted in 6 column volumes.

Figure 8 presents a typical chromatogram of BSA adsorption/elution onto DEAE fast flow sepharose at 5cm/min, where BSA has been loaded until 2% breakthrough. The column was washed for 79 column volumes and 40% of the loaded BSA slowly leached out.

Typical chromatogram for BSA adsorption/elution under saturation loadings at a linear velocity of 5cm/min at 21^{0}C and 37^{0}C onto DEAE cellulose beads (DP 200, 900 μm diameter) derivatized by procedure A are presented in Figure 9a. The breakthrough at 21^{0}C occurs over 9 column volumes to reach 75% of inlet concentration. The breakthrough at 37^{0}C occurs over 15 column volumes to reach 70% of inlet concentration. Typical chromatogram for BSA adsorption/elution under saturation loadings at a linear velocity of 5cm/min at 21^{0}C and 37^{0}C onto DEAE cellulose beads (DP 2070, 450 μm diameter) derivatized by procedure B are presented in Figure 9b. The breakthrough at 21^{0}C occurs over 30 column volumes to reach 75% of inlet concentration. The breakthrough at 37^{0}C occurs over 35 column volumes to reach 65% of inlet concentration.

Discussion

Effect in Bead Morphology and Flow Behavior

Our studies seek to correlate changes in uncrosslinked, cellulose bead morphology with transport, sorption kinetics, and protein binding site architecture due to different derivatization procedures. Because the chemical substitution of DEAE moieties on the hydroxyl group of the pyranose ring will likely result in changes in hydrogen bonding, a change in hydrogel structure and chemical stability was expected as the degree of substitution is increased. In fact, we have found that changing the reaction time and temperature of derivatization of cellulose beads having a DP of 200 resulted in bead shrinkage from a diameter of 1200 μm to 900 μm and 1100 μm by procedure A and B respectively. The higher substitution achieved by procedure B also resulted in bead instability at pH 5. The beads derivatized by procedure A were stable at pH 5. Furthermore, beads made by derivatization with procedure A and B also had different adsorption behavior.

Derivatization of DP 2070 and 870 beads by procedure B and DP 200 beads by procedure A resulted in bead shrinkage from a diameter of 1200 μm to 1000 μm with a corresponding increase in solids content from 2-3% to 5-7%. In contrast to the above results cellulose beads of DP 200 derivatized by procedure B, exhibited a greater solids content than predicted by the average change in bead diameter. The degree of

substitution appeared to be similar to that of DP > 870 beads derivatized by procedure B, with about one out of every 8 rings derivatized. The probable cause of the excess solids after derivatization could be attributed to precipitation of salts although these beads did not appear to have any difference in translucence.

The properties of non cross-linked polymers, like viscosity in aqueous solutions, can change over time even though their diffusion coefficient is small. The "aging" of a polymer over long periods of time is well documented in the literature and is usually attributed to rearrangement of the hydrogen bonds or to the presence of microorganisms in the aqueous medium [11,12]. Uncross-linked DEAE cellulose beads, derivatized by Procedure B, loose their mechanical strength when stored at 4°C over six months. But cellulose beads stored for equivalent amount of time at 4°C, we have encountered the loss of bead integrity only for highly substituted DEAE cellulose beads, and not for underivatized or DEAE beads derivatized by Procedure A. It is known that underivatized cellulose beads exhibit high mechanical strength due to the presence of hydrogen bonds between different chains of cellulose. These hydrogen bonds are disrupted when the beads are derivatized and at very high degree of substitution DEAE cellulose is soluble in aqueous medium [13]. Thus chemical cross-linking may be necessary to maintain bead integrity in highly substituted DEAE cellulose beads.

In our previous studies [8], a change in flow behavior characteristics for DEAE

cellulose beads (derivatized by procedure A) as compared to underivatized bead was observed. While the solids content of beads increased from 2-3% to 5-7% upon derivatization (procedure A or B), the change in size to smaller beads increased the surface area to volume ratio and therefore the frictional drag exerted per volume of bed. We have attempted to normalize the pressure drop data for derivatized beads to that of underivatized beads to account for bead shrinkage. The shift in the slope of pressure drop per unit bed length versus linear velocity predicted by the semi-empirical Ergun correlation [14] for flow in a packed bed is the same as found for underivatized versus derivatized cellulose beads. Moreover, DEAE cellulose beads which retain their diameter upon derivatization (DP 200, derivatized by procedure B) also show no change in pressure drop versus linear velocity. Thus the change in flow behavior characteristics of DEAE cellulose beads can be attributed to bead shrinkage and not loss of mechanical strength upon derivatization.

Effects on Transport Phenomena

The change in transport phenomena of cellulose beads upon derivatization as studied by gel permeation of underivatized and derivatized beads indicates that a structural change occurred in the beads during derivatization. We have defined bead contacting time in our previous studies [4] as a ratio of bead diameter to superficial velocity. Bead contacting time is useful for estimating the approximate time available for a species to penetrate the bead. It is noted that the characteristic time required for

diffusion of solute in a bead is directly proportional to the square of the radius of the particle [15]. Thus, the maxima of the elution profile for tryptophan (M_r 204) for underivatized and derivatized beads at an estimated bead contacting time of 2 seconds centering at one column is well described by diffusional transport. But the maxima of the elution profile for BSA (M_r 66,000) centering at one column volume (panel a, Figure 2c) at an estimated bead contacting time of 4 seconds (superficial velocity of 1 cm/min) indicates penetration of the bead was significantly more than predicted by purely diffusive transport. Our results for underivatized beads, show some characteristics of enhanced intraparticle mass transfer over that explainable by unhindered diffusion and are in agreement with the results of Kaster *et al*[4]. DEAE derivatized cellulose beads show a shift towards the void volume in the maxima of the elution profile of BSA for DEAE cellulose beads under nonbinding conditions (panel a, Figure 2d) for an estimated bead contacting time of 4 seconds (superficial velocity of 1 cm/min). As the contacting time is decreased by raising the superficial velocity to 5 cm/min the maxima of the elution profile of BSA for DEAE cellulose beads shifts to the void volume (panel c, Figure 2d). Thus molecular exclusion of BSA occurs near the edge of the DEAE cellulose bead (derivatized by procedure A or B) in contrast to greater permeability seen in underivatized beads.

Protein binding Site Architecture

The titration curves of DEAE cellulose beads DP 200, derivatized by procedure A and B, exhibited a small ion capacity of 0.03 and 0.05 meq/ml of gel respectively. Oligomeric DEAE ligands can be formed due to secondary reactions of the monomer depending on alkaline conditions such as used for procedure A versus procedure B. Thus, the small ion capacity can change in the presence of oligomeric DEAE. Moreover, beads derivatized by procedure B exhibited an inflection in the titration curve at pH 5 accompanied by swelling of the hydrogel until loss of bead integrity. Thus, derivatization by procedure B appears to lower the stability of the uncross-linked DEAE cellulose beads, probably by altering the hydrogen bonding between adjacent chains. Furthermore, a change in hydrogen bonding pattern can be expected to alter the adsorption site architecture and hence kinetics of adsorption.

We have used equilibrium adsorption studies to study the number of available adsorption sites for proteins present on the hydrogel. All the adsorption isotherms presented here are concave down isotherms and fit a typical Langmuir isotherm [16]. DEAE cellulose beads of DP 200 derivatized by procedure A exhibit a maximum capacity of 20 mg BSA/ml of gel compared to 60 mg BSA/ml of gel derivatized by procedure B. This result is consistent with lower small ion capacity and degree of substituion of the DEAE ligand by procedure A as determined by titration as well as NMR respectively. DEAE cellulose beads of DP 200, 870, and 2070, (~ 1000 μm

diameter) derivatized by Procedure B exhibit equivalent degree of substitution as well as equivalent maximum capacity of 60 mg BSA/ml of gel when normalized with respect to solids content. We have compared DEAE cellulose beads having same degree of polymerization (2070) and equivalent substitution, but different diameter. For example, 450 μm diameter beads exhibited higher maximum capacity of 100 mg BSA/ml of gel as compared to a maximum capacity of 60 mg BSA/ml of gel for 1000 μm diameter beads. The surface area of 450 μm diameter beads is two fold higher than 1000 μm diameter beads. Thus, a surface area dependent adsorption capacity in DEAE derivatized cellulose beads is evidence that only surface adsorption occurs for BSA. The relative dynamic binding capacity of DEAE cellulose beads by varying the procedure of derivatization, degree of polymerization and bead diameter were similar to those observed by equilibrium adsorption studies. DEAE cellulose beads (DP 2070) 450 μm diameter beads at superficial velocity of 5 cm/min also exhibited twice the binding capacity for BSA (12 mg/ml of gel) as compared to 1000 μm DEAE cellulose beads (6 mg/ml of gel). Thus, gel permeation studies, equilibrium adsorption studies and dynamic binding capacity studies are all consistent with BSA adsorption sites which are accessible existing only on the surface of DEAE cellulose beads.

The number of BSA binding sites on DEAE cellulose beads derivatized by procedure B is much greater than those derivatized by procedure A or DEAE fast flow sepharose. The maximum equilibrium adsorption capacity and dynamic binding capacity

for DEAE cellulose beads (DP 2070, 450 μm diameter) has a value of 100 and 12 mg BSA/ml of gel respectively, as compared to 40 and 8.3 mg BSA/ml of gel for DEAE fast flow sepharose. It is noted that these DEAE cellulose beads have ¼ the surface area of DEAE cross-linked agarose beads (7% solids content) and exhibit equivalent dynamic binding capacity and higher maximum adsorption capacity.

DEAE cellulose beads have a lower estimated number of DEAE ligands per BSA site as compared to commercially available hydrogels. Table 4 presents data available from manufacturer and data obtained by titration curves, solid state NMR and equilibrium adsorption studies. The meq of DEAE per ml of DE52, and DEAE cellulose beads derivatized by procedures A and B as determined by titration curve, had a value of 0.26, 0.03 and 0.05 respectively and were similar to values obtained by NMR. The estimated number of ligands per BSA site is 371 for DE52 (amorphous DEAE cellulose), 200 for DEAE fast flow sepharose, and 100 and 50 for DEAE cellulose beads derivatized by procedure A and B respectively. Since DEAE cellulose beads adsorb on the surface in batch loadings, and have the DEAE ligand evenly spatially distributed across the bead (as determined by FTIR), the estimated number of DEAE ligands per BSA site would be even lower than those calculated.

The kinetic behavior of the adsorption sites can be deduced from studying the adsorption/elution profile of BSA solution. Upon saturation of binding sites, column

80

loading of a solute to a packed bed having no transport or kinetic limitations would yield step increase to loading concentration at the column outlet. Subsequent column washing with loading buffer only would result in solute washout within one column volume of wash buffer. Elution of bound proteins would occur as a sharp gaussian peak if there was no significant transport limitations or axial dispersion. Surface bound protein would also exhibit similar elution behavior. DEAE cellulose beads derivatized by procedure A exhibit a sharp increase in the slope of the breakthrough curve, and washes out unbound or weakly bound BSA in 2 to 3 column volumes of loading buffer. The eluate peak for adsorbed BSA is a gaussian peak and elutes in 2 to 3 column volumes (Figure 7a). DEAE cellulose beads derivatized by procedure B exhibit a slow increase in the slope of the breakthrough curve, and washes out unbound or weakly bound BSA in 3 to 5 column volumes of loading buffer. The eluate peak for adsorbed BSA is a gaussian peak and elutes in 5 to 6 column volumes (Figure 7b). Thus, DEAE cellulose beads derivatized by procedure A is indicative of fast adsorption whereas DEAE cellulose beads derivatized by procedure B is indicative of slow adsorption with neither showing any significant transport limitations upon elution. In contrast, DEAE cross-linked agarose has a sharp breakthrough curve but takes about 16 column volumes to wash the weakly or unbound BSA from the bed. The elution volume and profile of BSA is similar to that of the DEAE cellulose beads (Figure 7c). Thus, the difference between these ion exchange hydrogels can be attributed to differences in the adsorption/desorption site kinetics and probably then to site architecture.

81

The above data is consistent with the existence of a minimum of three different binding sites for BSA. These are a site having fast adsorption and slow desorption kinetics, a site having fast adsorption and fast desorption kinetics, and a site having slow adsorption and slow desorption kinetics. The DEAE cross-linked agarose has a mixture of the former two sites as 40% of the bound of the weakly bound BSA desorbs during the wash step and the rest of the adsorbed material is tightly bound and elutes in less than 6 column volumes (Figure 8). While the DEAE cellulose beads have the same anion exchange moiety as the cross-linked agarose, they behave chromatographically as if only one type of site predominates i.e. fast adsorption and slow desorption sites for beads derivatized by procedure A, slow adsorption and slow desorption sites for beads derivatized by procedure B.

The different adsorption sites on DEAE cellulose beads due to different derivatizational procedures can be verified by studying the adsorption profiles of BSA at 21°C and at 37°C. The rate of mass transfer is proportional to the diffusivity, which is directly dependent on temperature and indirectly through the viscosity of the surrounding medium. From the Stokes-Einstein relationship, $D \propto T(K)/\mu$. Thus, an increase in temperature from 21°C to 37°C will have a small increment in the rate of mass transfer and would exhibit a small shift in the breakthrough profiles at the higher temperature. The rate of adsorption is proportional to the binding rate constant, which can be described by an Arrhenius equation, $k_f = A \exp [- E_a/RT]$. Thus, a small

increment in temperature will exponentially increase the binding rate constant and hence the rate of adsorption. Thus, kinetic limited supports would exhibit a shallower breakthrough profile at higher temperatures. The steepness of the initial breakthrough profiles for DEAE cellulose beads derivatized by procedure A at 21°C and 37°C are similar indicating that fast adsorption sites exist on these beads. However, the initial breakthrough profile of DEAE cellulose beads derivatized by procedure B at 37°C is shallower indicating that slow adsorption sites exist on these beads. Both these beads exhibit slower binding kinetics in the latter part of the breakthrough curve which maybe attributed to formation of oligomeric surface structures of BSA binding on the support. DEAE cellulose beads (derivatized by procedure A or B) also exhibited higher dynamic binding capacity of 4mgs and 21 mgs BSA/ ml of gel at 37°C. This maybe due to the swelling of the gel at a higher temperature.

Conclusions

DEAE cellulose beads have a higher degree of substitution when mild temperatures are used accompanied by long reaction time. This reaction condition gave the cellulose beads a degree of substitution which was equivalent to commercially available amorphous anion exchange cellulose. The DEAE ligand was evenly spatially distributed throughout the bead irrespective of the procedure of derivatization. However, accessible BSA binding sites occurred only near the surface

The dynamic binding capacity of DP 2070, 450 μm beads was higher than DEAE cross linked agarose. Equivalent binding capacity was maintained by DEAE cellulose beads (derivatized by procedure B) at ¼ surface to volume ratio over small cross-linked DEAE agarose beads. Thus, cellulose has a greater number of sites per surface area. Furthermore, the DEAE cellulose beads possessed less ion exchange ligands per BSA site as compared to commercially available DEAE hydrogels. The BSA adsorption sites on DEAE cellulose beads are kinetically more uniform than DEAE fast flow sepharose, but high density DEAE sites had slower binding kinetics than low density DEAE sites on cellulose beads as well as cross-linked agarose beads. Thus, the reaction time and temperature of derivatization of cellulose beads can be perturbed to engineer adsorption sites exhibiting fast or slow kinetics.

References

1. Yang C.-M., and Tsao G.T., *Adv. Biochem. Eng.*, (1982) **25**(1): 5.

2. Mikes O., "Fundamentals of Ion-Exchange Chromatography", *Liquid Column Chromatography A Survey of Modern Techniques and Applications*, Deyl Z., Macek K., and Janak J., (Eds.), Elsevier Scientific Publishing Co., Amsterdam, (1975) pp. 15-31.

3. Tyn M.T., and Gusek T.W., *Biotech. and Bioeng.*, (1990) **35**: 327-338.

4. Kaster J.A., Oliviera W.de., Glasser W.G., and Velander W.H., *J. Chromatogr.*, (1993) **648**: 79-90.

5. Arnold F.H., and Blanch H.W., *J.Chromatogr.*, (1986) **355**: 13-27.

6. Wu D., and Walters R.R., *J Chromatogr.*, (1992) **598**: 7-13.

7. Kalman F., Borsa J., Kemeny S., and Rusznak I., *Colloid and Polymer Science*, (1988) **266**: 716-720.

8. W.H. Velander, J.A. Kaster, G. Kumar, K. van Cott, W. de Oliviera and W.G. Glasser, *Cellucon '92 Selective Purification and Separation Processes: The Role of Cellulosic Materials* (1992).

9. Voelkel R., *Angew. Chem. Int. Ed. Engl.*, (1988) **27**: 1468-1483.

10. Frye J.S., and Maciel G.E., *Solid State NMR approaches for resolving components of Plant Materials*, Chapter 14, 389-402.

11. Kulicke W.M., and Kniewske R., *Macromol. Chem.* (1980) **181**: 823-838.

12. Chemlir M., Kunscher A., Barthell E., *Die Angewandte Makromoleculare Chemie,* (1980) **89**: 145-165.

13. Glasser W.G, intercommunication.

14. *Mass Transfer Operations*, 3rd Ed., Treybal R.E., Mcgraw-Hill, NY, (1980) pp. 200.

15. Transport Processes and Unit Operations, 2nd Ed., Geankoplis C.J., (1983) pp.419.

16. Ruthven D.M., *Principles of Adsorption and Adsorption Processes,* John Wiley, New York, (1984).

Table 1: Effect of derivatization on cellulose beads

Degree of Polymerization	Initial Diameter (μm)	Final Diameter (μm)	Initial Solids Content (Wt%)	Final Solids Content (Wt%)	% Volumetric Shrinkage
200*	1200 ± 200	900 ± 100	3.2 ± 0.2	7.1 ± 0.2	50
200	1200 ± 200	1100 ± 150	3.2 ± 0.2	6.2 ± 0.3	5
870	1200 ± 150	1000 ± 100	2.1 ± 0.2	3.5 ± 0.2	25
2070	1250 ± 50	1000 ± 50	2.3 ± 0.1	5.3 ± 0.1	40
2070	600 ± 100	450 ± 100	4.2 ± 0.1	6.3 ± 0.1	40

* Derivatized by Procedure A, others derivatized by Procedure B

Table 2: Comparison of degree of substitution of DE52 with DEAE cellulose beads

Material	Io (A)	Io (B)	Degree of Substitution
DE 52 (Whatman)	113	40	0.17
DEAE* Cellulose Beads			
DP 200, 1100μm 3.2% $\rightarrow$ 6.2%	114	29	0.12
DP 870, 1000μm 2.1% $\rightarrow$ 3.5%	117	30	0.12
DP 2070, 1000μm 2.3% $\rightarrow$ 5.3%	115	27	0.11
DP 2070, 450μm 4.2% $\rightarrow$ 6.3%	113	26	0.11
DP 200, 900μm[#] 3.2% $\rightarrow$ 7.1%	115	10	0.04

* Degree of Polymerization, bead diameter, solids content before and after derivatization

Derivatized by Procedure A, others derivatized by Procedure B

Table 3: Comparison of dynamic binding capacity of DEAE fast flow sepharose with DEAE Cellulose Beads

Material	Degree of Polymerization	Bead Diameter (μm)	Superficial Velocity (cm/min)	Capacity# (mg/ml gel)
DEAE FF Sepharose	NA	100	1 5	7.8 ± 0.2 8.3 ± 0.9
DEAE Cellulose * 3.2% → 7.1% **	200	900	5 10	1.8 ± 0.2 1.4 ± 0.1
3.2% → 6.2%	200	1100	5	5.5 ± 0.2
2.1% → 3.5%	870	1000	5 10	3.0 ± 0.2 1.5 ± 0.1
2.3% → 5.3%	2070	1000	1 5 10	14.0 ± 0.5 6.4 ± 0.3 1.4 ± 0.1
4.2% → 6.3%	2070	450	5 10	11.7 ± 0.0 8.0 ± 0.6

\# 1 mg/ml BSA solution loaded until >75% breakthrough
  Column: 1 x15 cm
* Solids content (wt%) before and after derivatization
**Derivatized by Procedure A, other beads derivatized by Procedure B

89

Table 4: Comparison of the estimated number of DEAE ligands/BSA site of DEAE cellulose beads with commercially available hydrogels

MATERIAL	meq of DEAE / ml of gel	meq of BSA bound / ml gel	meq BSA / meq of DEAE	Estimated number of ligands / BSA site
DE 52 30% solids content	0.26* (0.26)	0.0007*	0.003	371
DEAE FF Sepharose 7% solids content	0.11*	0.0006 @	0.005	200
DEAE Cellulose Beads, DP 200				
ProcedureA 7% solids content	0.03 (0.02)	0.0003 @	0.01	100
Procedure B 6% solids content	0.05 (0.05)	0.0010 @	0.02	50

( ) NMR value in paranthesis, beside titration values

* data available by manufacturer

@ data obtained from equilibrium adsorption studies at pH 8.5

90

Table 5: Comparison of BSA binding sites of DEAE fast flow sepharose with DEAE cellulose beads

Types of BSA Binding Sites	DEAE Fast Flow Sepharose	DEAE Cellulose Bead, DP 200
Fast k_A Slow k_D	~ 50%	> 90% *
Fast k_A Fast k_D	~ 50%	-------
Slow k_A Slow k_D	-------	> 90% **

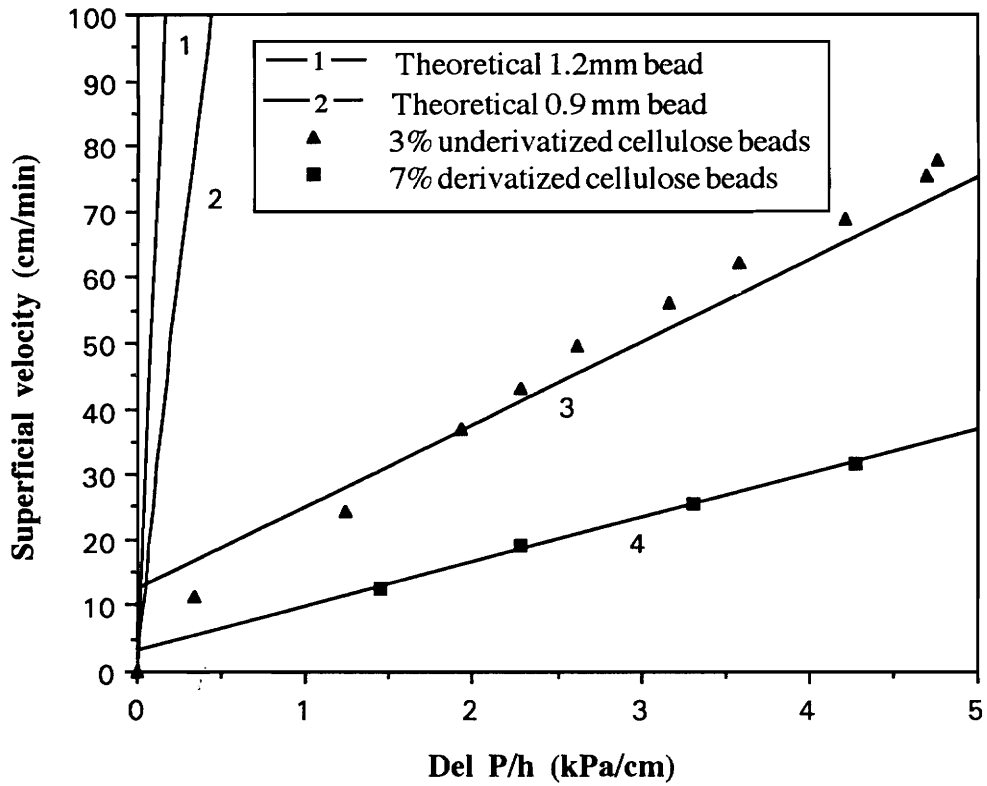* Derivatized by Procedure A
** Derivatized by Procedure B

Figure 1: Comparison of pressure drop versus linear velocity of underivatized and derivatized beads with respect to theoretical curves
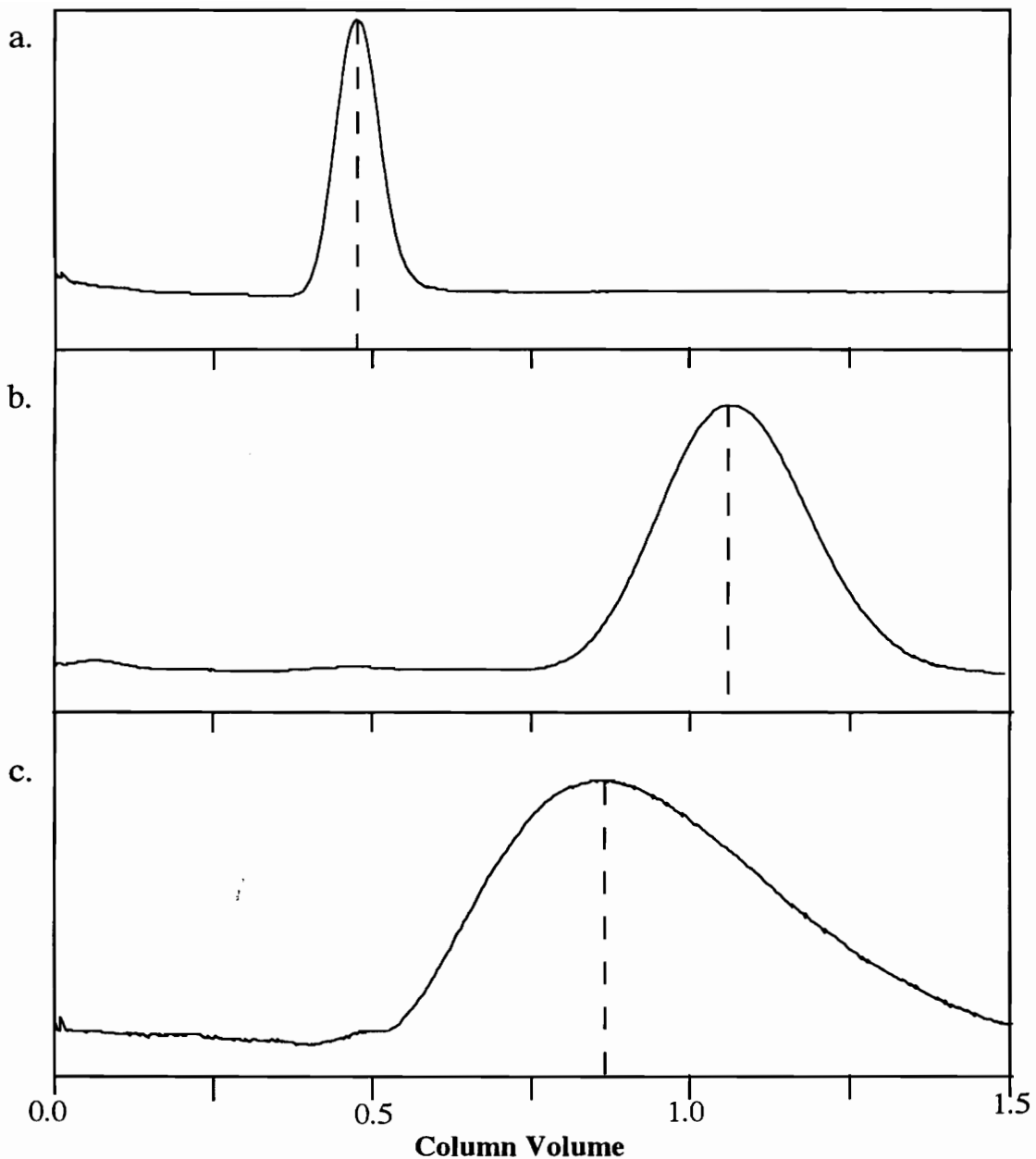
Figure 2a: Gel permeation chromatography on underivatized cellulose beads (DP 2070, 650 μm diameter, solids content 3.5%). Superficial velocity 2cm/min (estimated bead contacting time: 2 sec), Column 1.6 x 90 cm. a. Nanospheres 0.269 μm microspheres.
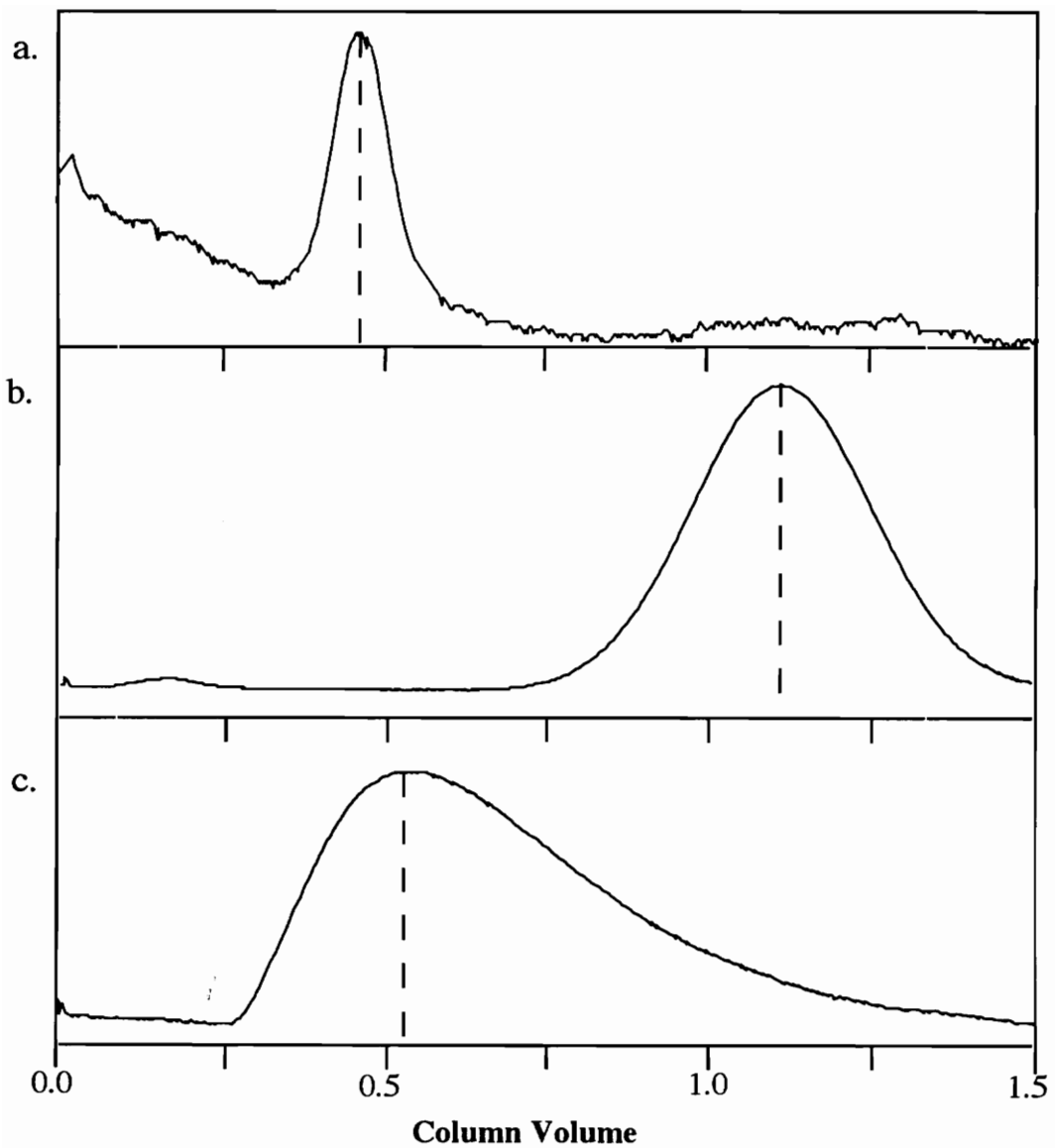b. Tryptophan, molecular weight 204. c. BSA, molecular weight 66,000.

Figure 2b: Gel permeation chromatography of DEAE cellulose beads (DP 2070, 500 μm diameter, solids content 6.8%). Superficial velocity 2 cm/min (estimated bead contacting time: 2sec), Column 1.6 x 90 cm. a. Nanosphere, 0.269 μm microspheres. b. Tryptophan, molecular weight 204. c. BSA, molecular weight 66,000.
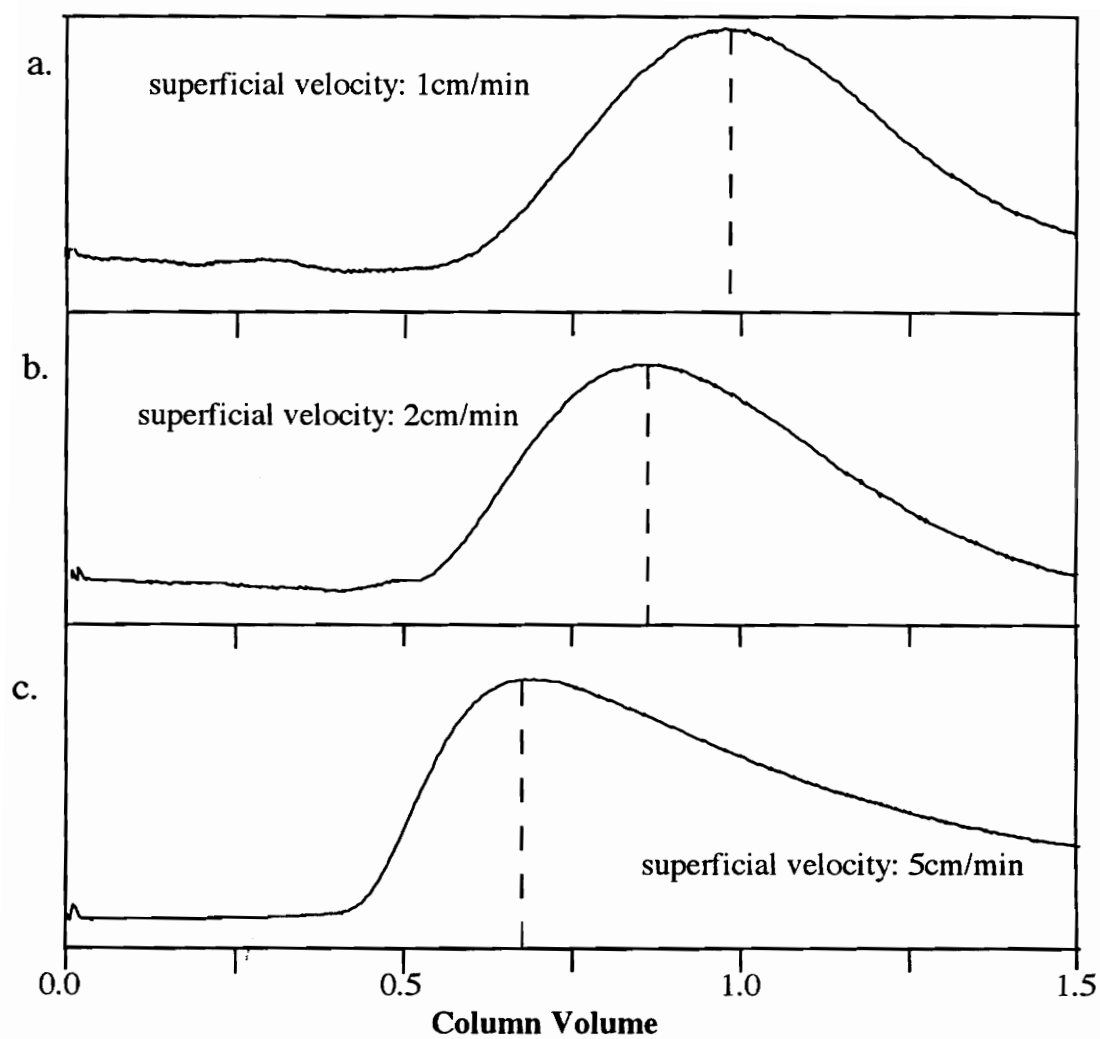
94

a. superficial velocity: 1cm/min

b. superficial velocity: 2cm/min

c. superficial velocity: 5cm/min

Column Volume

Figure 2c: Gel permeation chromatography on underivatized cellulose beads (DP 2070, 650 μm diameter, solids content 3.5%). Column 1.6 x 90 cm, BSA, molecular weight 66,000. a. superficial velocity 1cm/min. b. superficial velocity 2 cm/min. c. superficial velocity 5cm/min.
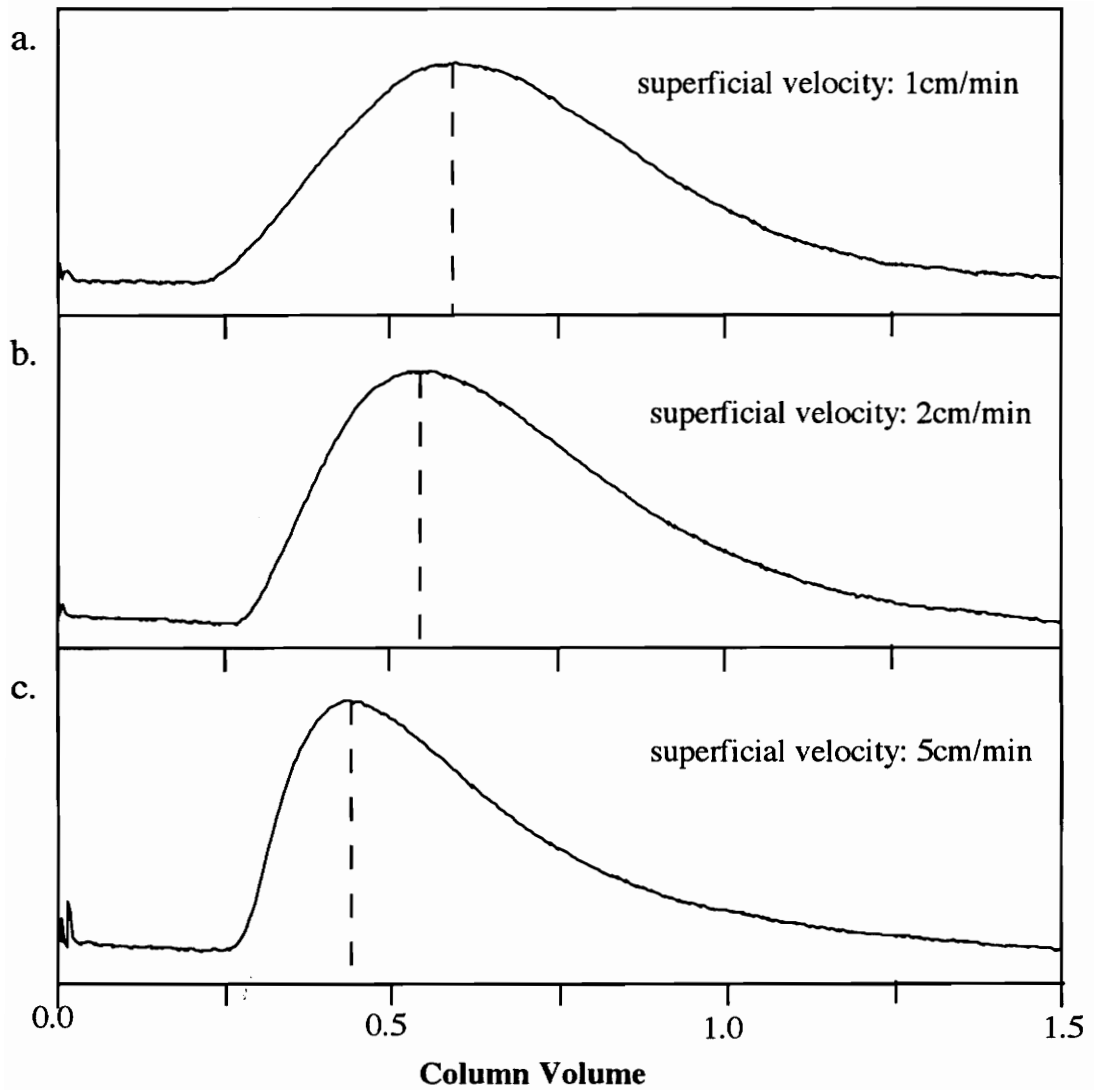
Figure 2d: Gel permeation chromatography on DEAE cellulose beads (DP 2070, 500 μm diameter, solids content 6.8%). Column 1.6 x 90 cm, BSA, molecuar weight 66,000. a. Superficial velocity 1 cm/min. b. Superficial velocity 2 cm/min. c. Superficial velocity 5cm/min.

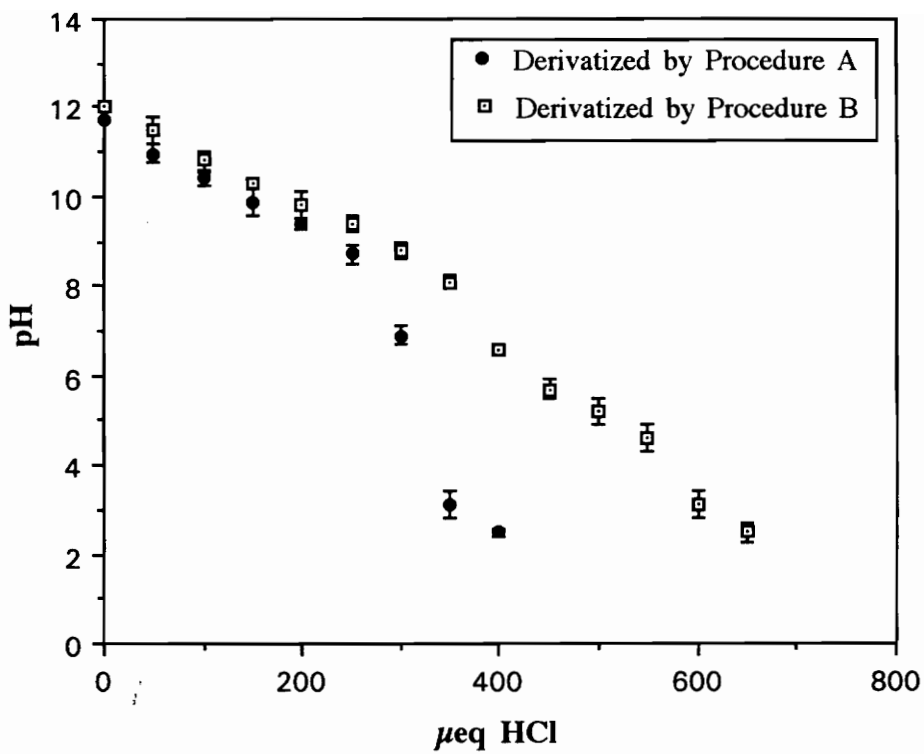**Figure 3:** **Titration curves of DEAE cellulose beads derivatized by procedures A & B**
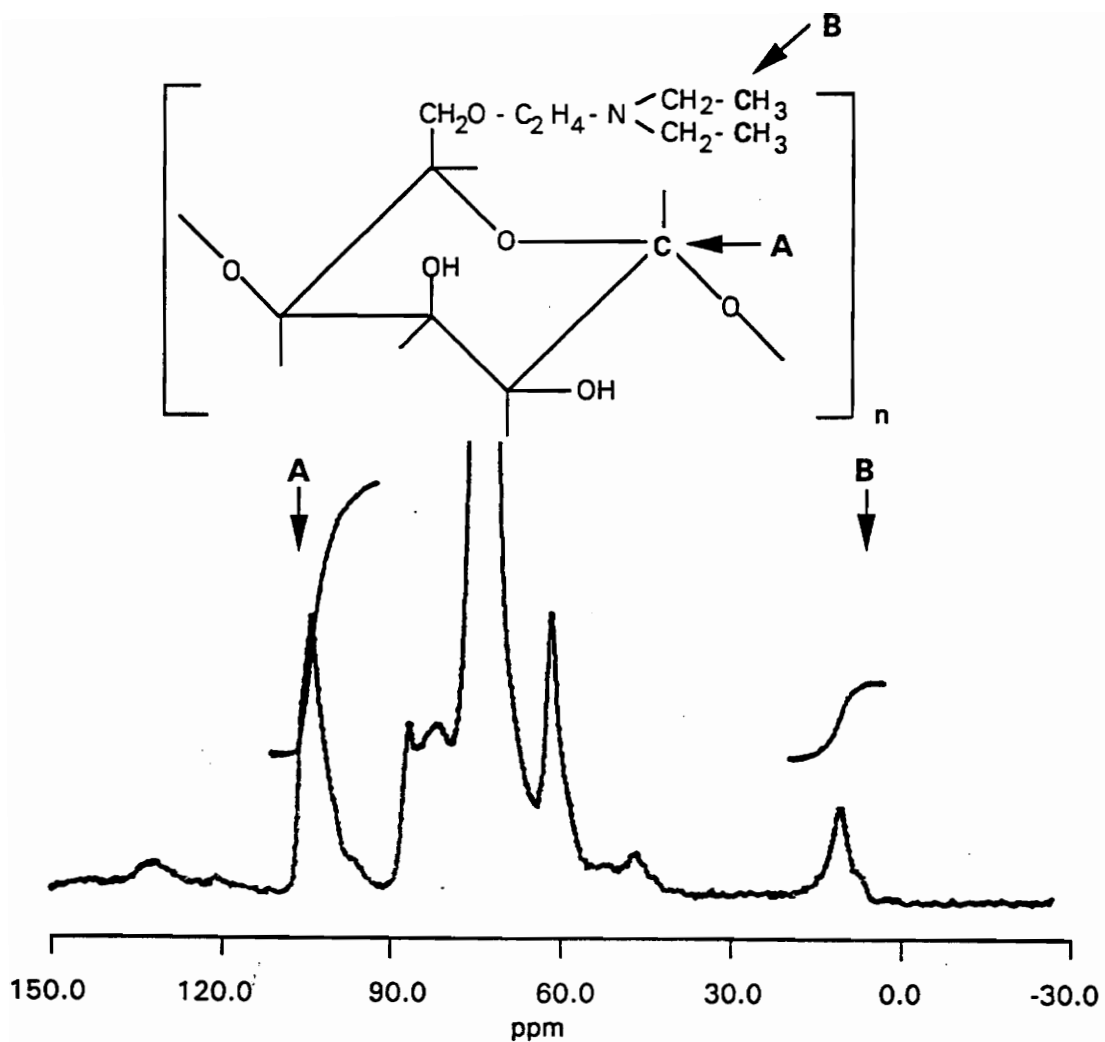
Figure 4: CP/MAS ^{13}C NMR of DE52 and partial molecular structure of DEAE cellulose
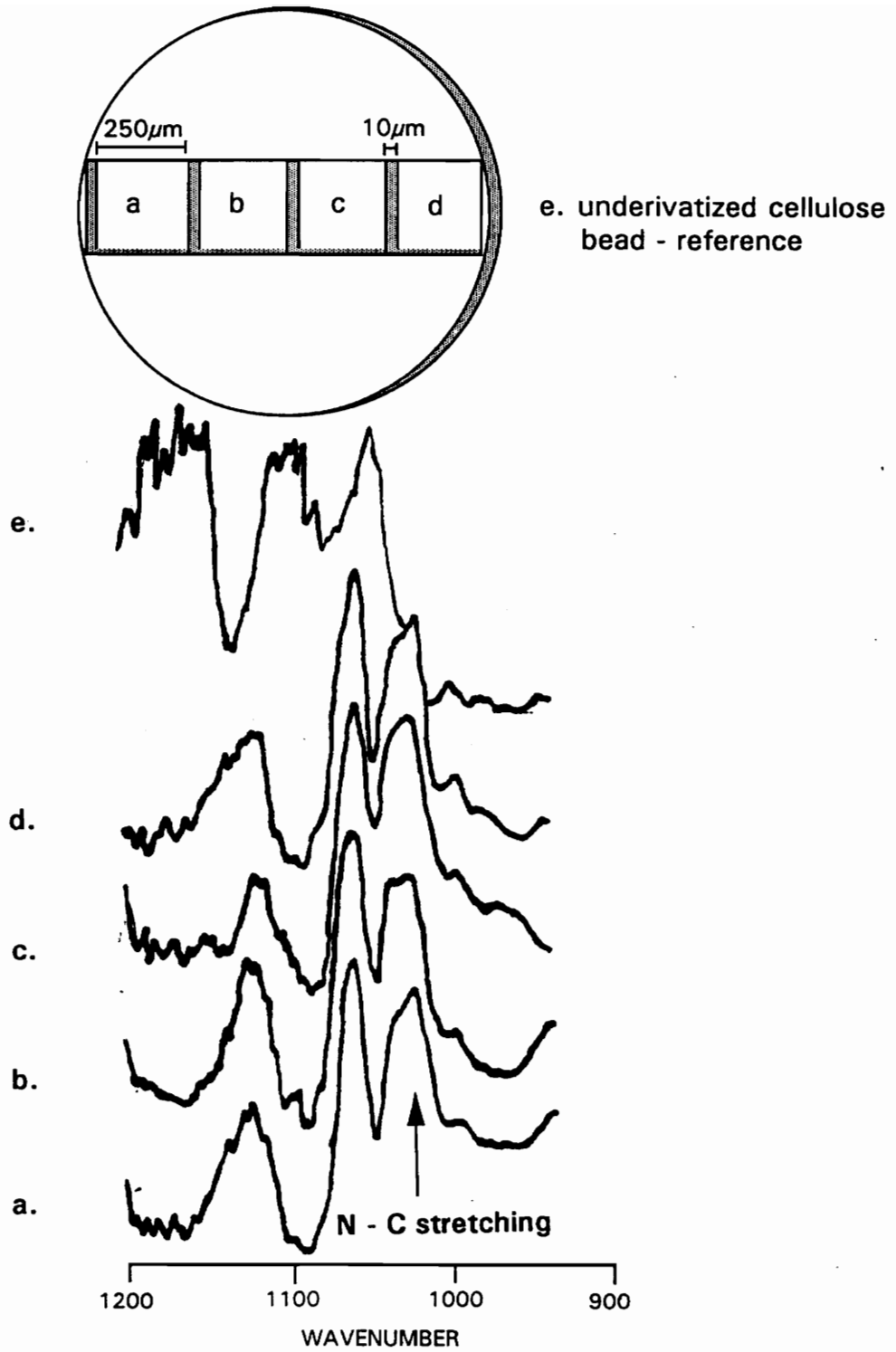
Figure 5: FTIR spectra across a DP 200, 1000 μm diameter, solids content 6.2% DEAE Cellulose Bead, compared to FTIR spectra of Underivatized Bead
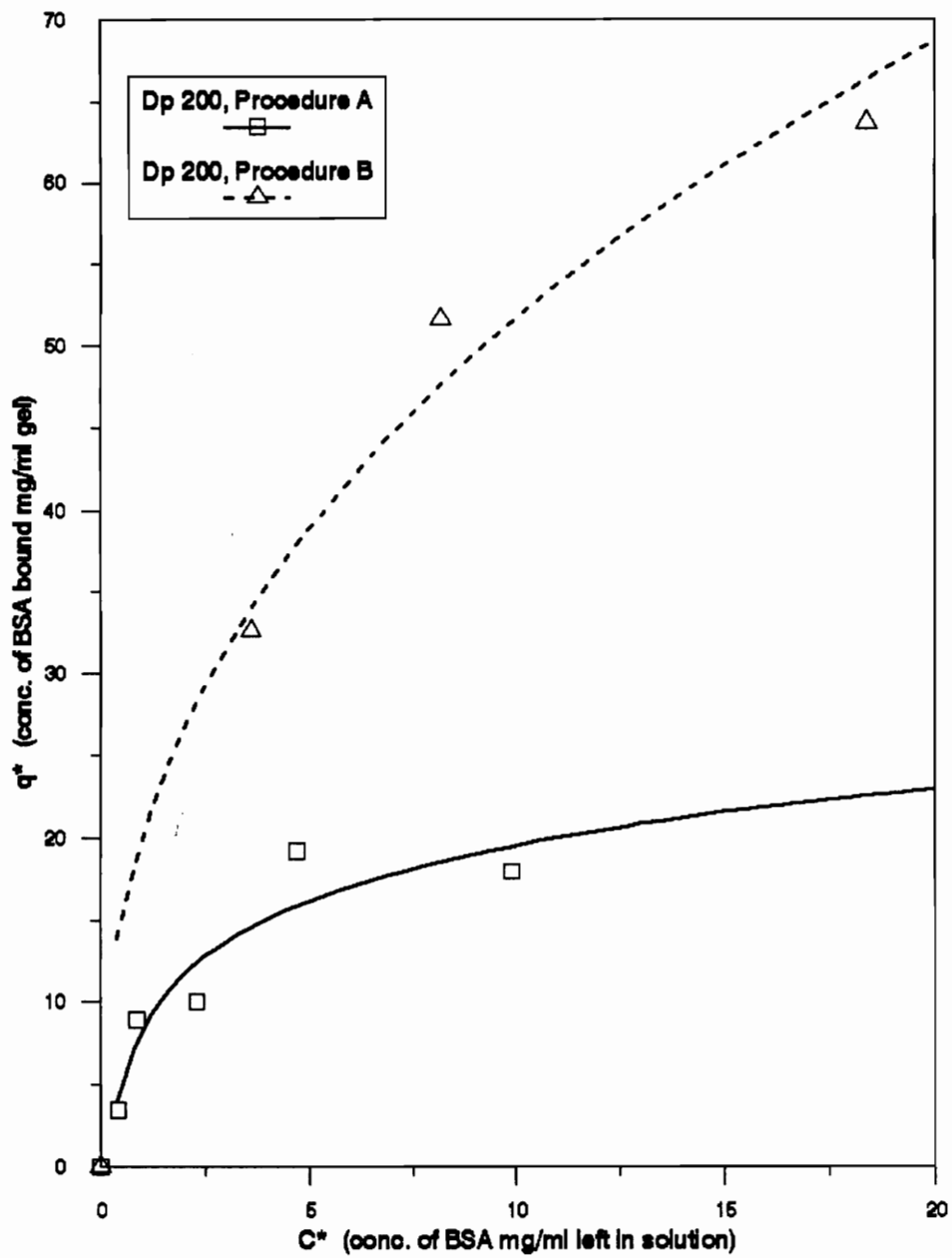
Figure 6a: Isotherm for DEAE cellulose beads derivatized by procedures A and B
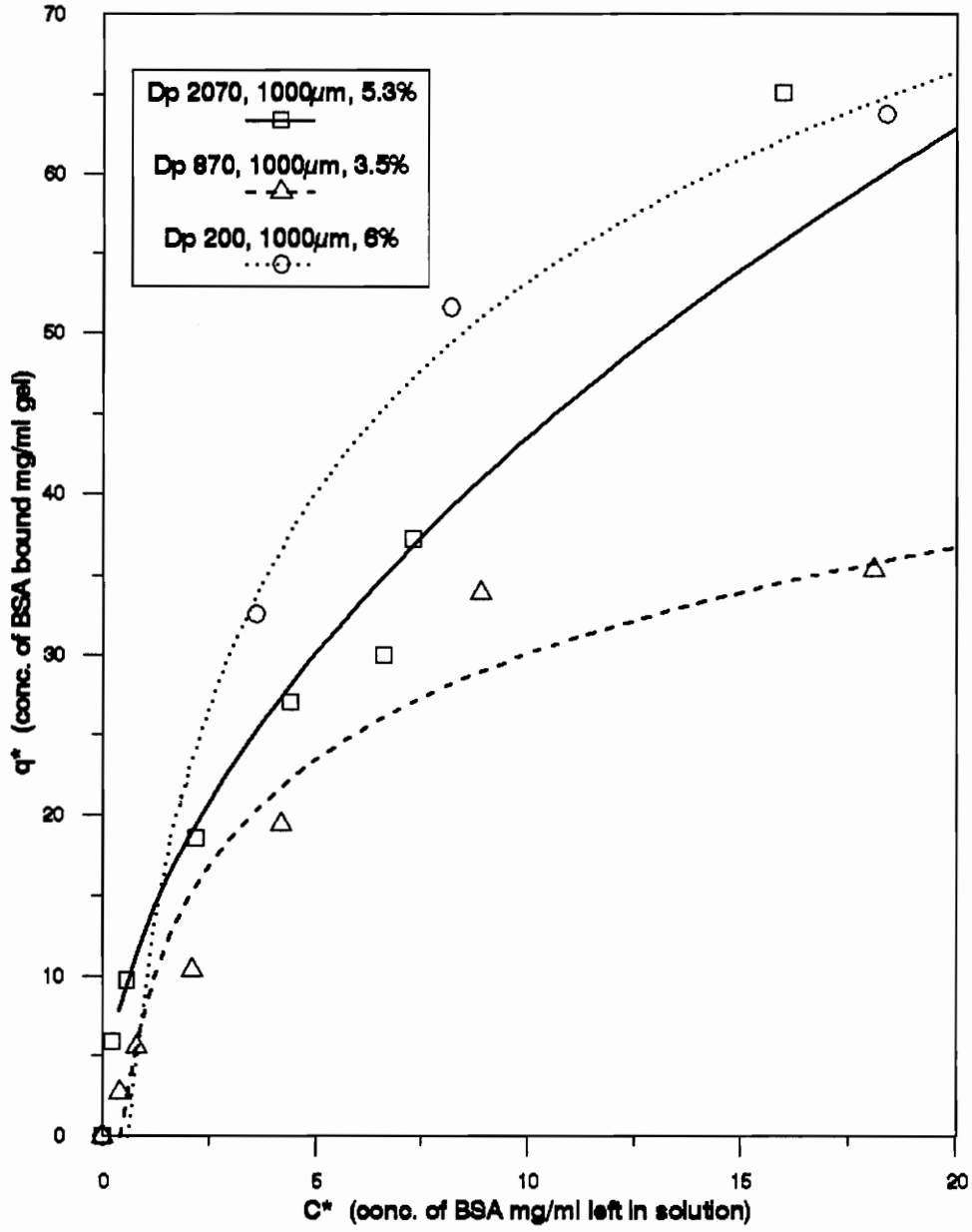
Figure 6b: Isotherms for varying degree of polymerization of DEAE cellulose beads
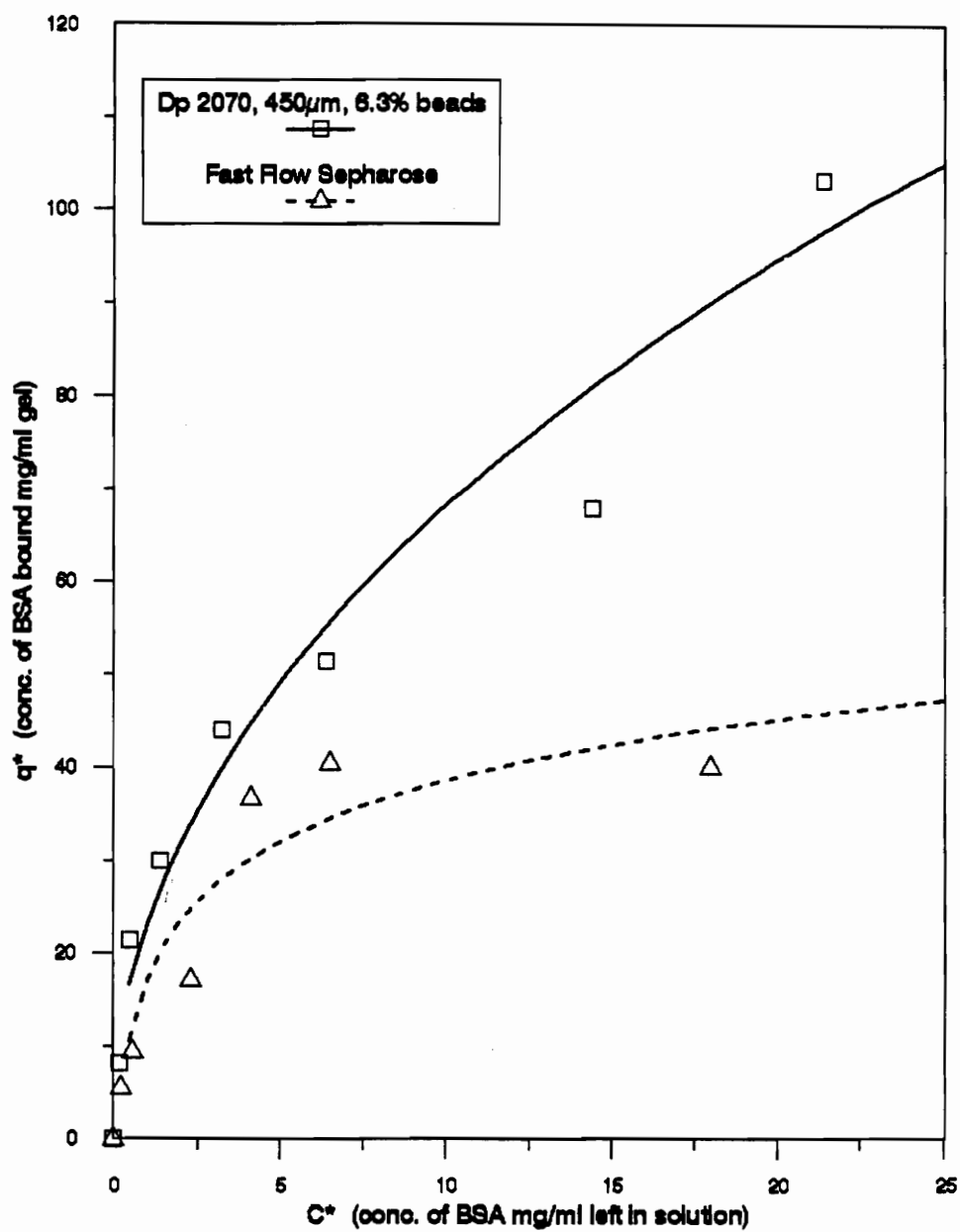
Figure 6c: Comaprison of isotherms of DEAE fast flow sepharose with DEAE cellulose beads
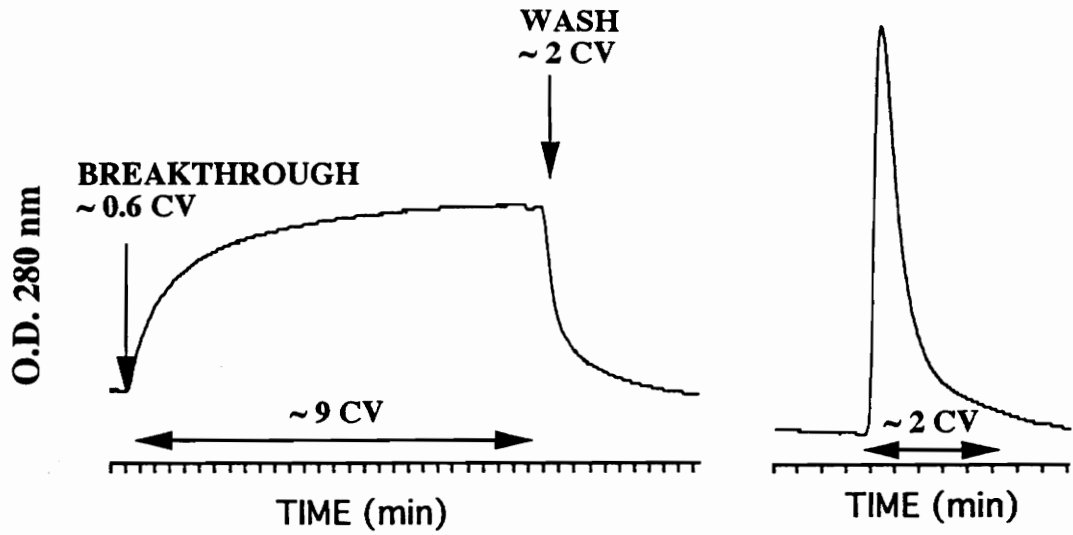
Figure 7a: Chromatogram of DEAE cellulose beads derivatized by Procedure A. Column 1x15 cm, Superficial velocity 5cm/min, load BSA 1mg/ml until > 75% breakthrough

Figure 6c: Comaprison of isotherms of DEAE fast flow sepharose with DEAE cellulose beads
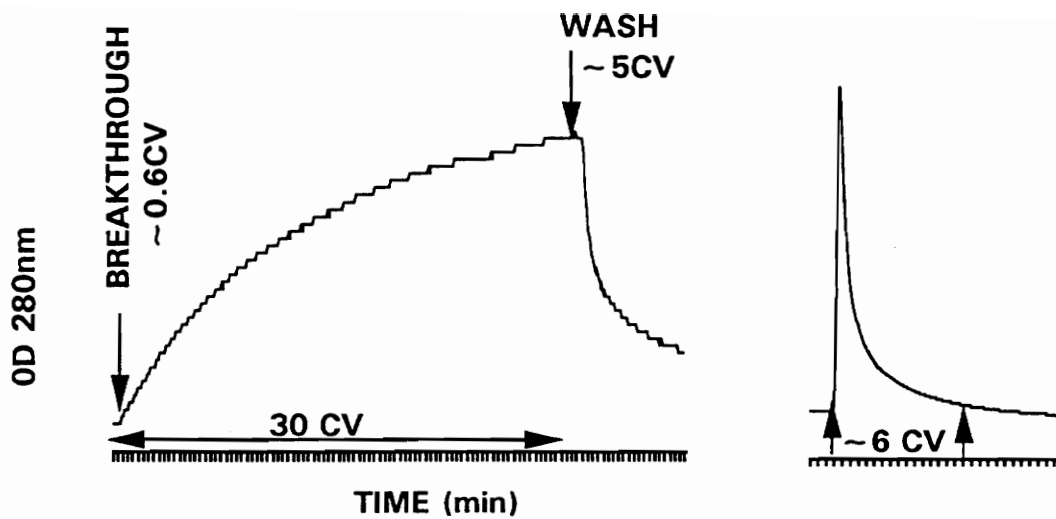
Figure 7b: Chromatogram of DEAE cellulose beads derivatized by procedure B. Column 1 x 15 cm, Superficial velocity 5 cm/min, 1 mg/ml BSA loaded until >75% breakthrough.

104
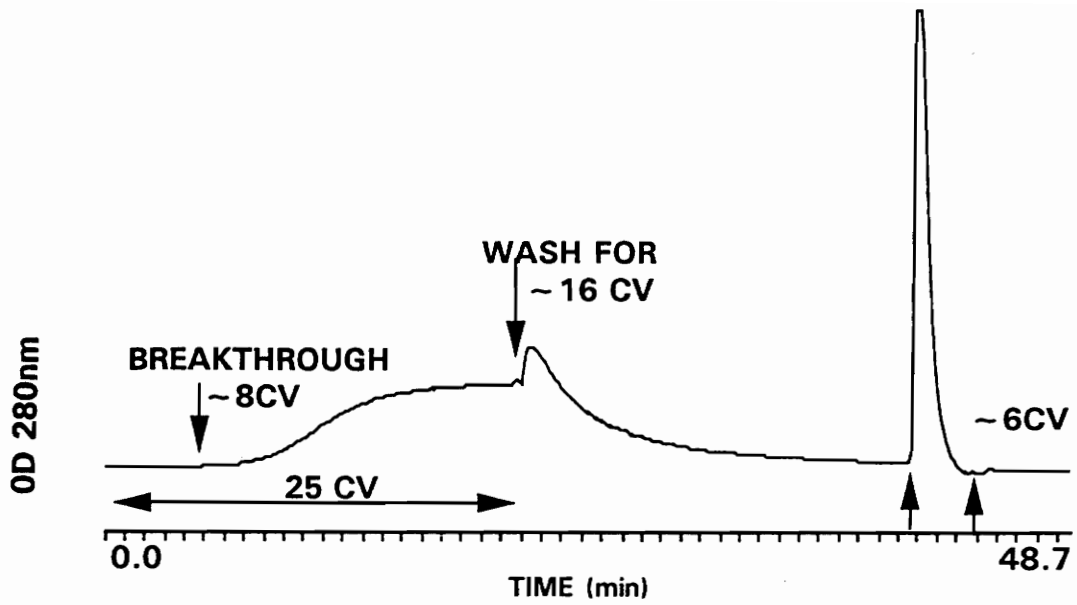
Figure 7c: Chromatogram of DEAE fast flow sepharose. Column 1 x 3 cm, Superficial velocity 5 cm/min, 1 mg/ml BSA loaded until > 80% breakthrough.
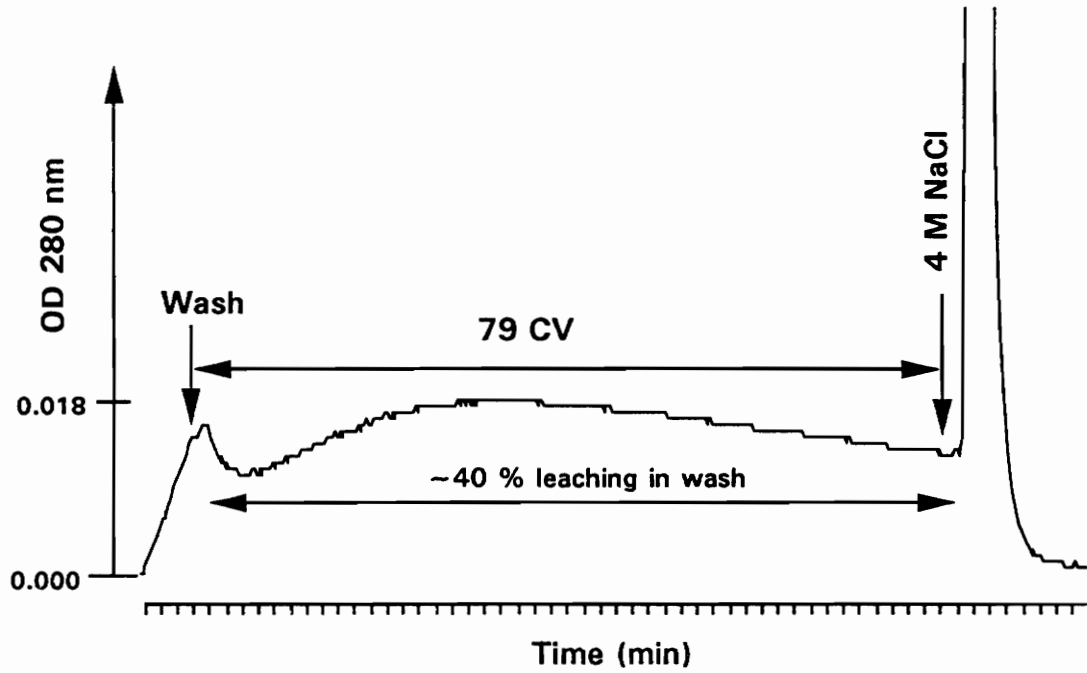
Figure 8: Chromatogram of partial saturation of BSA on DEAE fast flow sepharose. Column 1 x 3 cm, Superficial velocity 5 cm/min, 1 mg/ml BSA solution loaded until < 2% breakthrough.

106
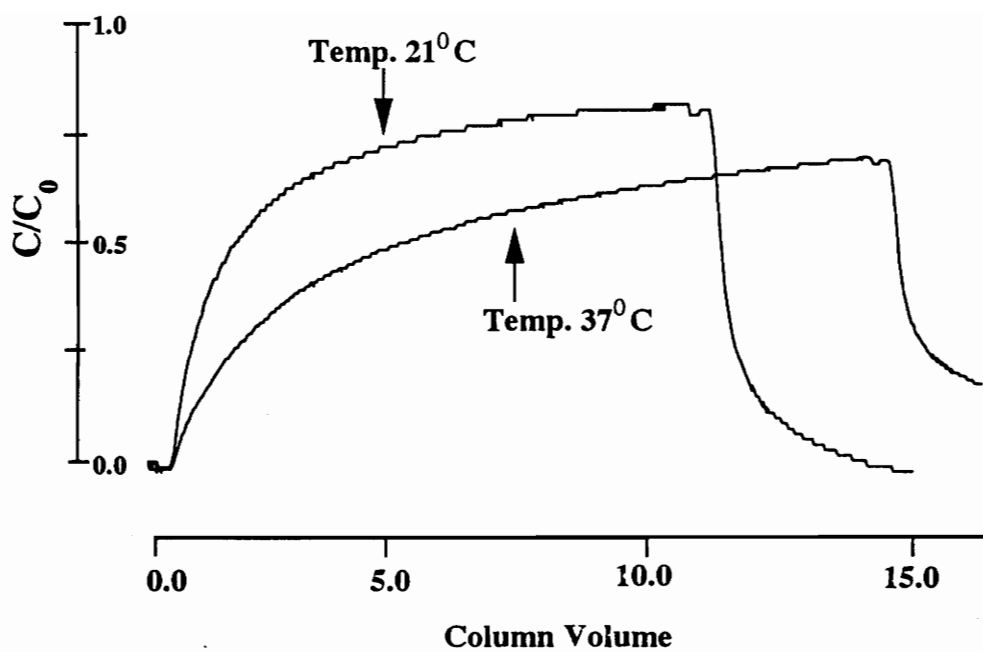
Figure 9a: Comparison of breakthrough curves for DEAE cellulose beads derivatized by Procedure A at temperatures 21^0C and 37^0C. Column 1 x 15 cm, Superficial velocity 5cm/min, 1mg/ml BSA solution loaded until > 70% breakthrough.
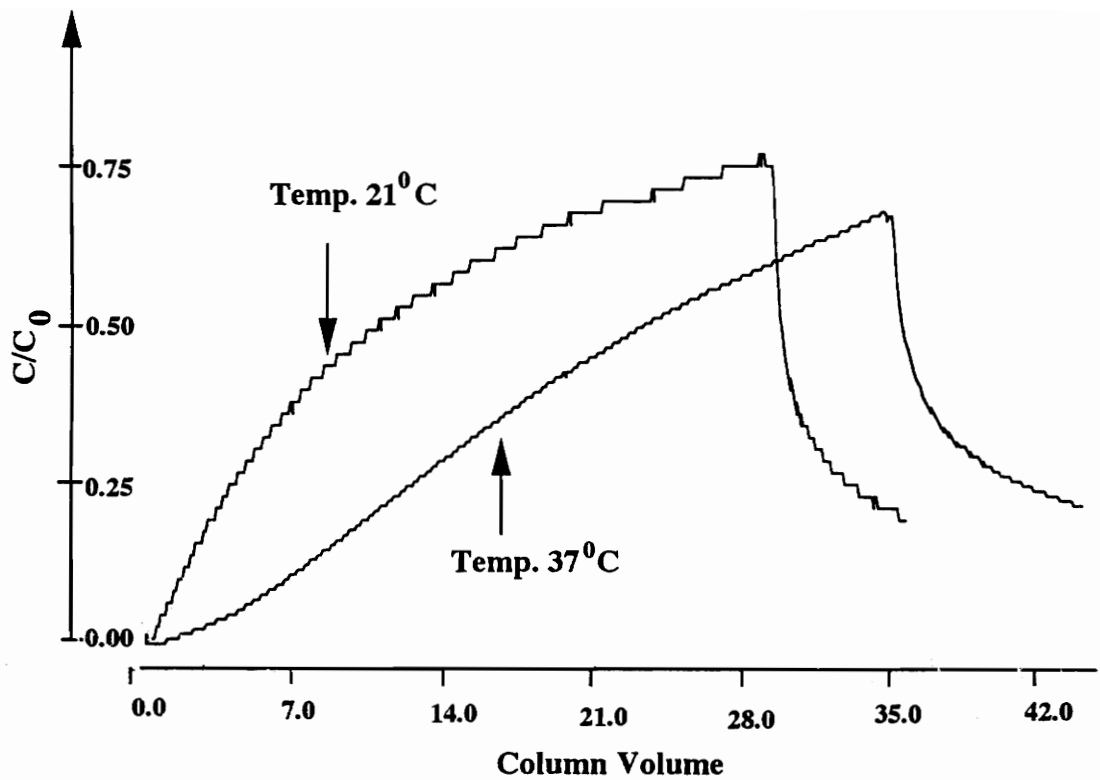
Figure 9b: Comparison of breakthrough curves for DEAE cellulose beads derivatized by procedure B at temperatures 21 ^{0}C and 37 ^{0}C. Column 1 x 15 cm, Superficial velocity 5 cm/min, 1mg/ml BSA solution loaded until > 70% breakthrough.

Chapter 5:

Expanded Bed Adsorption of Proteins Using Anion Exchange (DEAE-) Cellulose Beads

Abstract

A feasibility study was done for expanded bed adsorption application of DEAE cellulose beads. The beads exhibited comparable capacity for BSA in expanded and packed beds. A slow rise in breakthrough profile indicated that some transport limitations occur in DEAE cellulose expanded beds. The adsorption of recombinant human Protein C from transgenic porcine whey was limited by transport and sorption kinetics.

110

Introduction

The expanded bed is an attractive alternative to the packed bed of adsorbent beads for the direct adsorption of proteins from feedstocks containing whole cells or disrupted cells [1]. Feedstocks containing particulates can be directly applied to the bed without prior removal of the particulate by filtration or centrifugation. The application of particulate-containing feedstocks to conventional packed beds results in severe operational problems due to the rising pressure drop across the bed as the particulate matter gets filtered out by the bed and forms a filter cake. Processes including filtration, centrifugation, and solids settling, are generally expensive for large scale operations and may result in the loss of a considerable amount of desired protein. Thus a technique which enables the protein to be adsorbed from the feedstock, without a prior additional process to remove particulate matter, is of major interest.

The essential concept of the expanded bed is that as the bed expands due to the force of the liquid passing through it, the spaces between the adsorbent particles become larger allowing particulates to pass through the bed unhindered. Expanded beds have been used in the recovery of some bioproducts, namely antibiotics [2,3]. However, expanded beds for the adsorption of proteins have been envisaged only recently.

Ion exchange adsorbents are considered a suitable choice for expanded bed

111

procedures, as the ligands are very robust and can withstand the harsh operating cycles associated with the processing of crude feedstocks. Chase and Draeger [4] have used commercially available Q-fast flow sepharose to study expanded bed adsorption of proteins. A new product line by Pharmacia, Streamline, derivatized by ion exchange ligands has been recently introduced for use in expanded bed mode chromatography [5].

The aim of the work described here is to investigate the performance of large diameter DEAE cellulose beads in expanded bed mode using BSA as the model protein. This is followed by an investigation of the expanded bed adsorption performance of this adsorbent when used to purify recombinant human Protein C from porcine whey with particulates of precipitated proteins.

Methods and Materials

Large diameter DEAE cellulose beads of Dp 2070, 1000 μm and 450 μm diameter, solids content of 5.3% and 6.3% respectively, were derivatized by Procedure B as described in Chapter 4.

Recombinant human Protein C was obtained in the form of whey containing rhPC from transgenic pigs. These pigs were produced by the Department of Animal Sciences in conjunction with the American Red Cross and our laboratory.

Column Configuration

For packed beds the column configuration was similar to that described in Chapter 4. However, for expanded bed, screens with wider pore size were used on the adapter to allow unhindered passage of protein precipitate. Three-way valves were used, such that the protein could be loaded and washed in expanded bed mode and eluted in packed bed mode.

Binding and Elution Conditions

Binding and elution conditions for BSA in packed and expanded bed were as described in Chapter 4. Recombinant human Protein C feed stock was obtained in the form of precentrifuged milk whey-50 mM EDTA containing 300 μg/ml rhPC. Whey

was centrifuged for 30 minutes at 3400 x g (temperature, 4°C) and then gravity filtered to remove precipitates. Whey was then dialyzed against loading buffer (TBS, 0.05 M Tris, 0.1 M NaCl, pH 7.0) to remove all the EDTA. The whey thus obtained had an optical density of 35 and was stored at −90°C until further use. The whey was diluted in the ratio: one part whey to four parts TBS. Then 100 mM $ZnCl_2$ buffer solution was slowly added, while stirring, such that the whey had a final concentration between 5 to 10 mM $ZnCl_2$. The pH of the precipitate and supernatant mixture of whey proteins was adjusted to 7.0. The whey was allowed to stir for 30 minutes at 4°C before loading on the expanded bed. The whey was also loaded in batch (for three hours) and then column eluted. While loading, whey was continuously stirred to insure there was no settling of protein precipitate. The column was washed with loading buffer for two to three column volumes in the expanded bed mode to remove all the precipitate, and then the wash was continued in the packed bed mode for a total of six to seven column volumes. TBS 30 mM $CaCl_2$ was used to elute rhPC. All the other proteins bound to the column were eluted with 1 M NaCl. The column was regenerated with successive washes of TBS 5 mM EDTA and 4 M NaCl.

Protein C Assay

Protein C was assayed using sandwich ELISA with Polyclonal Assera C as the capturing antibody as described in Reference [6].

Electrophoretic Analysis

Non-reduced SDS-PAGE was performed on 12% gels. The gel was silver stained.

Results

Figure 1 presents a typical chromatogram for BSA adsorption/elution loaded onto DEAE cellulose beads (Dp 2070, 450 μm diameter) in packed and expanded bed. For packed bed, the breakthrough occurred at 0.6 column volumes and required 28 column volumes to attain 70% of inlet concentration. For expanded bed, the breakthrough occurred at 0.6 column volumes and required 40 column volumes to attain 70% of inlet concentration.

Table 1 presents the capacity for BSA/ml of DEAE cellulose beads in packed and expanded bed. DEAE cellulose beads of 1000 μm diameter have a capacity of 6.4 $\pm$ 0.3 mg BSA/ml of gel in packed bed and 6.0 $\pm$ 0.5 mg BSA/ml of gel in expanded bed. DEAE cellulose beads of 450 μm diameter have a capacity of 11.7 $\pm$ 0.0 mg BSA/ml of gel in packed bed and 9.0 $\pm$ 0.1 mg BSA/ml of gel in expanded bed .

A typical chromatogram for rhPC adsorption in expanded bed and elution in packed bed is presented in Figure 2. The whey was recycled for three to five column volumes with rhPC eluting in 2 column volumes in 30 mM $CaCl_2$ peak and 3 to 4 column volume in 1 M NaCl peak. SDS-PAGE (12%, non-reduced, silver stained) of the purification of rhPC in expanded bed mode is shown in Figure 3.

Table 2 presents the capacity for rhPC from porcine whey determined by batch and column loading on 450 μm diameter DEAE cellulose beads. The capacity for rhPC when batch loaded is 124 μgs for a 10 ml column, with a yield of 20%. The capacity for rhPC when column loaded is 82 μgs for a 10 ml column with a yield of 13%.

Discussion

Our studies have evaluated the feasibility of using DEAE cellulose beads in expanded bed, used for adsorption chromatography of mixture containing solids. These studies have correlated the difference between packed and expanded bed behavior with change in transport and sorption kinetics. The performance of expanded bed purification is a complex function of adsorbent design, feedstock properties and flow distributor design. For the protein adsorption to be efficient and reproducible, the expanded bed is required to exhibit stable fluid dynamics. DEAE cellulose beads at a superficial velocity of 5 cm/min expanded by 2.5 times and gave a very stable bed. We estimate the Dp 2070, 1000 and 450 μm diameter beads to have a density of ~ 1.08 g/cm^3. In comparison the densities of commercially available expanded bed beaded supports (DEAE Streamline/Pharmacia) are much higher (~ 1.45 gm/cm^3), to compensate for the fluid drag generated from their small size. This fluid drag would tend to cause flotation of the beads instead of expansion. The large size of the low density cellulose beads enables expansion without flotation in linear velocities ranging from 1 to 10 cm/min. An expansion between a factor of 2 to 3 is considered ideal, as the adsorbents do not loose too much of their capacity and there is enough voidage to allow unhindered passage of particulates through the column [1]. Thus, DEAE cellulose beads of 1000 μm and 450 μm diameter, Dp 2070, appear to have desirable fluid dynamic properties required for expanded bed applications.

The dynamic binding capacity of DEAE cellulose beads (Dp 2070), 1000 μm and 450 μm diameter beads is 6.4 and 11.7 mg BSA/ml of gel in packed bed and 6.0 and 9.0 mg BSA/ml of gel in expanded bed. In contrast, in expanded bed configuration the 450 μm diameter DEAE cellulose beads required 40 column volumes of feed to attain 70% of inlet concentration as compared to 28 column volumes of feed in packed bed. The slow rise of breakthrough curve is consistent with slow sorption kinetics due to protein binding site architecture, which these beads exhibit. However, a slower rise of breakthrough curve in expanded bed is indicative of slower mass transfer (Table 3), frequently found in expanded bed application [1].

The purification of rhPC from whey by conventional methods is a three step process: two ion exchange columns followed by an affinity column [7]. One of the major contaminants in porcine whey are α and β caseins, which bind under similar conditions to anion exchange columns as rhPC. Metal ions such as Ca^{2+}, Mg^{2+}, Zn^{2+}, and Cu^{2+} decrease the solubility of α and β caseins by forming coordinate complexes [8]. Moreover, transition metal ions like Zn^{2+}, at very low concentrations, can selectively precipitate proteins dependent on the free electrons available on the surface of the protein. For example, in the presence of 5 to 10 mM Zn^{2+}, β caseins are selectively precipitate out as compared to α casein or rhPC. Furthermore, this mixture of protein precipitate and supernatant loaded onto an expanded bed of DEAE cellulose beads can theoretically reduce the two step ion exchange step to one, giving relatively pure rhPC.

DEAE cellulose beads exhibit a low capacity of 82 μgs/10 ml of gel for rhPC in expanded bed, with a yield of 13%. Even when batch loaded, the capacity for rhPC is 124 μgs/10 ml of gel, with a yield of 20%. The rhPC eluted from DEAE cellulose beads is 3 fold purified, with a decrease in the ratio of β casein to rhPC (Figure 3). The low capacity for rhPC on DEAE cellulose beads is indicative of decreased adsorption due to transport and sorption kinetics. As already observed (for BSA), mass transfer limitations occur in expanded bed, but the presence of precipitate in feed (for rhPC) further reduces the mass transfer rate. It is also noted that rhPC has slow sorption kinetics as compared to BSA (data not shown) at the adsorption conditions used here. In addition, the formation of coordinate complexes of Zn^{2+} with negatively charged groups (essential for anion exchange chromatography) on rhPC can decrease the sorption kinetics further.

Conclusions

This study shows that expanded bed applications to large DEAE cellulose beads is feasible. The capacity for BSA in packed bed mode was similar to that in expanded bed mode. Low capacities for rhPC were not attributed to operation in the expanded bed configuration. Thus, the operating conditions (Zn^{2+} concentration) may need to be optimized for adsorption of a given system.

References

1. Draeger, N.M., and Chase, H.A., *Advances in Separation Processes (I. Chem. E. Symp. Ser. 118)*, (1990), 161-172.

2. Bartels, C.R., Kleiman, G., Korzun, N., and Irish, D.B., *Chem. Eng. Prog.*, (1958) **54**: 49-52.

3. Belter, P.A., Cunningham, F.L., and Chen, J.W., *Biotechnol. Bioeng.*, (1973) **15**: 533-549.

4. Chase, H.A., and Draeger, N.M., *Separation Science and Technology*, (1992) **27(14)**: 2021-2039.

5. *Streamline Expanded Bed Adsorption*, Method Handbook and Operators Manual, Pharmacia Fine Chemicals AB, Box 175, S-751 04 Uppsala 1, Sweden.

6. Morcol T., Akers R.M., Johnson J.L., Gwazdauskas F.C., Knight J., Lubon H., Drohan W.N. and Velander W.H., (in press).

7. Moore, T., unpublished data.

8. Thompson M.P., Gordon W.G., Boswell R.T., Farrell H.M.Jr., *J. Dairy Science*, (1969) **52(8)**: 1166-1173.

Table 1: Capacity of DEAE cellulose beads in packed and expanded bed

Material*	Packed Bed Height (cm)	Superficial Velocity (cm/min)	Packed Bed Capacity (mg BSA/ml gel)	Expanded Bed Capacity (mg BSA/ml gel)
DP 2070, 1000 μm 2.1% → 5.3%	13.0	5	6.4 ± 0.3	6.0 ± 0.5
DP 2070, 450 μm 4.2% → 6.3%	15.0	5	11.7 ± 0.0	9.0 ± 0.1

* Degree of Polymerization, bead diameter, solids content before and after derivatization

Table 2: Capacity for rhPC on expanded bed DEAE cellulose beads

Mode of operation	30 mM $CaCl_2$ peak (μgs)	1 M salt peak (μgs)	Total rhPC[*] (μgs)	Yield
Batch load-column elution	28	96	124	20%
column load & elution	53	29	82	13%

* column: 10 ml, superficial velocity: 5cm/min,
  DEAE cellulose beads: DP 2070, 450 μm diameter,
  solids content 6.3%.

Table 3: Comparison of rate limiting step in packed and expanded beds

Mode of Operation	Transport Limitations	Sorption Limitations
Packed Bed (BSA)	Fast	Slow
Expanded Bed (BSA)	Slower	Slow
Packed Bed (rhPC)		Slow
Expanded Bed (rhPc)	Very Slow (due to ppt)	Very Slow (due to Zn rhPC complex)
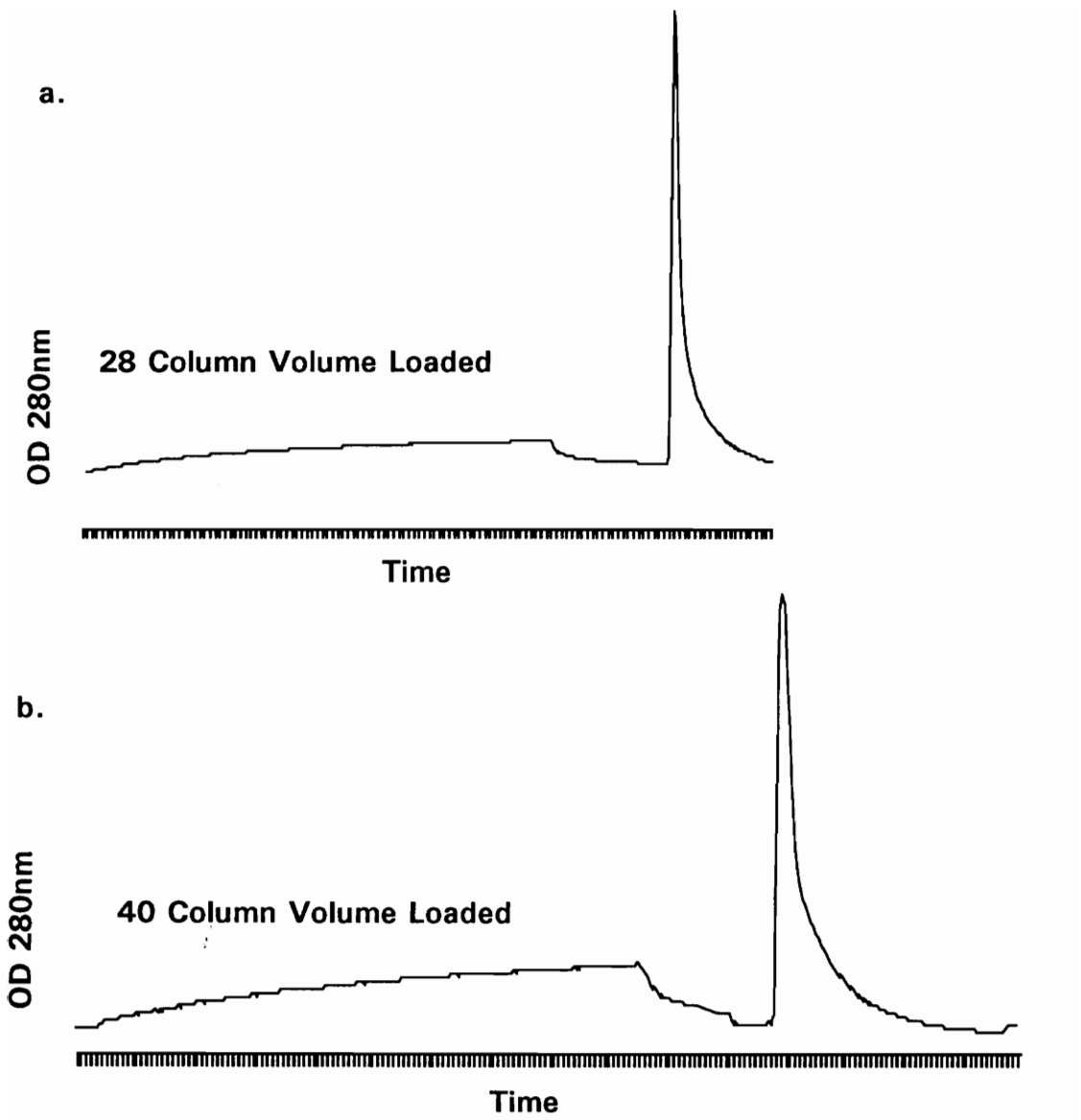
Figure 1: Chromatograms of DEAE Cellulose Beads (DP 2070, 450 μm diameter, solids content 6.3%) in: a. packed bed b. expanded bed. Column 1 x 15 cm, superficial velocity 5 cm/min, 1 mg/ml BSA solution loaded until > 70% breakthrough.
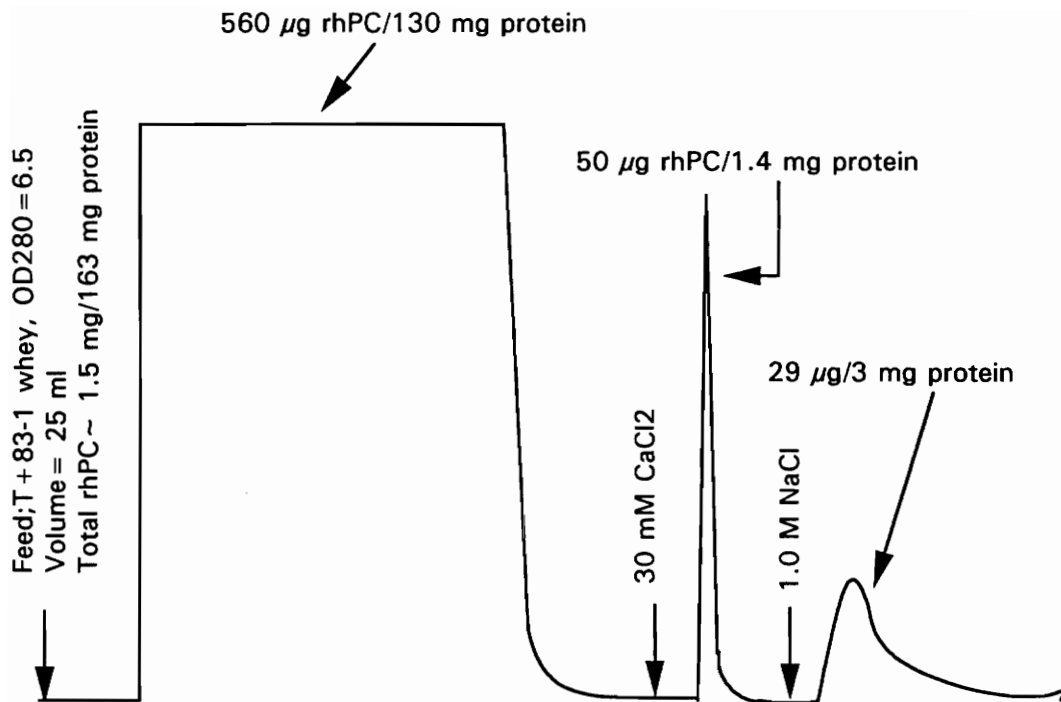
Figure 2: Chromatogram for purification of rhPC using (DP 2070, 450μm diameter, Solids content 6.3%) DEAE cellulose beads in expanded bed mode. Column: 1 x 13 cm, Superficial velocity: 5 cm/min, Total protein loaded: 16 mg protein/ml gel
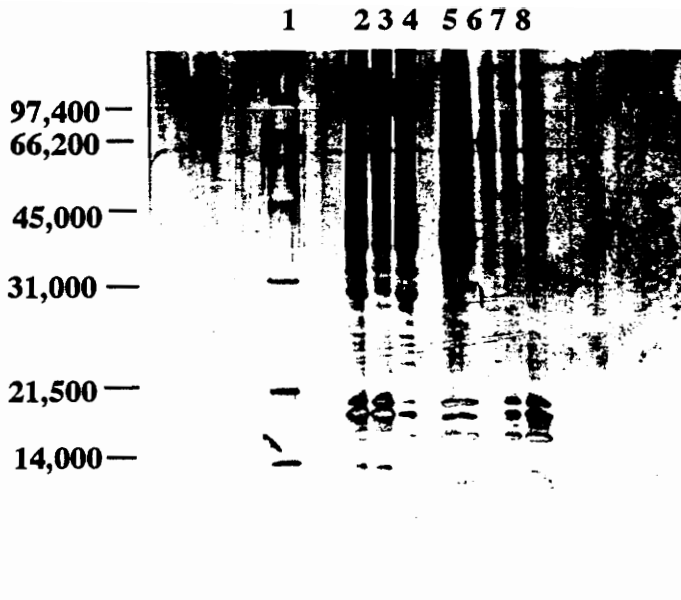
Figure 3: SDS-PAGE (12%, non-reduced, silver stained) for purification
of rhPC from whey in expanded bed using DEAE cellulose beads.
1. Molecular weight markers 2. Transgenic pig 83-1 milk whey 3.
Feed supernatant 4. Feed precipitate 5. 30 mM CaCl2 eluate
6. Immunopurified rhPC reference 7. 1M NaCl
8. Fall through (supernatant)

Chapter 6:

Purification of IgG from Hybridoma Cell Culture Supernatant Using Anion Exchange (DEAE-) Cellulose Beads

Abstract

The feasibility of using large diameter DEAE cellulose beads for preparative scale purification of proteins has been evaluated. IgG from hybridoma cell culture supernatant was purified using frontal chromatography on two successive DEAE cellulose bead columns. High throughput was achieved, as a 40 x 5 cm column could be operated at a superficial velocity of 10 cm/min without the pressure drop exceeding 20 psi. A yield of 85% and product purity of 70% was achieved at bench and preparative scale.

Introduction

A support matrix for process scale purification of proteins requires that the matrix have good mechanical strength to increase throughput along with other properties like high degree of porosity and hydrophilicity. In most commercially available matrices the lack of mechanical strength causes the matrix to compress at high flow rates and results in a rising back pressure. Moreover, in order to avoid contamination and keep the operating costs low, peristaltic pumps are preferred over HPLC pumps for loading proteins. However, peristaltic pumps cannot withstand a pressure drop greater than 20 psi across the column. To overcome these problems, large diameter DEAE cellulose beads have been used as a probable support matrix for preparative scale protein purification in this study. These beads exhibit low pressure drop across the column as well as exhibit high mechanical strength [1].

Immunoglobulins are being produced in large scale using Hybridoma cell culture technology [2,4] and purified by conventional methods using ultrafiltration, anion exchange chromatography or affinity chromatography followed by gel filtration [3,4]. The product purity achieved with anion exchange chromatography usually ranges from 40% to 90% [4]. The product purity achieved here, using DEAE anion exchange cellulose beads ranged between 70% to 80%.

Methods and Materials

Large diameter cellulose beads were produced by the Biobased Materials Center at Virginia Tech. Lignocellulose from yellow poplar was steam exploded and bleached by the classical CEH (Chlorination Alkali Extraction Hypochloride) method to remove all soluble lignin [5]. The cellulose thus obtained was beaded [6]. Modification of these beads by Procedure A was performed in batches of 500 ml. Underivatized cellulose beads had a diameter of 875 ± 140 μm and $4.2 \pm 0.2\%$ solids content. However, DEAE cellulose beads had a diameter of 760 ± 110 μm, and $6.5 \pm 0.5\%$ solids content.

Hybridoma Cell Culture supernatant of Anti human Protein C murine monoclonal antibody 7D7B10 was produced by Baxter Hyland and supplied by the American Red Cross. Anti human Protein C murine monoclonal antibody 7D7B10 standard was also kindly provided by the Holland Laboratory, of the American Red Cross, Rockville, MD.

Anti mouse IgG peroxidase conjugate and albumin reagent were purchased from Sigma. O-Phenylenediamine.2HCl was purchased from Abbot Laboratories. All reagents used to make buffers were of the highest grade.

Column Configuration

C10/20, and C10/40 jacketed columns (Pharmacia) were used to study operating

132

parameters for process scale purification of IgG.   A XK50/60 jacketed column (Pharmacia) was used to perform the preparative scale purification. To avoid excessive pressure drop the end fittings for XK50/60 jacketed column were custom-made in the departmental workshop for large diameter tubes for protein and buffer delivery.   A recirculating cold water bath, RM6 Lauda by Brinkmann, was used to cool the columns to 4-7°C. Protein rich feeds as well as buffers were pumped through a Master Flex pump (Cole-Palmer). Quick load 7513 pump head was used to study the operating parameters for scale-up and a 7017 pump head was used to perform the preparative scale purification. Protein output was measured with a Knauer UV detector with a high flow rate variable path length flow cell (Sonntek). Data collection was controlled through Rainin Dynamax system.

EIA to detect IgG

The data for IgG presented in Tables 1 through 4 was obtained from an EIA (Enzyme Immuno Assay) sandwich.   Microtiter plates (Immulon II, Dynatech Laborataries) were coated with 100 μl of Prothrombin solution of 50 μg/ml concentration in 0.1 M Sodium Bicarbonate, 0.2 M Sodium Chloride, pH 9.6 overnight at 0-4°C. The microtiter plates were washed with TBS, 25 mM EDTA, 0.05% Tween and stored at 0-4°C. The plate was washed again before usage and blocked at 25°C for 30 minutes with TBS, 25 mM EDTA, 0.1% PEG, pH 6.5. Following washing, varying concentrations of IgG standard and samples in TBS, 25 mM EDTA, 0.1% PEG, pH 6.5 were added to

the coated wells and incubated at room temperature for 3 hours with shaking. The wells were then washed and incubated with 1:1000 diluted HRP conjugated goat anti mouse immunoglobulin in TBS, 25 mM EDTA, 0.1% PEG, pH 6.5 for 3 hours at room temperature with shaking. The wells were again washed and HRP activity detected with OPD substrate by absorbance at 490 nm using a EL308 microplate reader (Bio-Tek).

BSA Assay

The dye binding assay with albumin reagent to detect BSA is described in Chapter 4.

Electrophoretic Analysis

SDS-PAGE was performed according to the method of Laemmli [7], using 8-25% gradient Phastgel (Pharmacia) as well as 4-15% gradient gel from Bio Rad. The area percent purity of IgG SDS-PAGE was performed using a Shimadzu CS9000 flying spot scanning densitometer at wavelength 570 nm. The SDS-PAGE was stained with 2% Coomassie brilliant blue R.

Optimization of operating parameters for scale-up

The supernatant was concentrated by a hundred fold using the Millipore pellicon cassette, having a nominal molecular weight cut off value of 30,000. The retentate

obtained was used as feedstock for optimization as well as preparative scale purification. The superficial velocity was optimized to attain maximum throughput and minimize loss of capacity. The capacity of DEAE cellulose beads at varying superficial velocities of 5, 10, and 15 cm/min was determined. The retentate was diluted 1:10 with TBS pH 8.0 buffer and loaded until breakthrough occurred. Protein bound to the column was eluted with 1 M salt and assayed for BSA and IgG (Table 1). The effect of protein concentration on the capacity of DEAE cellulose beads was also determined. The retentate was diluted 1:1, 1:2, 1:10, and 1:100 with TBS pH 8.0 buffer and loaded until breakthrough occurred. The protein bound to the column was eluted with 1 M salt and was assayed for BSA and IgG (Table 2). The capacity as a function of pulse loading retentate containing 25, 50, 75 and 100% BSA (dynamic binding capacity of BSA per volume of gel at a linear velocity of 10 cm/min) was determined (Table 3). The fall-through from pulse loading retentate containing 50 and 75% BSA chromatographies, were reloaded on the column. This was repeated until required product purity was achieved (Table 4).

Results

Table 1 presents the effect of superficial velocity on the dynamic binding capacity of large DEAE cellulose beads loaded until 90% breakthrough. At a superficial velocity of 5 cm/min, 556 $\pm$ 17 μg of BSA and 12.4 $\pm$ 6.7 μg of IgG bound per ml of gel. At a superficial velocity of 10 cm/min, 483 $\pm$ 27 μg of BSA and 13.4 $\pm$ 5.0 μg of IgG bound per ml of gel. At a superficial velocity of 15 cm/min, 431 $\pm$ 31 μg of BSA and 7.7 $\pm$ 2.0 μg of IgG bound per ml of gel.

Table 2 presents the effect of protein concentration on the dynamic capacity of DEAE cellulose beads as well as the selectivity of the column. At a 1:100 dilution of retentate loaded until 90% breakthrough, the capacity of the beads is 225 $\pm$ 20 μg BSA/ml of gel, with 5% of total protein bound to the column being IgG. At a 1:10 dilution of retentate loaded until 90% breakthrough, the capacity of the beads is 573 $\pm$ 20 μg BSA/ml of gel, with 3% of total protein bound to the column being IgG. At a 1:2 dilution of retentate loaded until 90% breakthrough, the capacity of the beads is 690 $\pm$ 44 μg BSA/ml of gel, with 3% of total protein bound to the column being IgG. At a 1:1 dilution of retentate loaded until 90% breakthrough, the capacity of the beads is 974 $\pm$ 112 μg BSA/ml of gel, with 3% of total protein bound to the column being IgG.

Table 3 presents product purity as a function of pulse loading retentate containing

25, 50, 75 and 100% BSA (dynamic binding capacity of BSA per ml of gel at a linear velocity of 10 cm/min). Upon pulse loading retentate containing 25% BSA, 48% product purity and 86% yield was achieved. Upon pulse loading retentate containing 50% BSA, 42% product purity and 90% yield was achieved. Upon pulse loading retentate containing 75% BSA, 31% product purity and 92% yield was achieved. Upon pulse loading retentate containing 100% BSA, 31% product purity and 93% yield was achieved.

Table 4a presents the data of reloading fall-through from the above chromatographies until required product purity was achieved. When fall-through from pulse loading retentate containing 50% BSA chromatography was reloaded, 70% product purity and 97% yield was achieved. The overall yield for the two step process was 87%. When fall-through from pulse loading retentate containing 75% BSA chromatography was reloaded, 51% product purity was achieved. The fall-through from the above chromatography was reloaded to achieve a product purity of 78%. The overall yield for the three step process was 83%

Figure 1 presents the schematic for the purification process of IgG. Typical chromatograms for the two step purification process of IgG on DEAE cellulose beads are presented in Figure 2. The product purity as determined by electrophoresis is shown in Figure 3.

Discussion

We seek to optimize operating parameters for the purification of IgG from Hybridoma cell culture supernatant and study the feasibility of scale-up using DEAE cellulose beads. The capacity of hydrogels is a complex function of superficial velocity, feed concentration, column length, and adsorbent design. DEAE cellulose beads from yellow poplar cellulose used here had twice the dynamic capacity for BSA at a superficial velocity of 10 cm/min as compared to cotton cellulose with similar diameter and degree of substitution (data not shown). Moreover, these beads exhibit no limitations with respect to transport or sorption kinetics (detailed in chapter 4). Furthermore, DEAE cellulose beads have high mechanical strength as well as exhibit low pressure drop across a packed bed [1]. Thus, these DEAE cellulose beads of 760 ± 110 μm diameter and $6.5 \pm 0.5\%$ solids content have the required properties for preparative scale application.

Frontal chromatography (usually give higher yields as compared to elution chromatography) was performed on DEAE cellulose beads to purify IgG from hybridoma cell culture supernatant. To stimulate growth, bovine serum albumin is supplemented to the culture medium and is a major contaminant in the supernatant. Thus, these studies concentrated on the removal of BSA for the purification of IgG. The conditions for frontal chromatography were obtained from an analytical (elution) chromatography performed by Stickler *et al* [8]. The ionic strength and pH of the loading buffer allowed

BSA to bind to the column giving an IgG-rich fall-through.

While DEAE cellulose beads, exhibited lower dynamic binding capacity of 483 μg BSA/ml of gel at a superficial velocity of 10 cm/min compared to 556 μg BSA/ml of gel at a linear velocity of 5 cm/min they have a higher throughput at the higher velocity. Moreover, the percentage of IgG bound with respect to BSA bound at superficial velocities 5 and 10 cm/min was similar and ranged between 2 to 3 %. At a superficial velocity of 15 cm/min, the pressure drop through the 5 cm diameter column was determined to be too high for peristaltic pumps to work efficiently. Thus, a superficial velocity of 10 cm/min was identified for scale up.

As the concentration of retentate loaded on the DEAE cellulose bead column increases, the dynamic capacity of DEAE cellulose beads per volume also increases from 225 μg BSA/ml of gel at 1:100 dilution to 975 μg BSA/ml of gel at no dilution. Moreover, the ratio of IgG bound to BSA bound over 1:1, 1:2, and 1:10 dilutions ranges between 3 to 5%. Thus, the retentate was used for loading during scale-up.

Pulse loading retentate containing 50 and 75% BSA (dynamic binding capacity of BSA at a linear velocity of 10 cm/min) on DEAE cellulose beads gave a product purity of 42 and 31% and a yield of 90 and 92% respectively. While the fall through from pulse loading retentate containing 50% BSA chromatography was loaded once on

a DEAE cellulose column to achieve 70% product purity and an overall yield of 87%, the fall through from pulse loading retentate containing 75% BSA chromatography was loaded twice on a DEAE cellulose bead column to achieve 78% product purity and an overall yield of 83%. Thus, the two step procedure was chosen for preparative scale purification.

As suggested in literature [9,10] scale up of an ion exchange column requires that the column diameter be increased while keeping the bed height constant. However, for DEAE cellulose beads, no significant change in capacity was observed when the bed height was increased from 15 to 30 cm (data not shown). Thus, for preparative scale purification, the retentate was loaded on a 41 x 5 cm column at a superficial velocity of 10 cm/min.

As evident from the chromatograms of preparative scale purification of IgG, the time scale for each run is about 16 minutes and is extremely short for a 41 x 5 cm column. Considering time required for regeneration of the column, 30 minutes is ample run time for each purification step. This provides a very cost effective throughput, with 125 to 150 mgs of IgG being produced every hour, and about a gram in a day of 8 working hours.

The product purity of 70% and overall yield of 85% achieved at preparative scale

were very similar to product purity of 70% and overall yield of 87% achieved at bench scale. The product purity can be further increased by gel filtration chromatography. As the purified IgG was mainly used *in vitro*, for diagnostic purposes and preparation of affinity columns the purity achieved was considered sufficient for this application.

Conclusions

The study shows that large diameter DEAE cellulose beads have feasibility and inherent advantages for large scale purification applications. High throughput was achieved, as beads exhibited good mechanical strength and low pressure drops across a a 5 cm diameter column at a superficial velocity of 10 cm/min. Moreover, product purity and yields at large scale were similar to those obtained at bench scale.

References

1.   W.H. Velander, J.A. Kaster, G. Kumar, K. van Cott, W. de Oliviera and W.G. Glasser, *Cellucon '92 Selective Purification and Separation Processes: The Role of Cellulosic Materials* (1992).

2.   Yarmush, M.L., Antonsen, K.P., Sundaram, S., Yarmush, D.M., "Immunoadsorption: Strategies for Antigen Elution and Production of Reusable Adsorbents", *Biotechnol. Prog.*, (1992), **8** (**3**): 168-178.

3.   Schmidt, C., *Journal of Biotechnology*, (1989) **11**: 235-252.

4.   Ostlund, C., "Large-scale purification of monoclonal antibodies", *Tibtech.*, (Nov 1986), 288-293.

5.   Singh, R.P., "Handbook of Pulp and Paper", second edition, Britt, K.W., ed., Van Nostran Reinhold, NY, NY (1970), p. 249.

6.   Velander, W.H., Kaster, J.A., Glasser, W.G., "Lignocellulosic and Cellulosic Beads for use in Affinity and Immunoaffinity Chromatography of High Molecular Weight Proteins". US Patent Application No. 07/496314.

7.   Laemmli, U.K., *Nature (London)*, (1970) **227**: 680-685.

8.   Strickler, M.P., and Gemski, M.J. (1987), "Single-Step Purification of Monoclonal Antibodies by Anion Exchange High-Performance Liquid Chromatography", Bioprocess technology, vol 2, "Commercial Production of Monoclonal Antibodies: A Guide for Scale-Up, Seaver, S.S., editor.

9.   Janson, J.C. and Hedman, P., "On the Optimization of Process Chromatography of Proteins", *Biotechnology Progress*, (1987), **3 (1)**: 9-13.

10. Tsai, A.M., Englert, D., Graham, E.E., "Study of the dynamic binding capacity of two anion exchangers using bovine serum albumin as a model protein", *J. of Chromatography*, (1990) **504(1)**: 89-95.

Table 1: Capacity of BSA and IgG on DEAE cellulose beads at varying superficial velocities

Superficial Velocity (cm/min)	IgG Bound[a] (μg/ml beads)	BSA Bound[b] (μg/ml beads)	% BSA[c] Bound
5	12.4 ±6.7	556 ± 17	97.8
10	13.4 ±5.0	483 ± 27	97.3
15	7.7 ±2.0	431 ± 31	98.2

a IgG concentration as determined by EIA
b BSA concentration as determined by BSA assay
c % of BSA bound with respect to the total protein bound/ml of beads

Table 2: Capacity of BSA and IgG on DEAE cellulose beads at varying feed concentration

Dilutions of Retentate	IgG Bound[a] (μg/ml beads)	B.S.A Bound[b] (μg/ml beads)	Ratio of [c] IgG /B.S.A. Bound
1:100	11.9 ± 1.4	225 ± 20	0.053
1:10	17.8 ± 1.4	573 ± 20	0.031
1:2	23.4 ± 3.1	690 ± 44	0.034
1:1	29.5 ± 5.0	974 ± 112	0.030

Superficial velocity:10cm/min.
a IgG concentration as determined by EIA
b BSA concentration as determined by BSA assay
c Ratio of IgG : BSA bound /ml of beads

Table 3: Optimization of pulse loading retentate volume

Fraction of [a] Total Capacity Loaded	Purity of Product [b]		IgG Bound [c] (μg/ml of beads)	BSA Bound [d] (μg/ml of beads)	Yield (%)
	%BSA	%IgG			
0.25	42	48	7.5 ± 2.3	142 ± 30	86
0.5	48	42	7.5 ± 0.0	200 ± 10	90
0.75	57	31	6.8 ± 2.2	249 ± 10	92
1.0	59	31	7.5 ± 0.4	280 ± 20	93

a Total capacity of beads as determined in Table 2 is~1000 μg/ml
b Purity of fall through as determined by scanning a SDS-PAGE
c IgG concentrations as determined by EIA
d BSA concentrations as determined by BSA assay

147

Table 4a: Product purity and yield upon pulse loading fall through

Run #	Fraction of Total Capacity Loaded[a]	Purity of IgG[b] (% of Total Protein)	% Recovery[c]	Overall Yield
1a	0.5	42 ± 3	90 ± 0.4	87 ± 0.5
1b	Fall through from run 1a	70 ± 3	97 ± 0.5	
2a	0.75	31 ± 2	92 ± 1.0	
2b	Fall through from run 2a	51 ± 2	94 ± 0.5	83 ± 1.0
2c	Fall through from run 2b	78 ± 3	96 ± 0.8	

a Total capacity of beads as determined in Table 2 is ~ 1000 μg/ml
b Purity of fall through as determined by scanning a SDS-PAGE
c % of IgG recovered in the fall through as determined by material balance

Table 4b: Product purity and yield from preparative scale purification

1a	0.5	41 ± 3	89 ± 1.6	84 ± 2.0
1b	Fall through from run 1a	70 ± 2	93 ± 1.0	
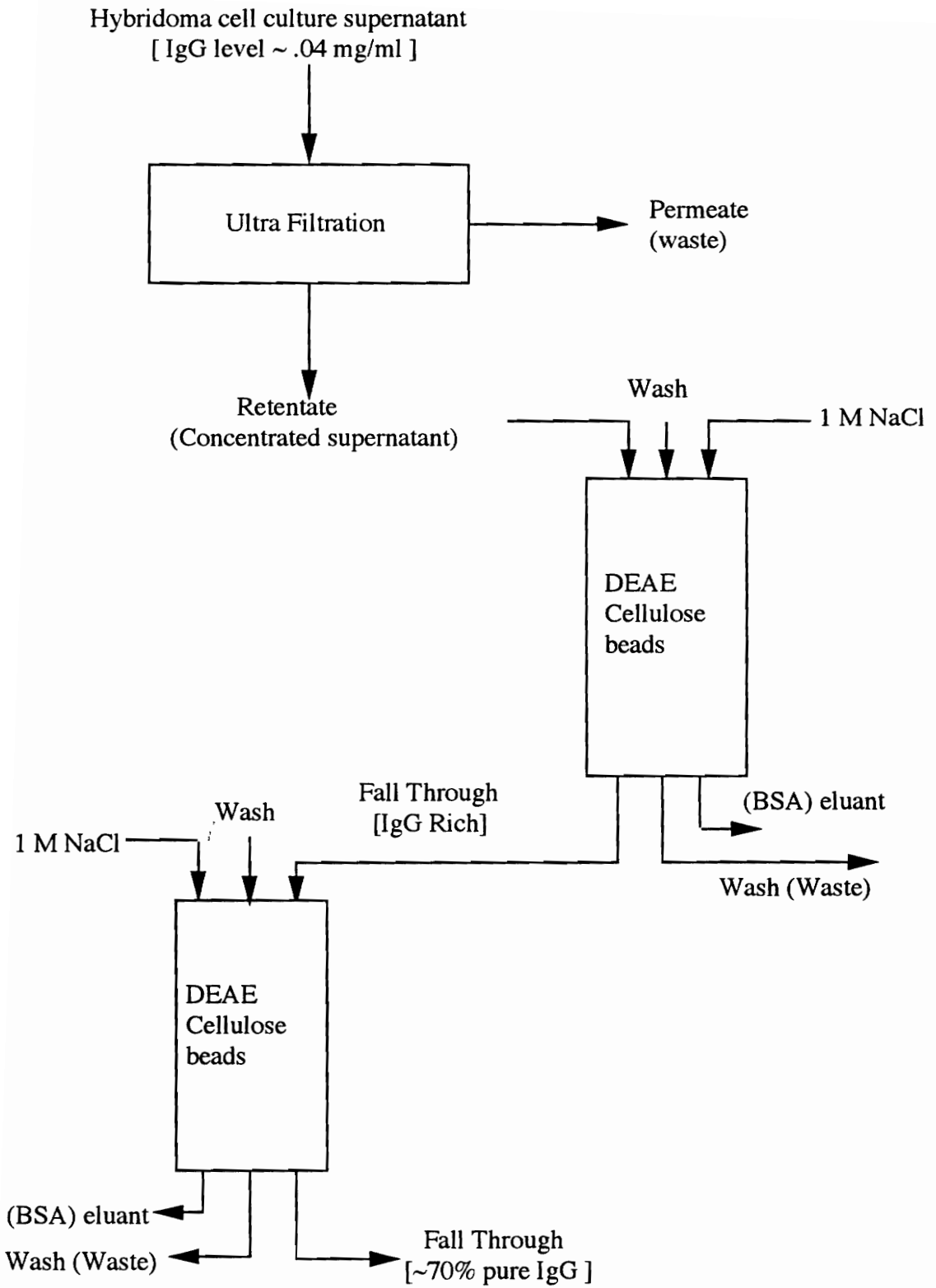
Figure 1: Schematic for IgG Purification Process

Retentate loaded onto a 41* 5cm DEAE cellulose column

Step 1

Fall through [IgG rich]

1 M NaCl

BSA

0.1   Time (min)   15.2
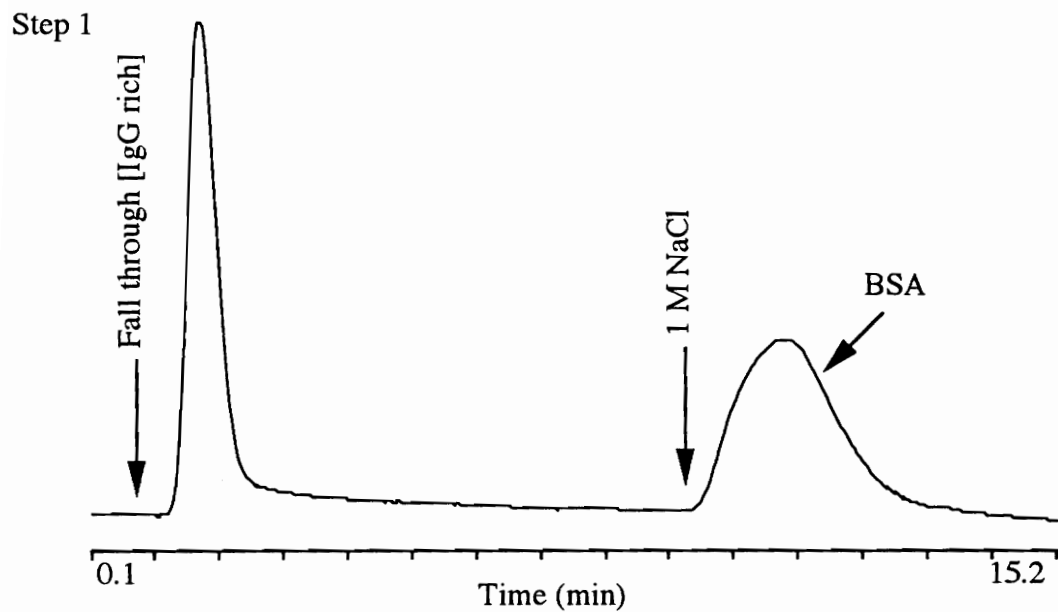
IgG rich Fall through loaded onto a 41*5cm Deae cellulose column

Step 2

[Fall through [~70% pure IgG]

1 M NaCl

BSA

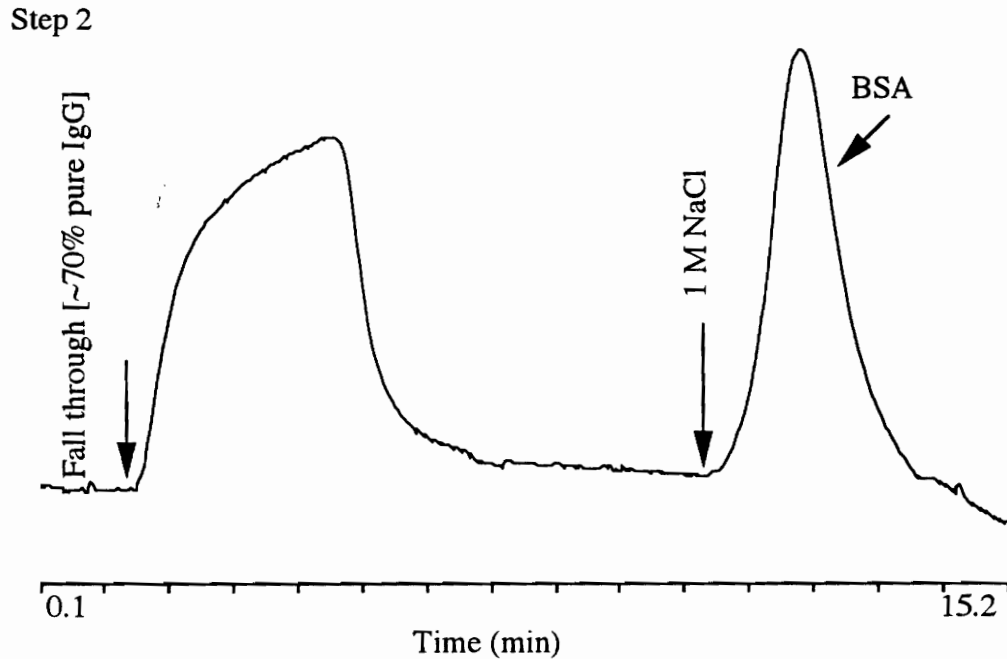0.1   Time (min)   15.2

Figure 2: Chromatograms for the 2-step purification process for IgG using DEAE Cellulose beads
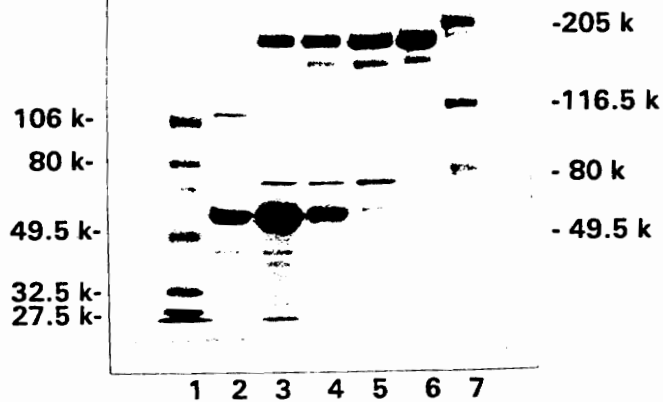
150

Figure 3: SDS-PAGE (4-15% gradient, non-reduced, Coomassie-blue stained) for purification of IgG from hybridoma cell culture supernatant using DEAE cellulose bead column. 1.Low range molecular weight markers 2. Standard BSA 3. Retentate 4. Fall through after first ion-exchange column 5. Fall through after second ion-exchange column 6. Standard IgG (7D7B10) 7. High range molecular weight markers

Chapter 7:

Conclusions

Conclusions

Past studies on the development of spherical hydrogel supports for ion exchange of proteins have emphasized matrices having diameters about 300 μm or less. Here we modify beaded cellulose about 500-1000 μm in diameter, 200-2070 Dp and 2-4% solids content with DEAE using procedures A and B. DEAE-cellulose beads derivatized by procedure B had equivalent degree of substitution as commercially available amorphous anion exchange cellulose which is 1 out of every 8 pyranose rings. The DEAE ligand appeared to be distributed evenly across the bead irrespective of procedure of derivatization. Upon derivatization the beads had a volumetric shrinkage ranging from 25% to 50% which corresponded with an increase in solids content from 2-4% to 5-7%. The decrease in bead size upon derivatization increased the surface area to volume ratio and therefore the frictional drag exerted per volume of bed. No apparent decrease in mechanical strength was seen when pressure drop per unit bed length was normalized for the decrease in bead size. Also, no deformation of beads at flow rates upto 90 cm/min was observed.

The DEAE cellulose beads derivatized by procedure A had lower degree of substitution as compared to DEAE cellulose beads derivatized by procedure B as well as lower static and dynamic binding capacity for BSA. The BSA dynamic binding capacity of Dp 2070, 450 μm DEAE cellulose beads derivatized by procedure B was higher than

100 μm DEAE cross-linked agarose beads. These cellulose beads had ¼ the surface area of cross-linked agarose beads, but permeation studies showed that the accessible binding sites existed only on the outer surface of the bead. Thus, high BSA binding capacity of these cellulose beads is attributed to greater number of sites per accessible area. DEAE cellulose beads exhibit lower small ion capacity compared to commercially available ion exchangers. The milliequivalent of BSA bound per milliequivalent of DEAE ligand is 0.01 for DEAE cellulose beads derivatized by procedure A and 0.02 for DEAE cellulose beads derivatized by procedure B, which is higher compared to 0.015 for DEAE fast flow sepharose and 0.003 for amorphous DEAE cellulose (DE52). Thus, DEAE cellulose beads have the least number of ion exchange ligands per BSA site.

DEAE cellulose beads derivatized by procedure B exhibited slower adsorption kinetics as compared to DEAE cellulose beads derivatized by procedure A or DEAE fast flow sepharose. The BSA adsorption site architecture of DEAE cellulose beads derivatized by procedure A and B are kinetically more uniform than DEAE cross-linked agarose BSA adsorption sites. Thus, kinetic characteristics clearly defined a minimum of 2 different types of protein binding site architecture. Diffusional transport does not appear to be a significant rate limiting step for BSA adsorption on DEAE cellulose beads as suggested by the large diameter of the bead. Furthermore, large diameter DEAE cellulose beads maybe useful for process scale anion exchange purification of proteins (as indicated by purification of rhPC from Zn^{2+} precipitated milk solids in expanded bed

mode and IgG from cell culture in fixed bed mode) if adsorption kinetics can be made

faster while maintaining high degree of substitution.

Chapter 8:

Recommendations for Future Work

Recommendations for Future Work

The feasibility of using large cellulose beads as anion exchange supports which can operate at fast flow rates and possess dynamic capacities comparable to small particle hydrogel supports has been demonstrated. However, there is a greater need to understand the influence of derivatizational chemistry with respect to extent of derivatization and adsorption kinetics on anion exchange binding sites. This phenomena appears to be dependent on reaction time and temperature as well as the surface morphology of the derivatized hydrogel and the constitutive nature of adsorption kinetics of given proteins.
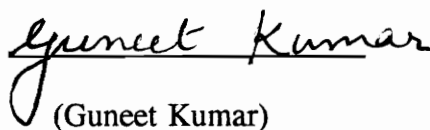
The highly derivatized cellulose beads loose their mechanical strength over a period of six months. Gel permeation chromatography studies seem to indicate that the interior of recently derivatized cellulose beads is not accessible to large molecules such as BSA. Thus the kinetics of "aging" could be studied by gel permeation chromatography and also help in understanding the change in accessibility of the interior of the bead caused by the decrease in hydrogen bonds. Moreover, the derivatized bead could be cross-linked to provide greater mechanical strength when the accessibility in the hydrogel had increased; thus forming a bead exhibiting different transport phenomena in packed beds.

DEAE cellulose beads have been used in the packed bed mode and its potential in expanded bed have been studied. Although the preliminary studies have been encouraging, further investigation of the effects of size and solids content of the beads would aid in understanding the stability of the expanded bed, an aspect that is important for scale-up.

We have shown that large cellulose beads can be used for affinity and anion exchange purification of proteins. The nature of the transport phenomena is different for beads derivatized with affinity and anion exchange chemistries. Cellulose beads derivatized by CNBr ligand show no physical change but beads derivatized by ion exchange ligand exhibit a decrease in bead size, thus changing the transport behavior of ion exchange beads. These studies could be extended to immobilized metal ion affinity chromatography (IMAC), as interest in this field is steadily growing because of the ability of metals to form coordinate bonds with proteins and elute them at very mild conditions. It would also help us further understand intraparticle transport mechanisms in cellulose beads.

Vita

Guneet Kumar was born in Calcutta, India, on October 27th, 1962. At the age of fifteen, she moved with her parents, Bhagat Mohinder Kumar and Usha Kumar, to Bangalore, where she graduated from Bishop Cotton High School in 1981. She received her Bachelor of Science in Chemistry and Master of Science in Organic Chemistry from Indian Institute of Technology, Kharagpur in May 1984 and 1986 respectively. In the future, Guneet intends to work in industrial engineering research in the field of Biotechnology. Guneet and her husband, Amit Pramanik, have one son, Abhik Kumar Pramanik, and presently live in Blacksburg.

(Guneet Kumar)